INTERGOVERNMENTAL OCEANOGRAPHIC COMMISSION (OF UNESCO)

WORLD METEOROLOGICAL ORGANIZATION

DATA BUOY COOPERATION PANEL

DEVELOPMENTS IN BUOY TECHNOLOGY AND DATA APPLICATIONS

PRESENTATIONS AT THE DBCP TECHNICAL WORKSHOP

(La Réunion, France, October 1997)

DBCP Technical Document No. 12

INTERGOVERNMENTAL OCEANOGRAPHIC
COMMISSION (OF UNESCO)

WORLD METEOROLOGICAL
ORGANIZATION

DATA BUOY CO-OPERATION PANEL

DEVELOPMENTS IN BUOY TECHNOLOGY AND DATA APPLICATIONS

PRESENTATIONS AT THE DBCP TECHNICAL WORKSHOP

(La Réunion, France, October 1997)

DBCP Technical Document No. 12

1998

NOTES

The designations employed and the presentation of material in this publication do not imply the expression of any opinion whatsoever on the part of the Secretariats of the Intergovernmental Oceanographic Commission (of UNESCO), and the World Meteorological Organization concerning the legal status of any country, territory, city or area, or of its authorities, or concerning the delimitation of its frontiers or boundaries.

Editorial note: This publication is for the greater part an offset reproduction of typescripts submitted by the authors and has been produced without additional revision by the Secretariats.

FOREWORD

The success of technical workshops at both the eleventh and twelfth sessions of the Data Buoy Cooperation Panel (DBCP) (respectively Pretoria and Henley-on-Thames, see DBCP Technical Publication No. 10) encouraged the panel to make such workshops a regular feature of its annual session, as a practical means of promoting cooperation and information exchange amongst all sections of the global buoy community, including buoy deployers, data users and communication systems providers.

Consequently, a technical workshop on *Developments in buoy technology and data applications* took place during the first day and a half of the thirteenth session of the panel, held in St Denis, La Réunion, France, in October 1997. Around 20 papers were read to more than 50 participants during the workshop, and the texts of 13 of these are included in this DBCP technical publication. In all cases the papers have been reprinted as received, without additional editorial intervention.

TABLE OF CONTENTS

Comparison of Drifting Buoy and Ocean Model Surface Currents

Richard W. Reynolds (National Centers for Environmental Prediction, Camp Springs, MD, 20746, USA)

Comparisons (e.g., see Acreo-Schertzer, et al, 1997) between tropical surface currents estimated from drifting buoys and surface currents from the National Centers for Environmental Prediction (NCEP) ocean model have shown important differences along the equator. Because of changes in the model and the availability of more recent data, the differences have been reexamined for the 1992-96 period. This version of the model used assimilation of temperature data and was forced by NCEP surface winds. In addition, the model surface temperatures were relaxed to the NCEP sea surface temperature analysis.

The mean buoy field was obtained by first computing monthly mean locations and currents for all buoy observations which had an attached drogue. When the drogues are operational, the buoy is designed to follow the currents at 15 m. The buoy observations were averaged on a 1° latitude by 1.5° longitude grid which was spatially smoothed by a 5° latitude by 10.5° longitude box average. The model averages were computed in two ways. In the first version, the model fields at a depth of 15 m were simply averaged onto the 1° by 1.5° grid. In the second version, monthly averaged model fields were sampled at the average buoy location. These "model" current observations were then processed in exactly the same way as the original buoy observations. The differences, defined as buoy minus model, for the zonal component of the current are shown in Figure 1. The upper panel shows the difference using the simple model average. This result is similar to the result of Acreo-Schertzer, et al. (1997) and shows large differences within 10° the equator with magnitudes as large as 30 cm s^{-1}. In general all model near equatorial currents, the westward flowing North and South Equatorial Currents and the eastward flowing North Equatorial Countercurrent, are too strong. However, when the model is sampled only at the buoy locations, the differences, which are shown in the lower panel, are much smaller with magnitudes usually below 5 cm s^{-1}. Although the differences in the lower panel are smaller, there are still important differences near the equator. However, the figure shows that the sampling strongly impacts the comparisons.

To examine these results in more detail, an optimum interpolation (OI) analysis (e.g., see Reynolds and Smith, 1994) of the currents from drifting buoys was computed. This was done by using the monthly averaged buoy and model currents. The model fields were used as a first guess, and the analysis was performed on the difference between the buoy data and the first guess. This resulted in monthly averaged analysis of the differences which was added to the first guess to produce the final OI field. To determine if the OI field using the drifting buoys is better that the original model field, the two fields were compared with independent currents measured at the Tropical Atmosphere Ocean (TAO) moorings. An example of these results for the zonal component of the current is shown at the equator and 165°E in the upper panel of Figure 2. The results show that the OI, which is based both on the model and the buoys, is generally closer to the independent TAO current data than the model alone. In addition, the OI relative error, shown in the lower panel of the figure, gives an indication of data availability. If there are no data, the relative error is one, and the OI and the model are identical; if the relative error is zero, the buoy data are perfect, and the OI is based only on the buoy data. During this period, the data has an

important impact on the OI, with a relative error less than 0.5, except in the first half of 1994. However, in the eastern equatorial Pacific at 110°W and 140°W, the buoy data were more sparse. Thus, the relative errors were often above 0.5 and the data could not correct the model currents.

These results are encouraging. They show a comparison of buoy and model currents must use the same time and space sampling. In addition, they show that an OI analysis of the buoy current data can improve model surface currents. However, these results are only preliminary. The drifting buoy data were not actually assimilated into the model. Thus, the dynamical effect of these corrections on the model is unknown. Furthermore, the drifting buoy data are only available at one level. It is necessary to determine how assimilation at this level would influence other model levels. We plan to first improve the model assimilation using S(z) and then extend the assimilation to use surface current observations from drifting buoys and current observations from the TAO array.

Figure Captions:

Figure 1. Difference between the zonal surface currents from the drifting buoys and the model for 1992-96. In the upper panel all the model data were used; in the lower panel the model was only sampled at the buoys locations (see text). The contour interval is 5 cm s^{-1}, with negative contours dashed. Eastward moving currents are positive.

Figure 2. Monthly zonal currents at the equator and 165°E from the TAO mooring, the model with assimilation, and the OI analysis which is based on both the drifting buoy data and the model. The lower panel shows the relative OI error where one indicates no data and zero indicates perfect data.

References:

Acreo-Schertzer, C. E., D. V. Hansen and M. S. Swenson, 1997: Evaluation and diagnostics of surface currents in the NCEP ocean analyses. *J. Geophys. Res.*, **102**, 21037-21048.

Reynolds, R. W. and T. M. Smith, 1994: Improved global sea surface temperature analyses. *J. Climate*, 7, 929-948.

Figure 1

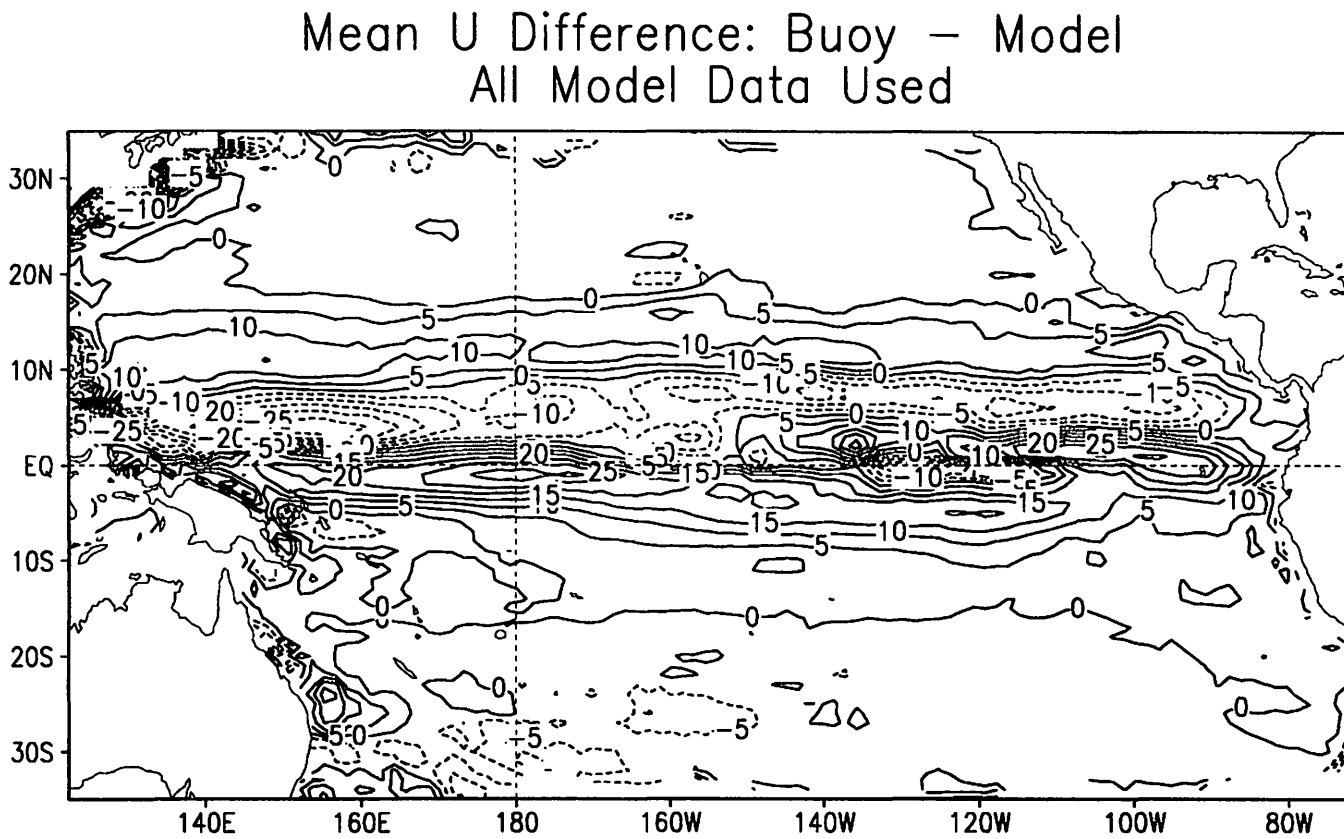
Mean U Difference: Buoy – Model
All Model Data Used
30N
20N
10N
EQ
10S
20S
30S
140E
160E
180
160W
140W
120W
100W
80W

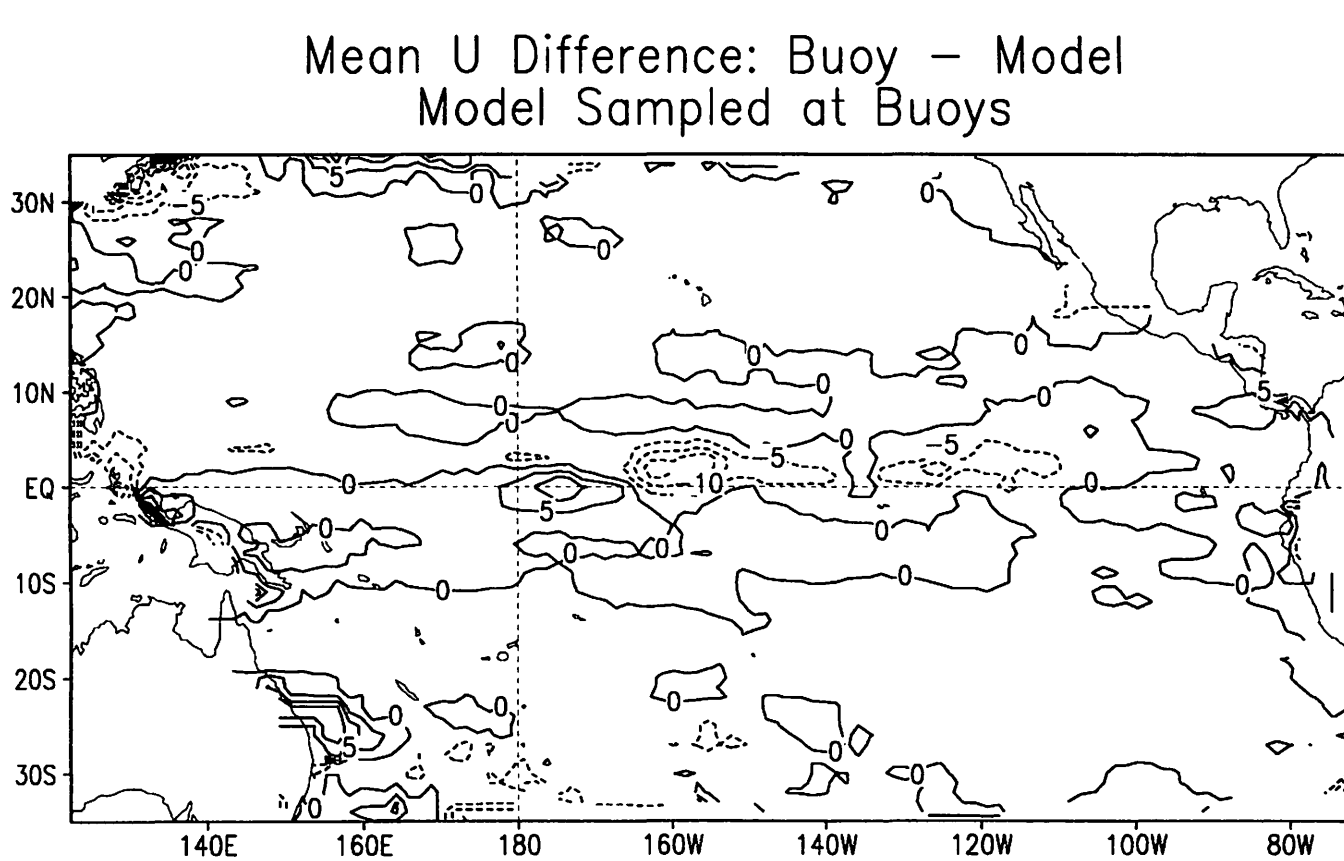
Mean U Difference: Buoy – Model
Model Sampled at Buoys
30N
20N
10N
EQ
10S
20S
30S
140E
160E
180
160W
140W
120W
100W
80W

Figure 2

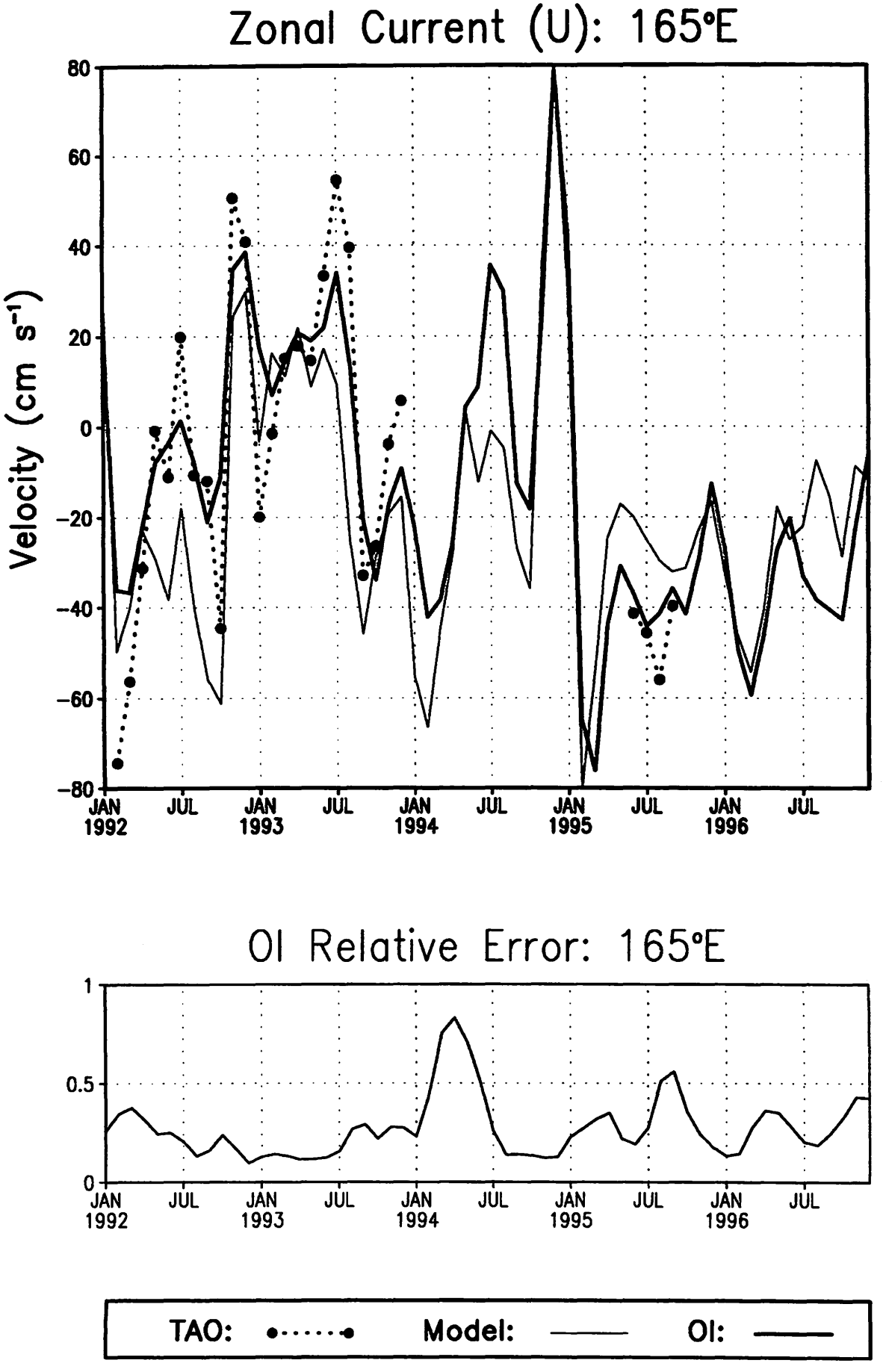
Zonal Current (U): 165°E
Velocity (cm s⁻¹)
80
60
40
20
0
-20
-40
-60
-80
JAN 1992
JUL
JAN 1993
JUL
JAN 1994
JUL
JAN 1995
JUL
JAN 1996
JUL
OI Relative Error: 165°E
1
0.5
0
JAN 1992
JUL
JAN 1993
JUL
JAN 1994
JUL
JAN 1995
JUL
JAN 1996
JUL
TAO:
Model:
OI:

Louis Vermaak, South African Weather Bureau

DRIFTING BUOY DATA AND OPERATIONAL WEATHER FORECASTING

A CASE STUDY

1. INTRODUCTION

The weather systems that develop in the South Atlantic move from west to east and in most cases develop between Gough island and South Africa. The lack of intime weather observation data has caused problems for weather forecasters for many years to identify and analyse weather systems. Satellite Imagery has aided the forecaster but the satellite imagery has it's limitation to identify the intensity of the weather systems. The deployment of drifters has aided the forecasters to identify and analyse the intensity of the weather systems.

The Southwestern Cape is well known as the Cape of storms and in this presentation actual chart analyses with drifter data were used to show the result of drifting buoy data in operational weather forecasting affecting the South-western Cape.

2. CASE STUDY MAY 1983

In the middle 1980's only a few drifters were deployed in the South Atlantic. Fig 1, the chart of the 18th May 1983 showed a frontal trough southwest of the country with a vortex of 1004hPa. Between the 18th and 19th intens cyclogenesis took place as can be seen on fig 2, the chart of the 19th. The vortex deepened from 1004hPa to 988hPa. The system moved gradually southeastwards on the 20th, fig 3. During the 19th and 20th gale force wind in the excess of 35knots occurred along the Southwestern Cape coast with over 100mm of rain in places.

CASE STUDY MAY 1984

A destructive hurricane force storm hit the Southwestern Cape on the 15th and 16th with strong-gale force winds with heavy rain. Millions of rands of damage were caused with roofs blown off, roads washed away, power and telephone comms disrupted and communities cut-off. In this period over 200mm of rain was recorded at places. Fig 4, the chart of the 14th showed a low pressure system of 1000hPa in the vicinity of Gough island. Intens cyclogenesis took place as the low deepened to 968hPa on the 15th.

Reports from the drifter buoy 20648 and 20649 show that the pressure dropped to 911hPa and 996hPa respectively on the morning of the 15th(fig 5). It is assumed that the low started to deepen after it moved north of the drifter buoy's. The low deepened further to 960hPa but moved southeastwards to south of the country on the 16th(fig 6). Fig 7, the buoy time series clearly shows how strong the pressure dropped at buoy 20642(40S,15E) from the 14th to the 15th.
The ECMWF-model predicted a low pressure system of 988hPa at 45S,08E on the 15th. The low pressure system was 28hPa deeper and slightly more northwards.

The South-African forecasters, predicted gale force winds for the Southwestern Cape coast in light of the ECMWF-model prediction. The data from the weather buoy's 20648 and 20649 at first was not trusted by the forecasters indication that the low was already further north and deeper than expected. It was only when buoy 20642 pressure dropped drastically on the 15h that is was realized the intensity of the system. It was only then that more intens conditions was predicted.

The highest wind gust,of 180km/h recorded in South-Africa occurred at Beaufort-West on the morning of the 16th before the anemometermast blew down.

3. CASE STUDY 21-22 JUNE 1997

Fig 8, 9 and 10 showed a vortex moving from 39S,6E on 21 June 1997 to 48S,24E on 22 June 1997 at 1200UT. In this period the central pressure fell from 984hPa to 959hPa. The associated cold front reached Cape Town on Sunday afternoon and Port Elizabeth by the evening.

Winds:

The attached time series of wind from the Cape Point AWS (fig 11), indicate that wind in excess of 30kts blew for over 24hours from the N/NW and even at times over 40kts.

Waves:

The CSIR waverider buoy in 76m of water off Slangkop recorded a max wave height of 14,9m on Sunday 22 June 1997 at 12H20 with the wave period at 18,9sec. The high sea was accompanied with a spring tide.

All the various numerical models: ETA regional, Bracknell global, Global spectral and ECMWF predicted the intensive system as well as the high wave conditions. This was well supported by the drifter buoy data on the 21st and 22nd.

The Cape Town regional office was well as Central Forecast Office followed the Bracknell global wave model and predicted a total sea of 7m on Saturday and raised this warning to 8m on Sunday morning.

Extensive damage occurred to property along the coastal areas, flooding due to the unusually high water levels and actual structural damage due to the direct impact of the waves. In the harbour several mooring lines parted and tugs had to go to the aid of some vessels.

The fact that a spring tide occurred together with the high seas and gale force winds caused higher wave conditions than predicted and hence all the damage.

CASE STUDY 27-28 JUNE 1997

This storm followed close on the heals of the storm during 21st and 22nd June 1997. The Southwestern Cape coast at this stage had not recovered from the previous storm. A developing low pressure system on 27th June 1997 at 0000UT(Fig 12) at approximately 36S,05E moved gradually southeastwards and deepened to 970hPa by 1800UT(fig 15), at approximately 42S,20E at 1800UT when the associated cold front reached Cape Town.

The wind along the Southwestern Cape coast increased dramatically during the morning of the 27th and peaked in the morning. Cape Point AWS recorded an average wind of 56kts from the NW with a max windgust of 84kts. The wind moderated gradually in the evening as the low started to move further southeastwards.

The CSIR waverider at Slangkop recorded a max wave of 7,2m at 13,5sec on the morning of the 28th.

Fortunately the storms duration was shorter than the storm of the 21st and 22nd but mopping-up operations where delayed as further wind damage was caused to weak building structures.

The numerical models did predict the position of the system well but the buoy data showed is slightly deeper and hence its effect greater.

The forecasters used the model predictions and issued a gale warning for the Southwestern Cape coast. The forecast was however adapted when the drifter data showed a deeper system.

4. CONCLUSION

Finally if we consider the fast ocean areas around Southern Africa with the lack of observation data previously it is evident from these case studies that the availability of drifter buoy data plays a major role in the analyses of weather systems and the final forecasting of weather conditions that affect the Southwestern Cape.

Fig 1. 18 MAY 1983 1200UT

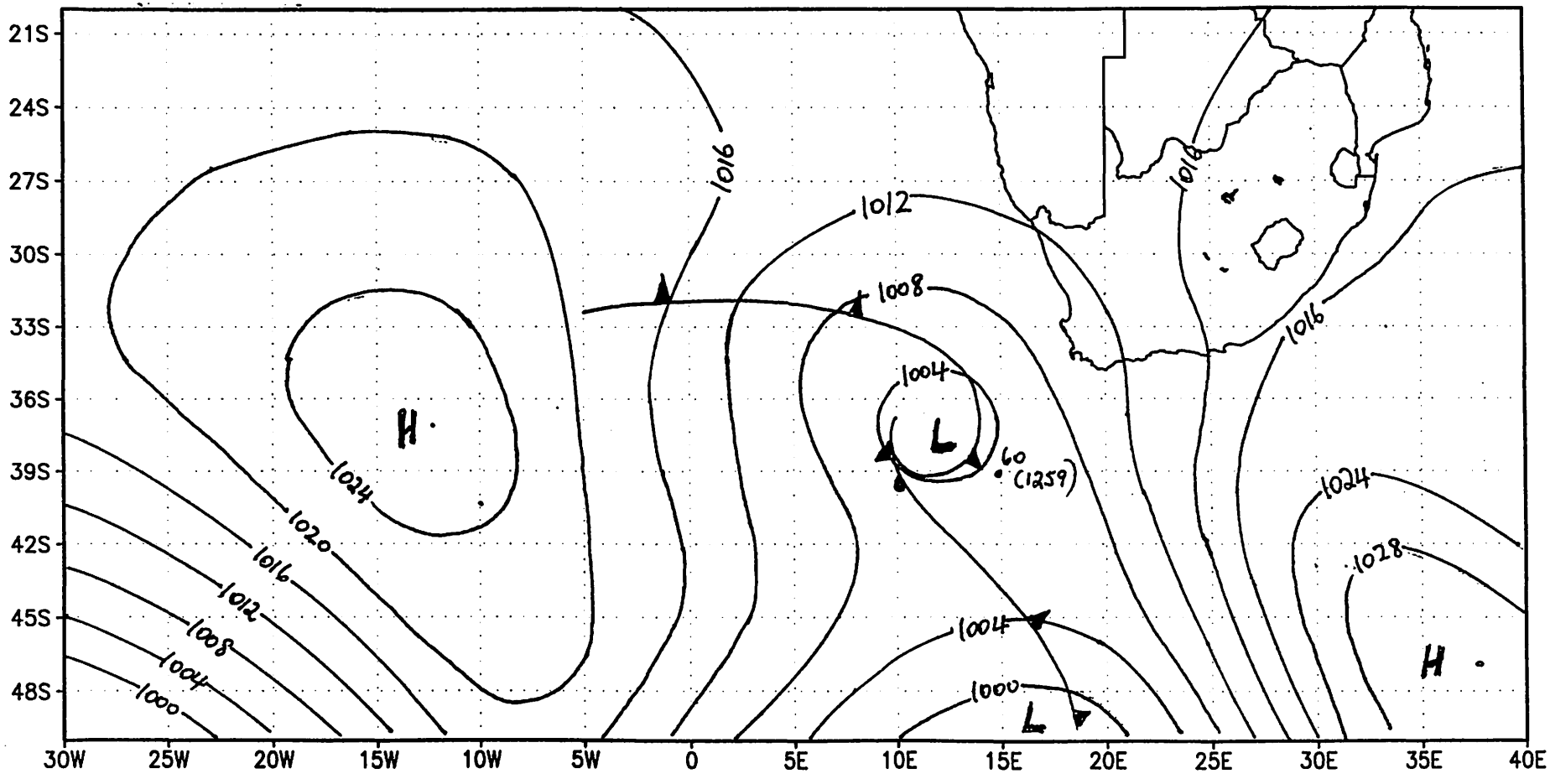

Fig 2. 19 MAY 1983 1200UT

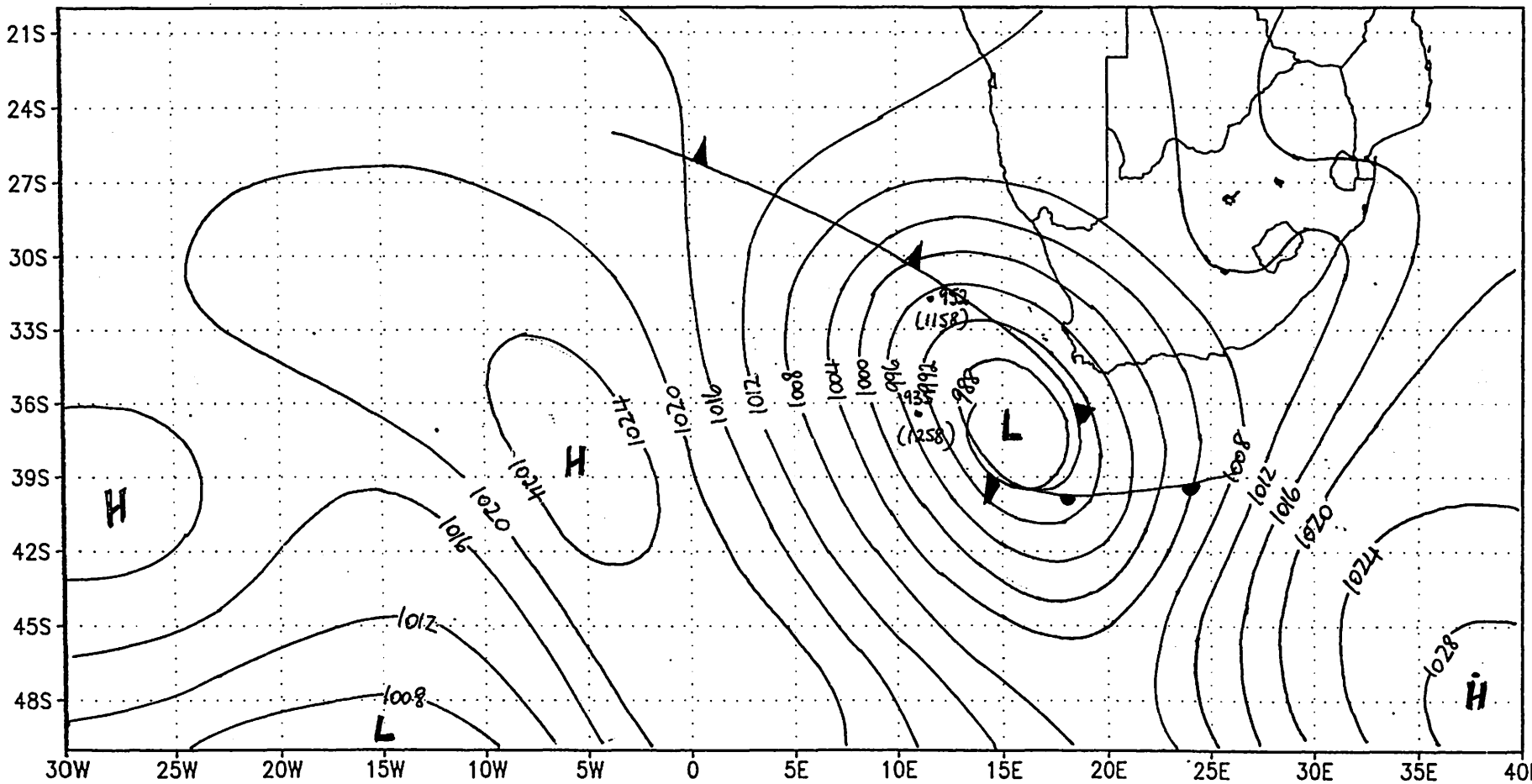

Fig 3. 20 MAY 1983 1200UT

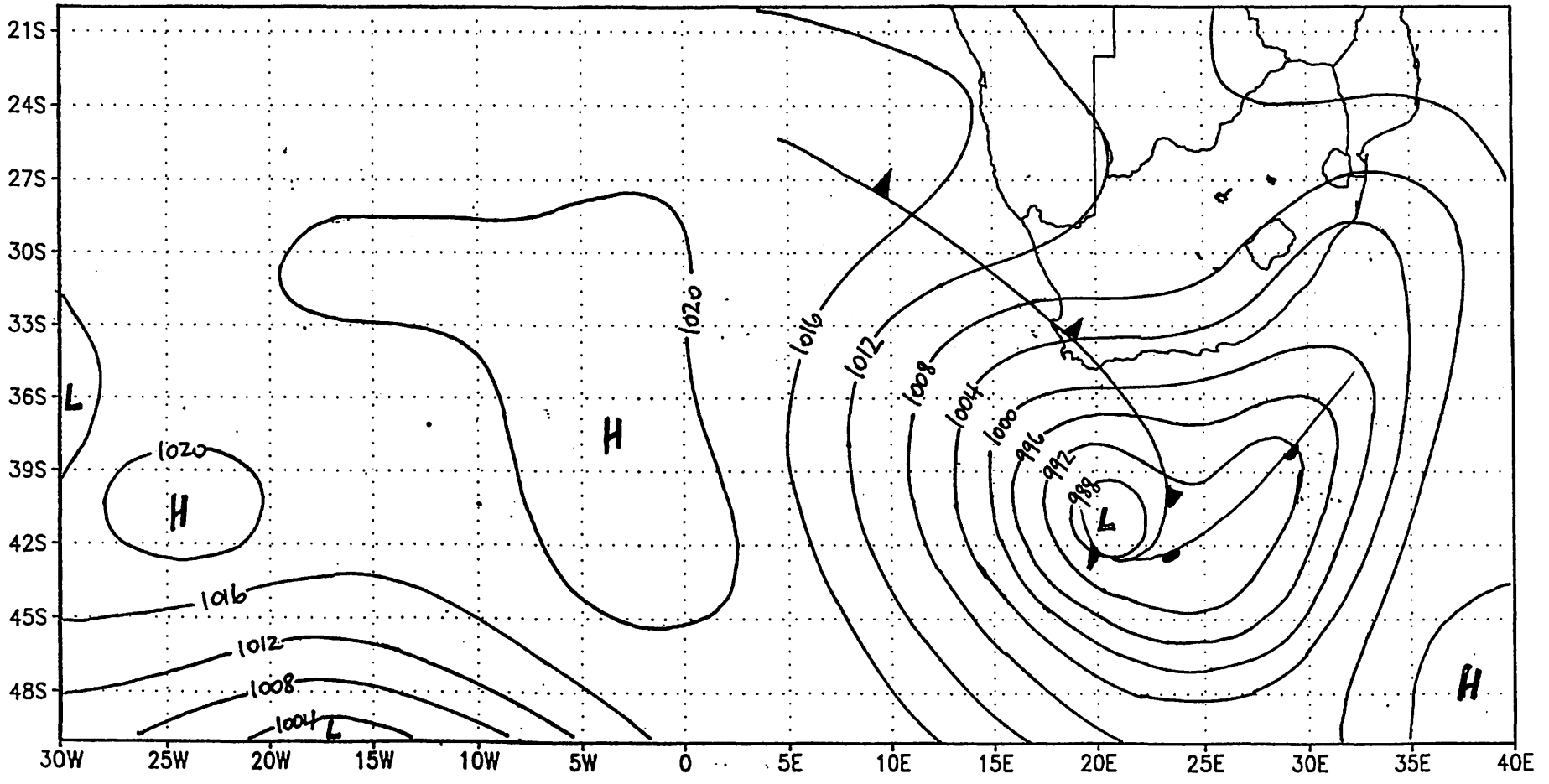

Fig 4. 14 MAY 1984 1200UT

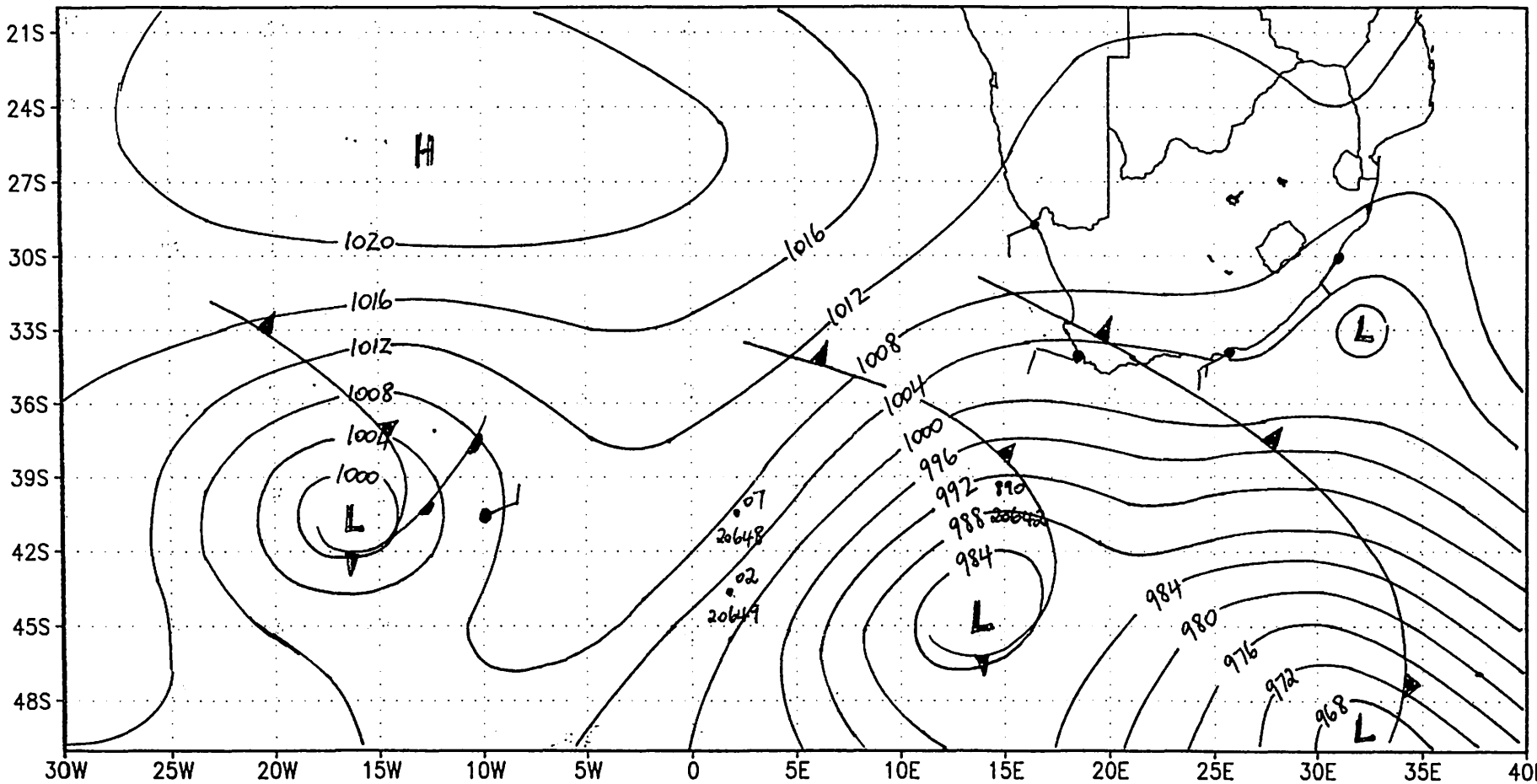

Fig 5. 15 MAY 1984 1200UT

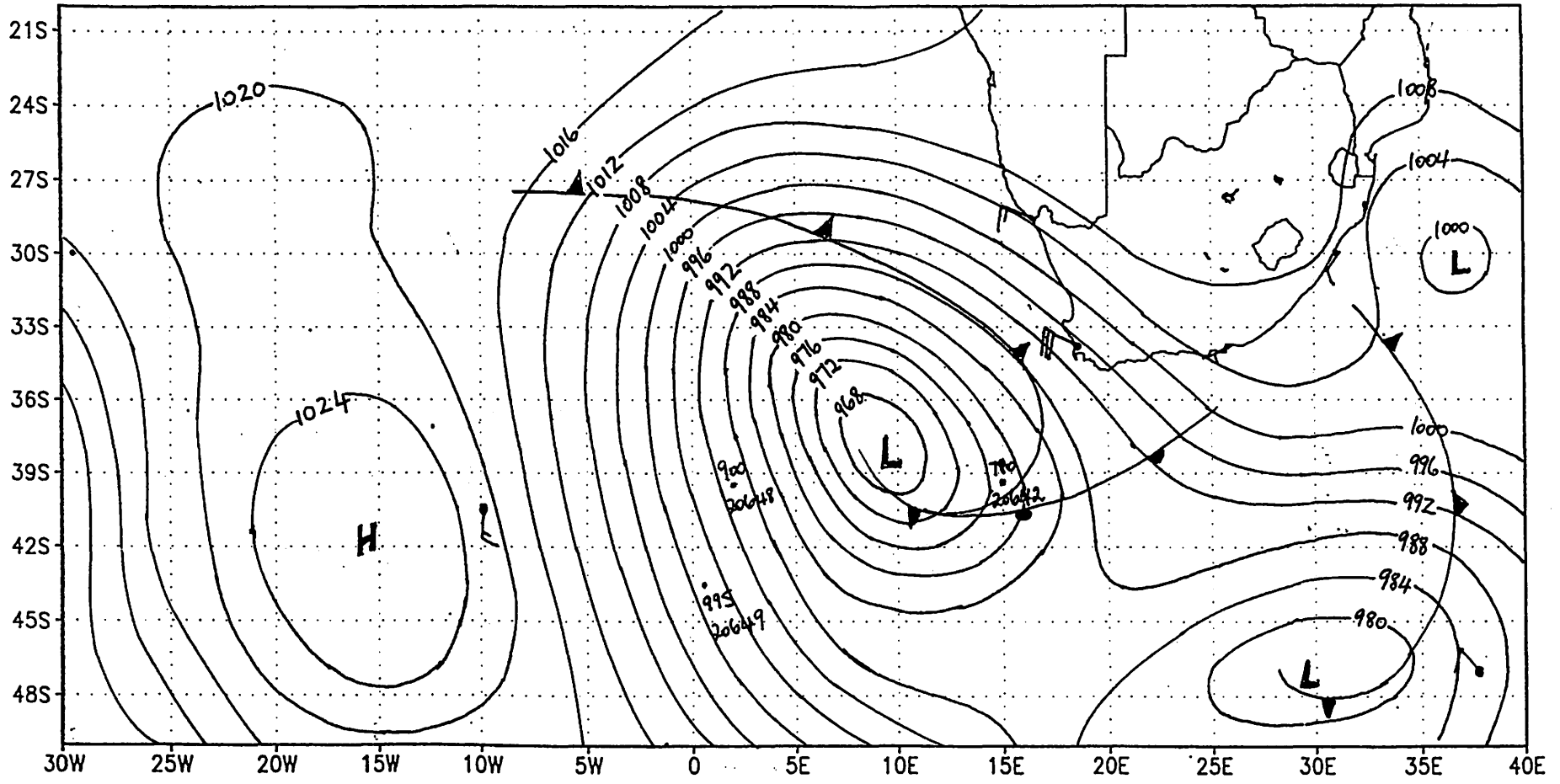

Fig 6. 16 MAY 1984 1200UT

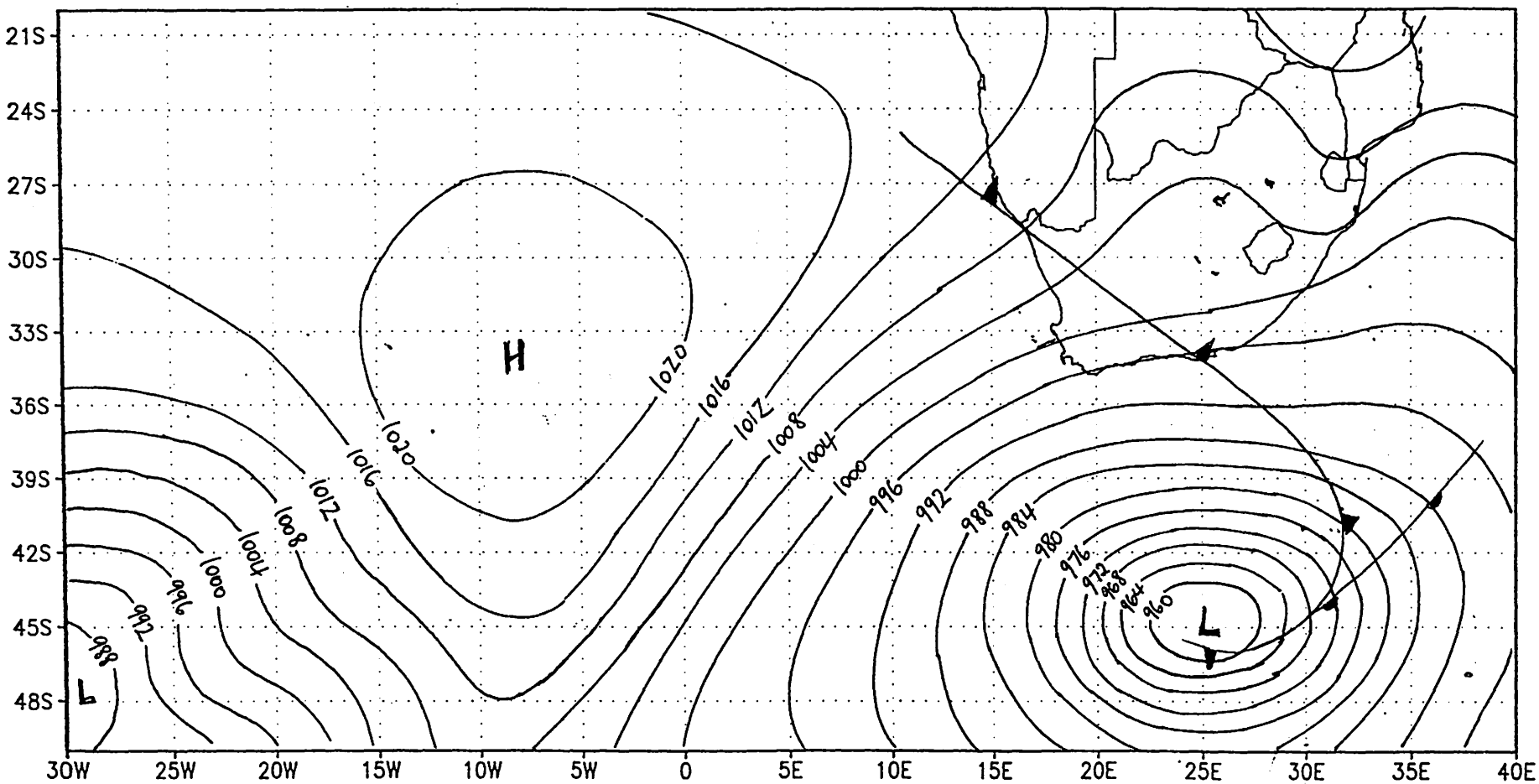

Fig 7. BUOY TIME SERIES

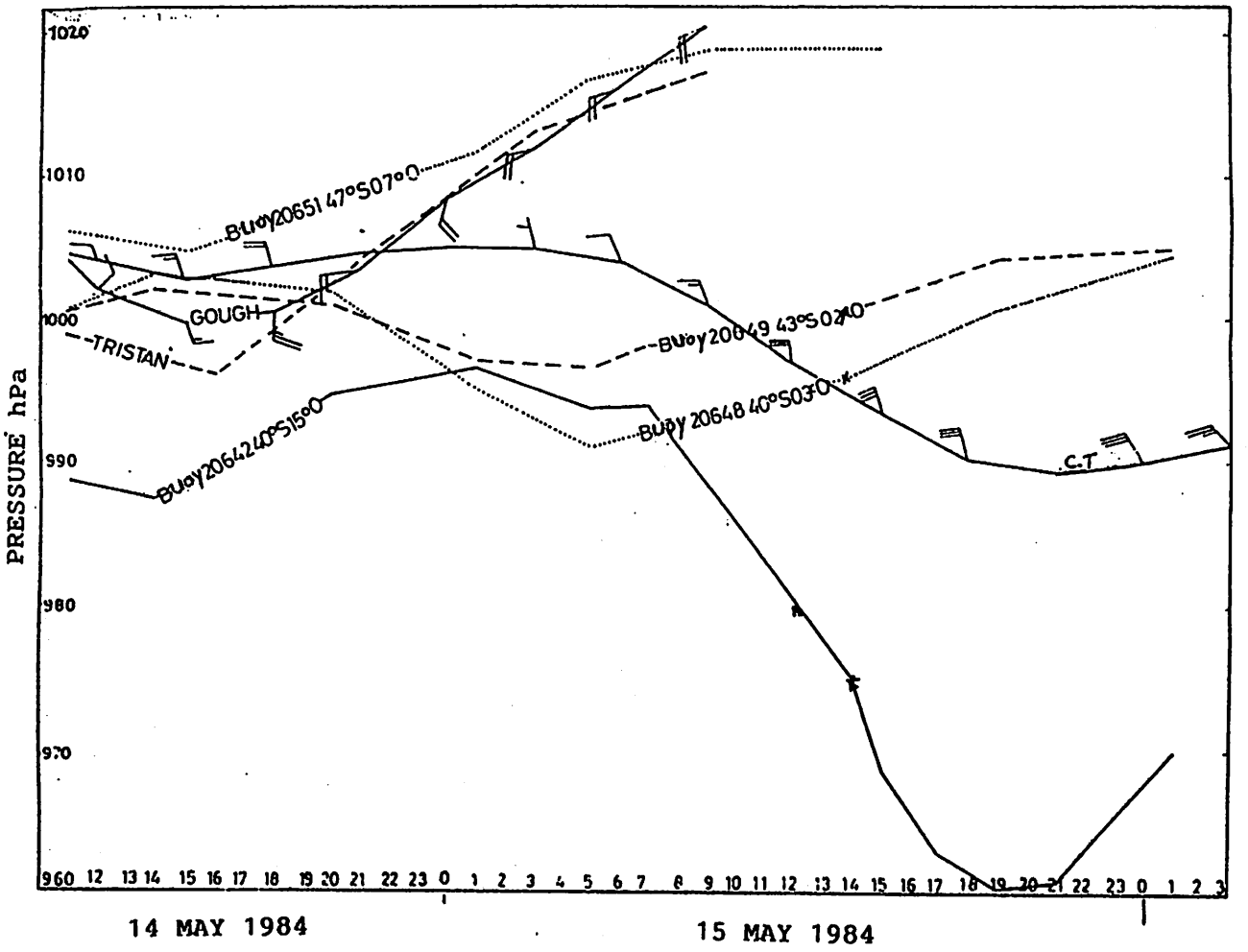

Fig 8. 21 JUNE 1997 1200UT

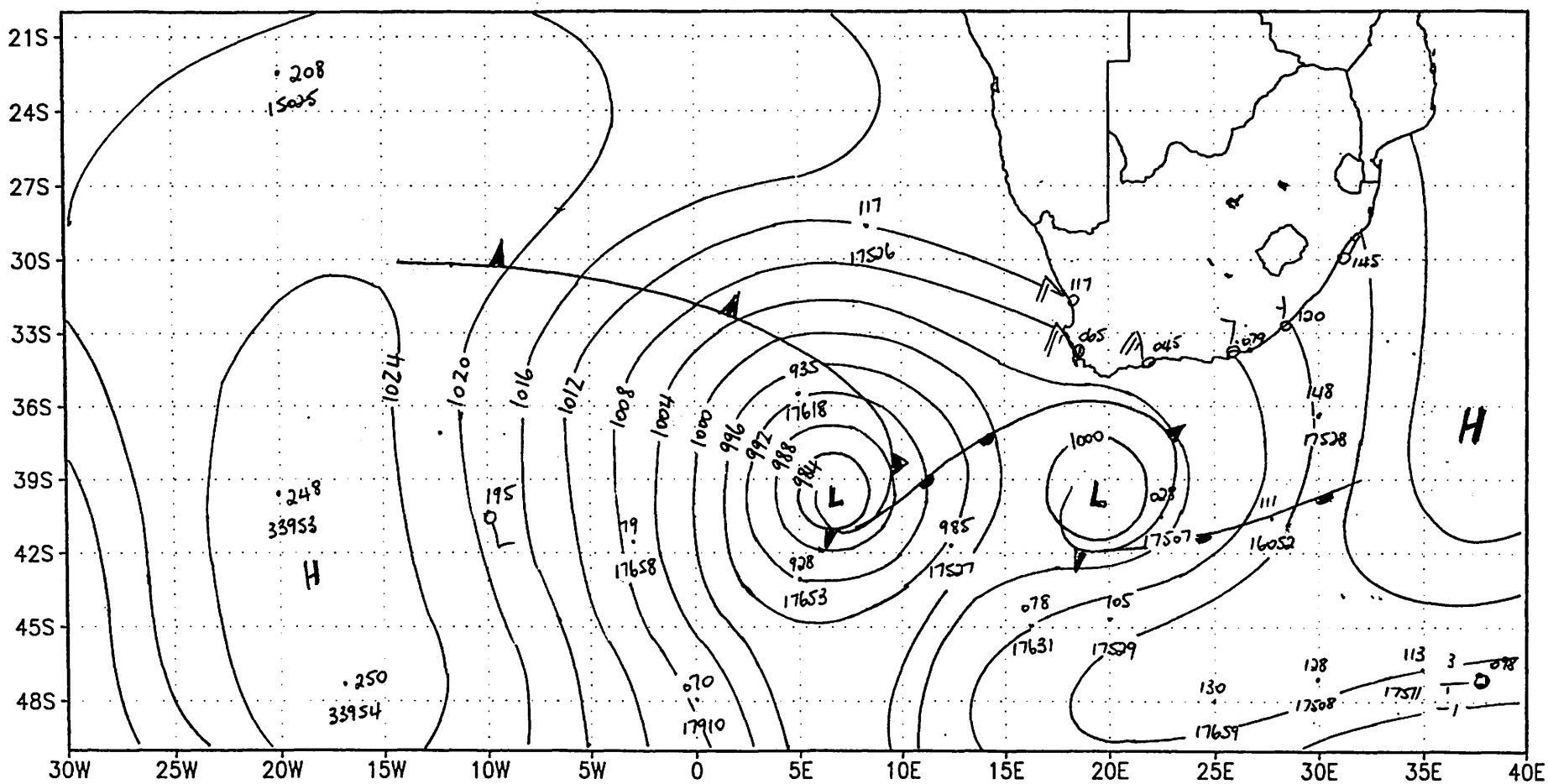

Fig 9. 22 JUNE 1997 0600UT

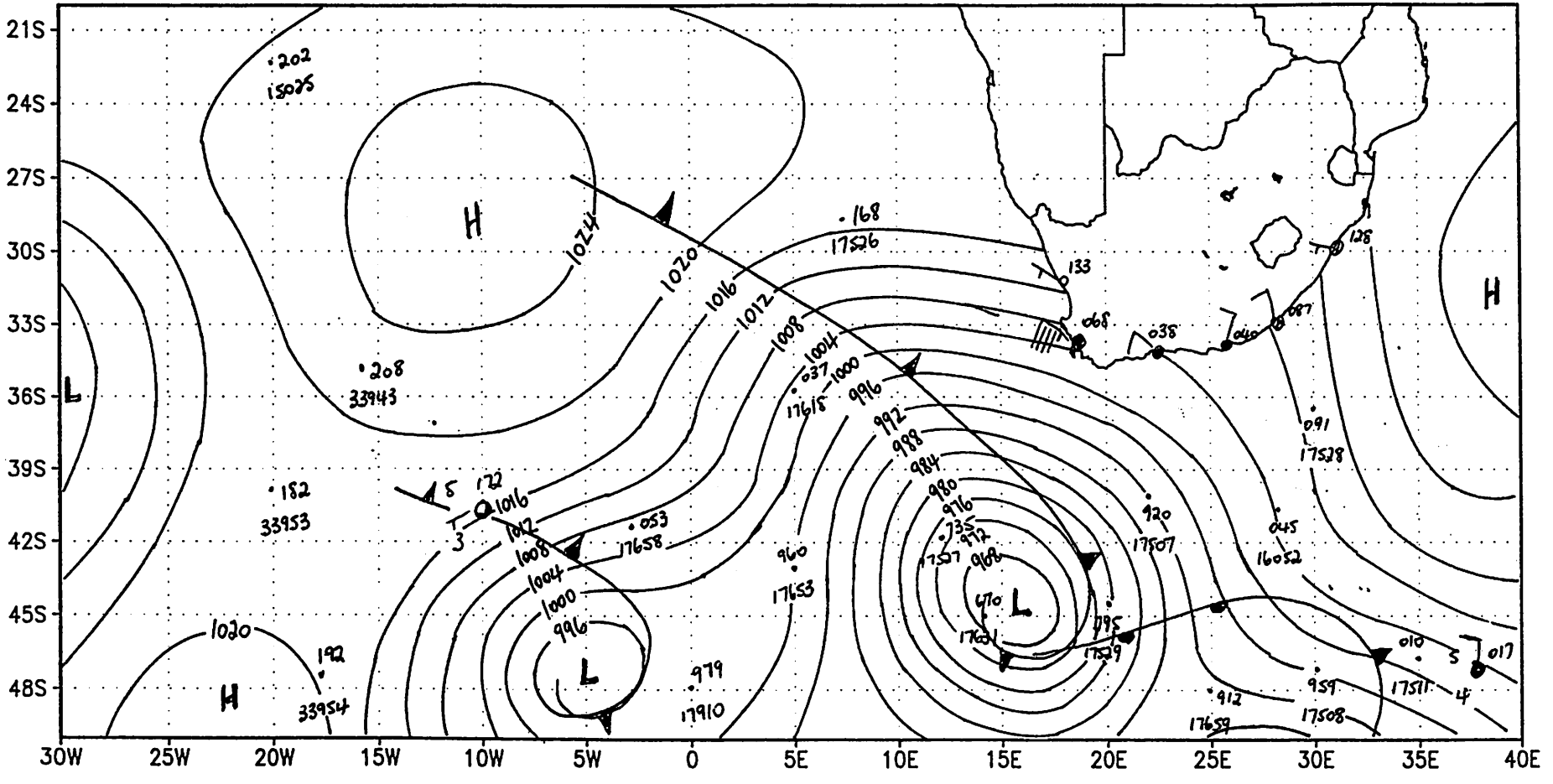

Fig 10. 22 JUNE 1997 1200UT

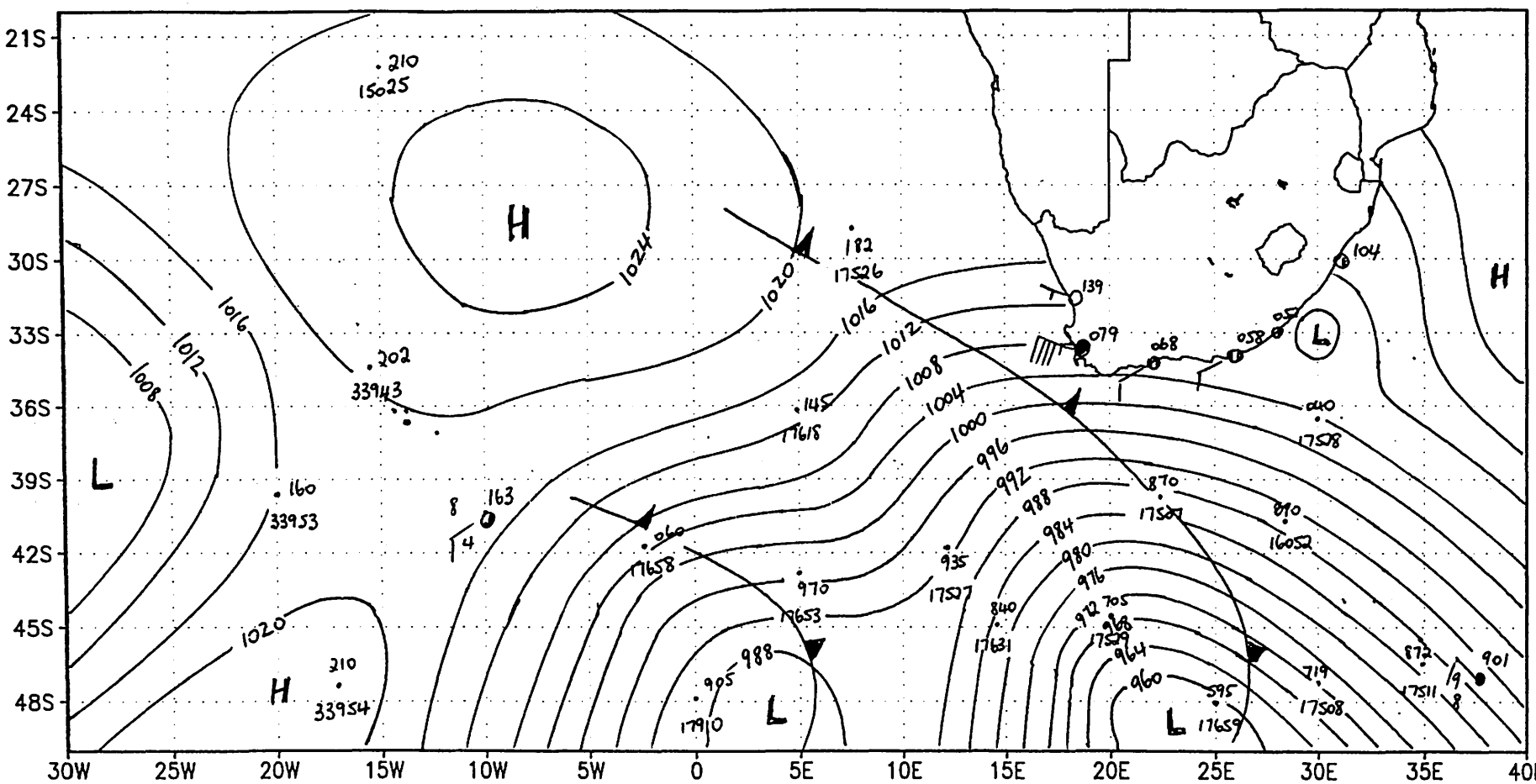

Fig 11. WIND PROFILE CAPE POINT 21-22 JUNE 1997

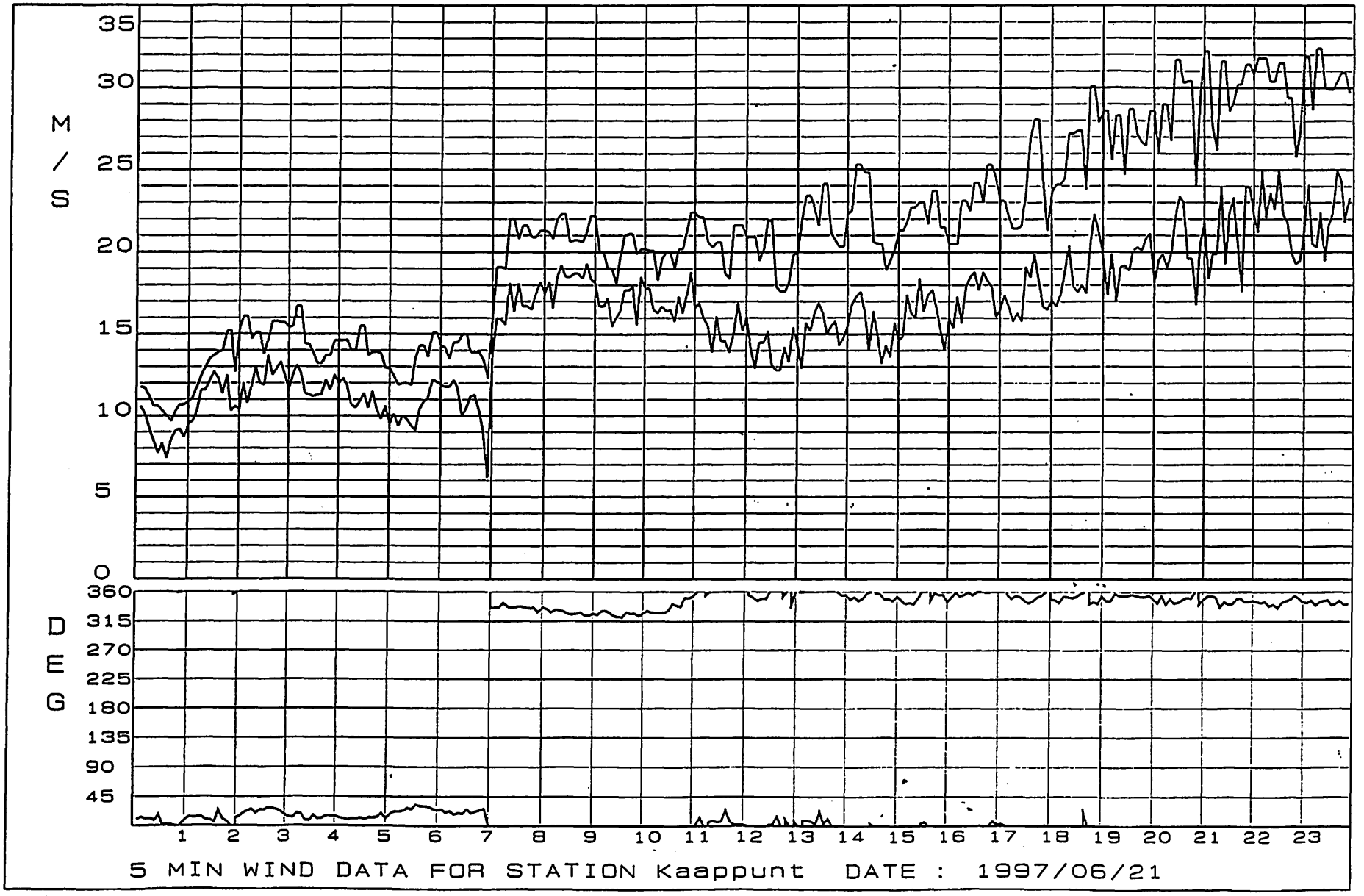

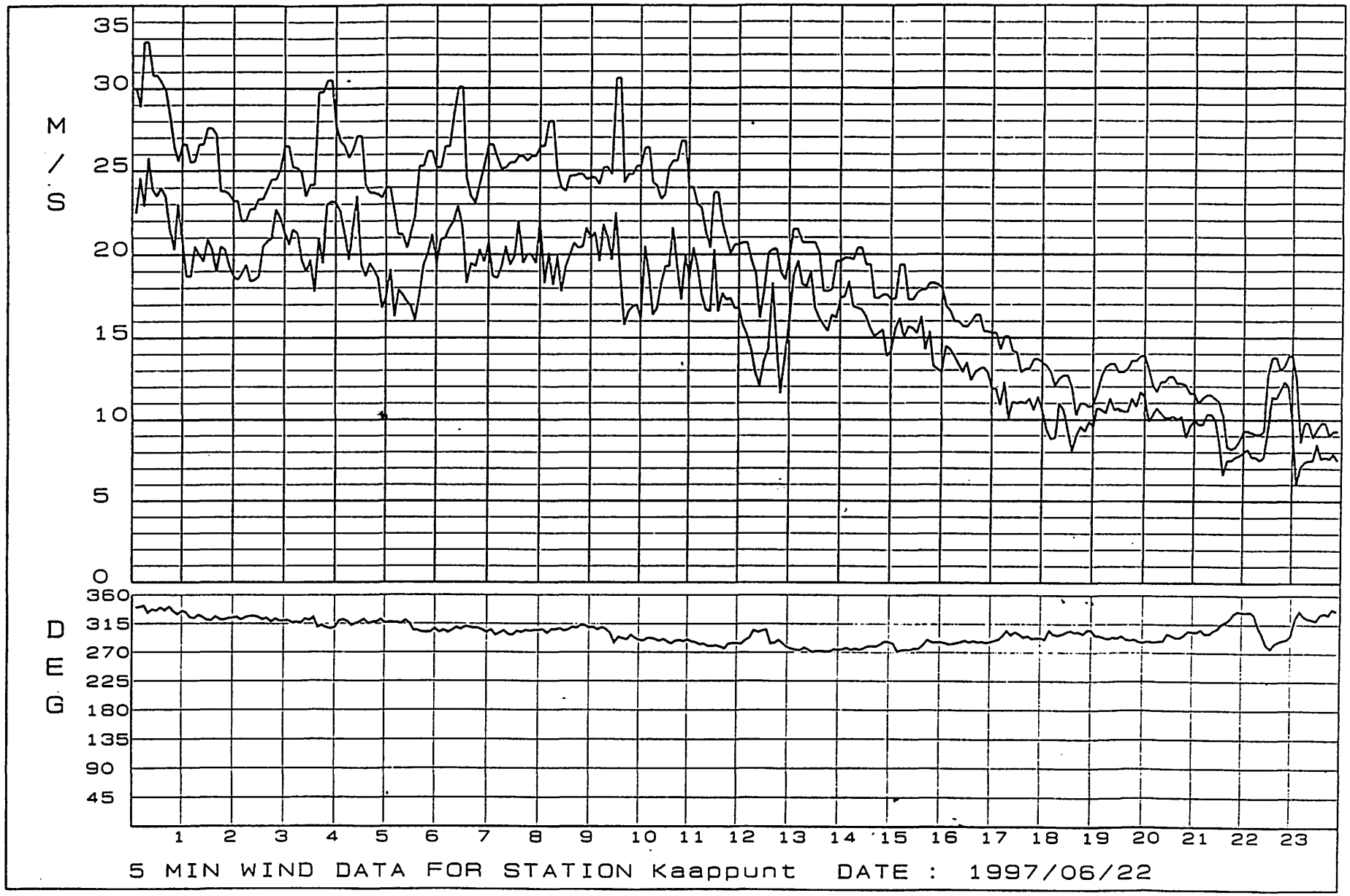
M / S
35
30
25
20
15
10
5
0
DEG
360
315
270
225
180
135
90
45
1 2 3 4 5 6 7 8 9 10 11 12 13 14 15 16 17 18 19 20 21 22 23
5 MIN WIND DATA FOR STATION Kaappunt DATE : 1997/06/22

Fig 12. 27 JUNE 1997 0000UT

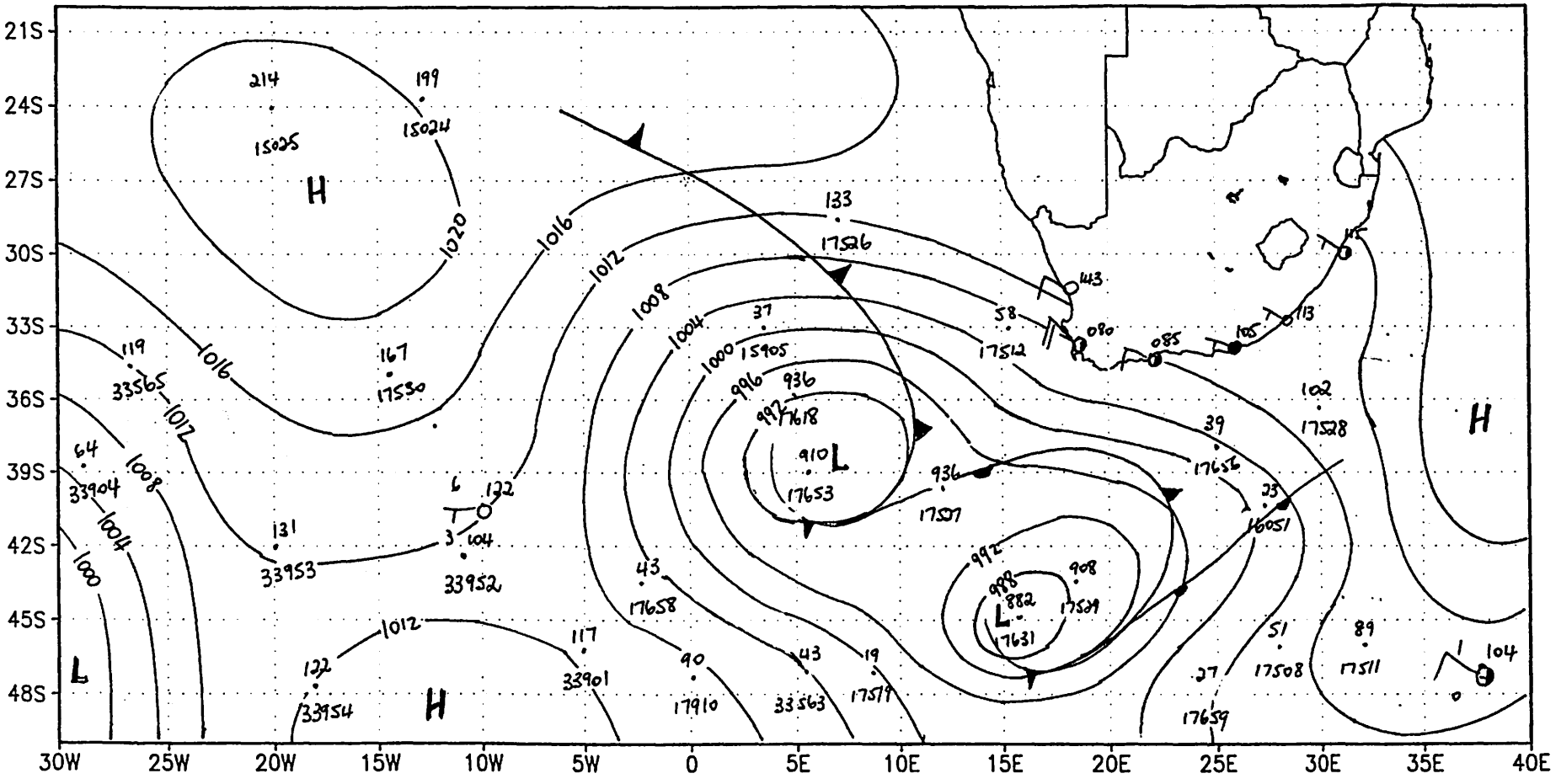

Fig 13. 27 JUNE 1997 0600UT

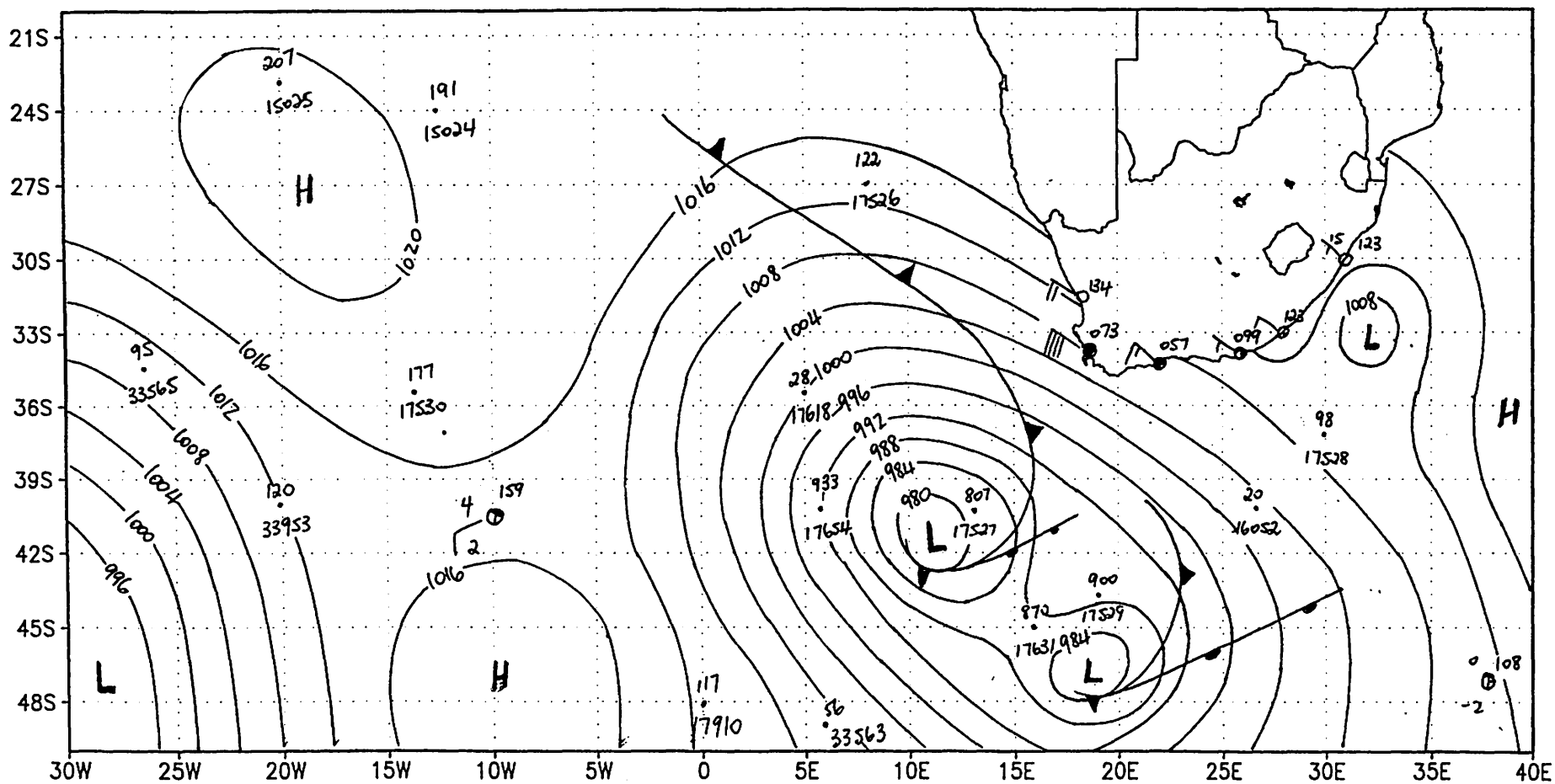

Fig 14. 27 JUNE 1997 1200UT

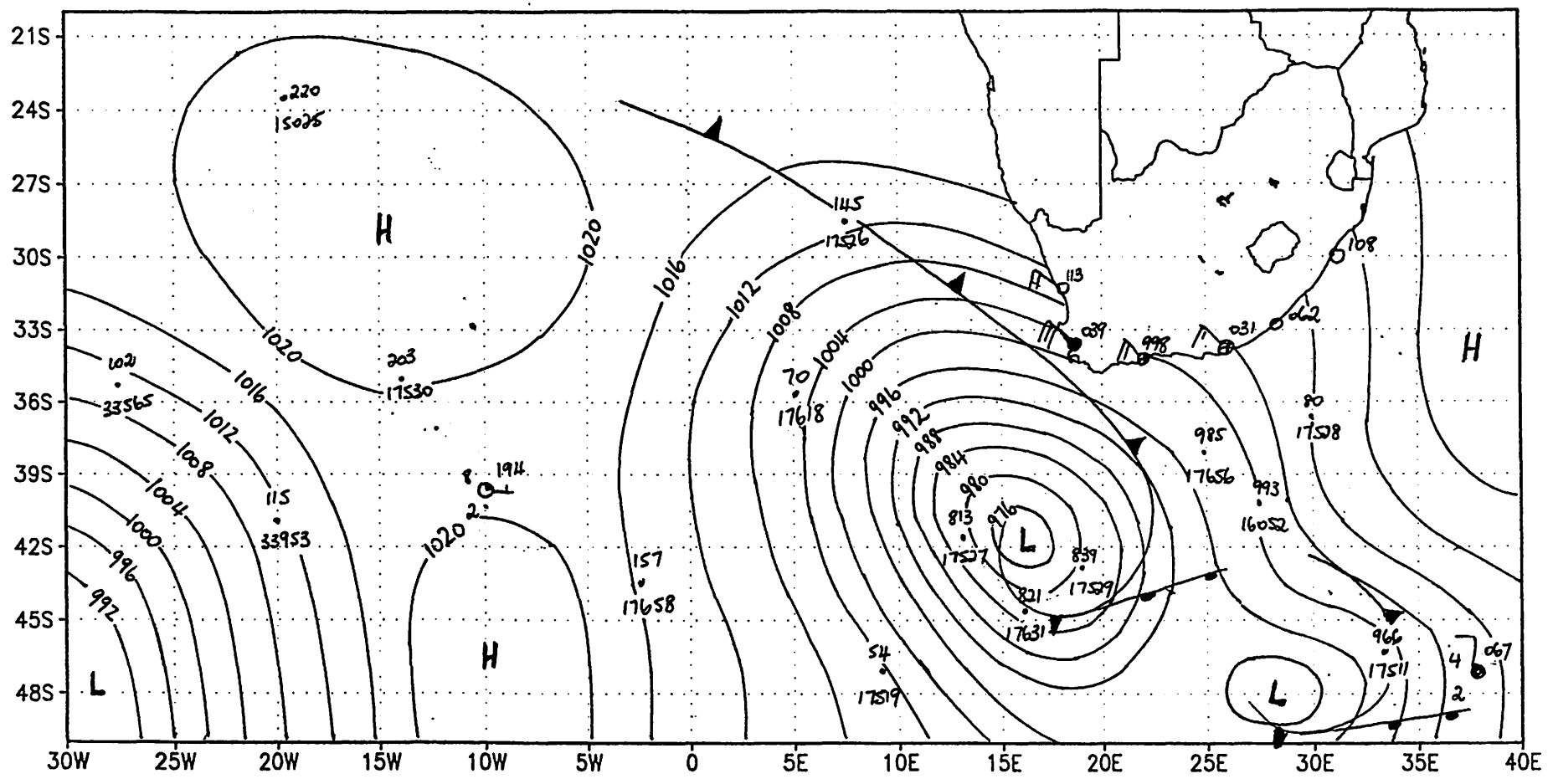

Fig 15. 27 JUNE 1997 1800UT

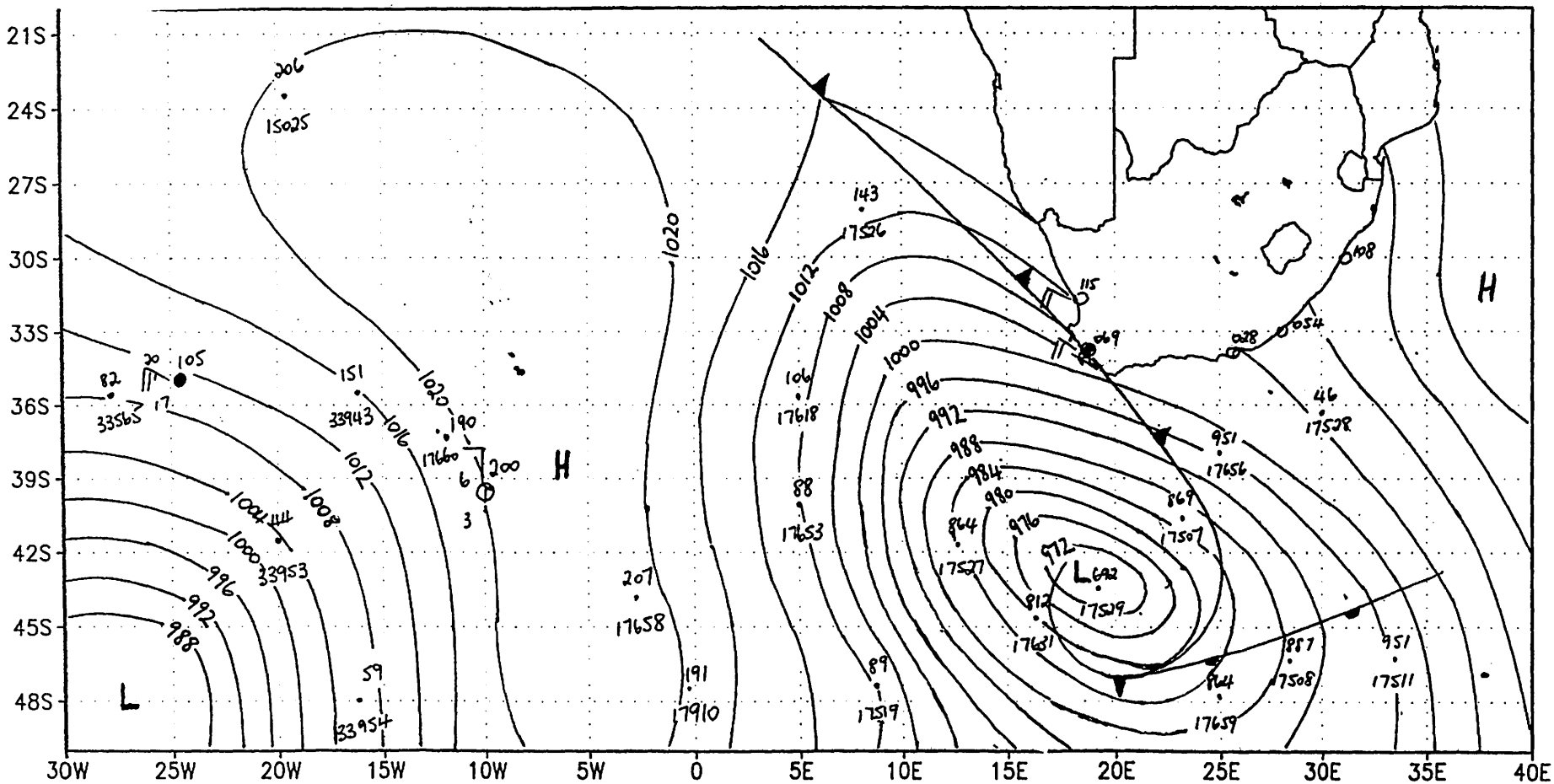

Fig 16. METEOSAT 27 JUNE 1997 20:30UT

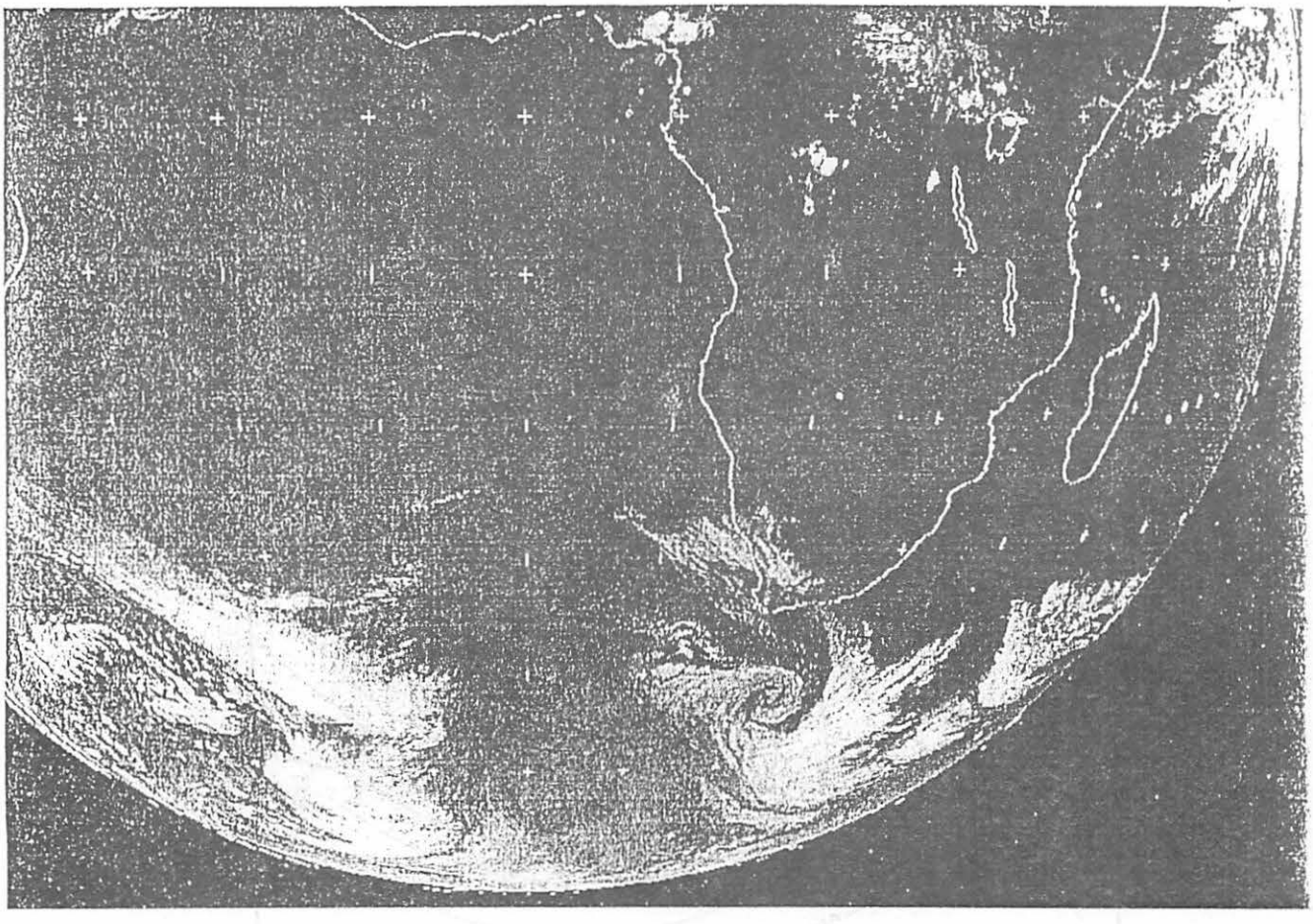

Fig 17. 28 JUNE 1997 0000UT

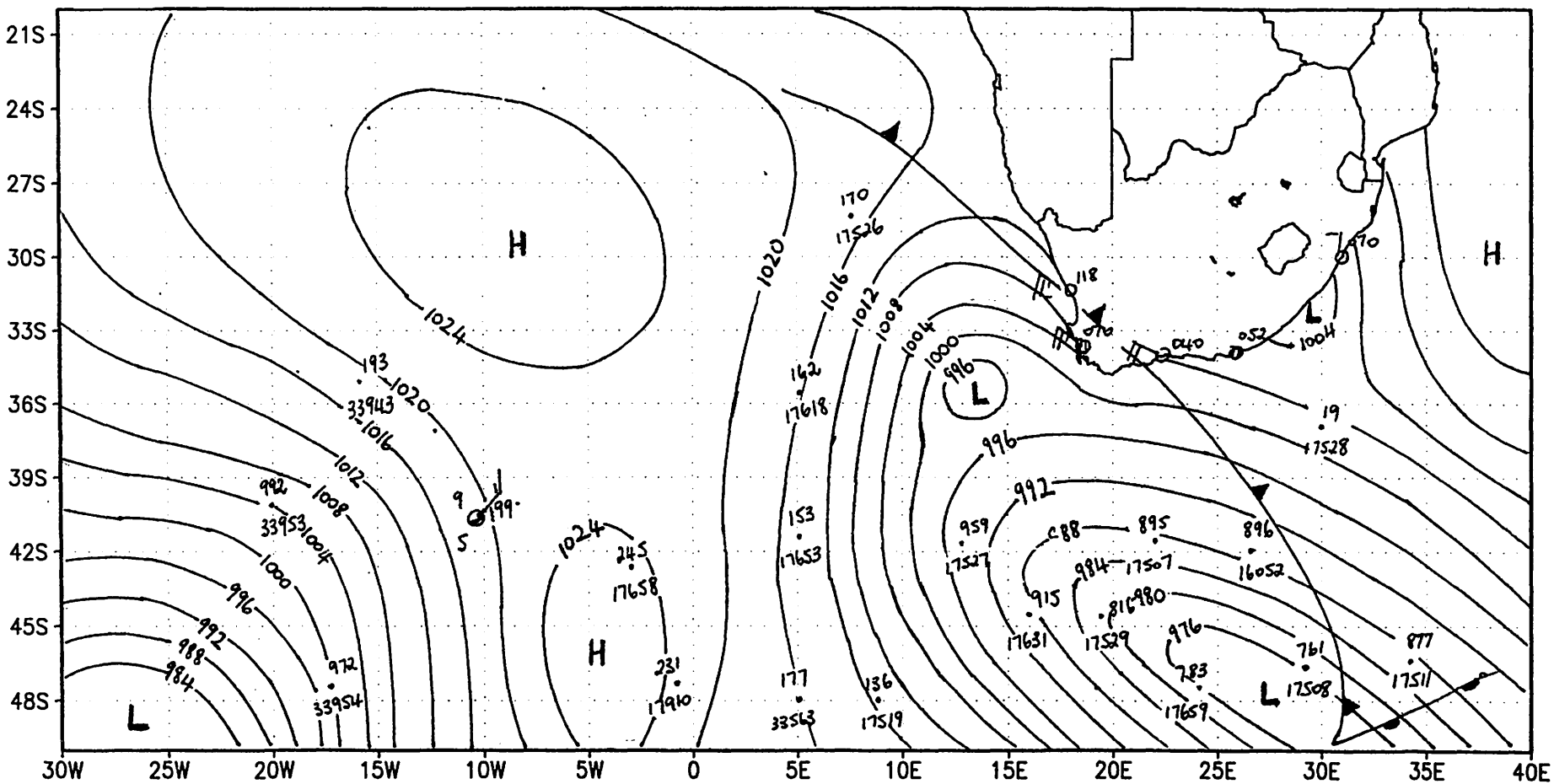

DRIFTING BUOY PERFORMANCE DURING TOGA

Eric A. Meindl
National Data Buoy Center
U.S.A.

INTRODUCTION:

The 10-year Tropical Ocean Global Atmosphere (TOGA) Research Program officially ended in 1995. A key observation platform was the meteorological drifting buoy developed for the First Global Atmospheric Research Program (GARP) Global Experiment (FGGE) that measured barometric pressure, air temperature, and sea surface temperature. A small number (fewer than 10) of wind speed and direction (WSD) drifting buoys, which were FGGE drifting buoys modified only to add wind measurement capability, were deployed around 1990.

The performance record of the FGGE drifting buoy during TOGA is summarized here.

FGGE Drifting Buoy Description and Deployments

A cut-away diagram of the FGGE drifting buoy is shown in Figure 1. It was a 3.2-m-long cylinder approximately 10 cm in diameter with a frustum-shaped flotation collar located approximately 1 m from the top.

All sensors, electronics, and batteries were located within the cylinder, with the batteries near the bottom to provide ballast. A 100-m drogue line, weighted at the bottom, was attached to the base of the cylinder in an attempt to couple buoy drift with the near-surface ocean current. As it turned out, the drogue line neither caused the drifting buoy to follow the surface current very well nor did it remain attached to the buoy for a sufficiently long period; therefore, it was eliminated by the late 1980's.

Figure 2 shows the number of buoys deployed between 1984 and 1995 by WMO area; Figure 3 is a graph of the number of buoys deployed by calendar year.

Drifting Buoy System Performance

Data from the TOGA drifting buoys was sent via the U.S. National Oceanic and Atmospheric Administration (NOAA) polar-orbiting satellites and the Service Argos data collection and processing system. Following Argos processing and gross data quality control checks, the data underwent further quality control in real-time using the NDBC algorithms at the National Weather Service Telecommunications Gateway (NWSTG). When a sensor failed, data were deleted from distribution to the GTS.

Table 1 shows the mean-time-to-failure (MTTF) in days of each sensor and the buoy transmitter; the MTTF shown is the average for all buoys deployed that year. Note the poorest performance record is associated with deployments in 1989; the best were in 1993 and 1994, when the last batch of TOGA drifting buoys was manufactured by a new contractor. The MTTF of the sensors (excluding the transmitter and drogue) during all of TOGA was between 407 and 468 days. The longest performance by a single buoy was 1,171 days — or more than 3 years and 2 months.

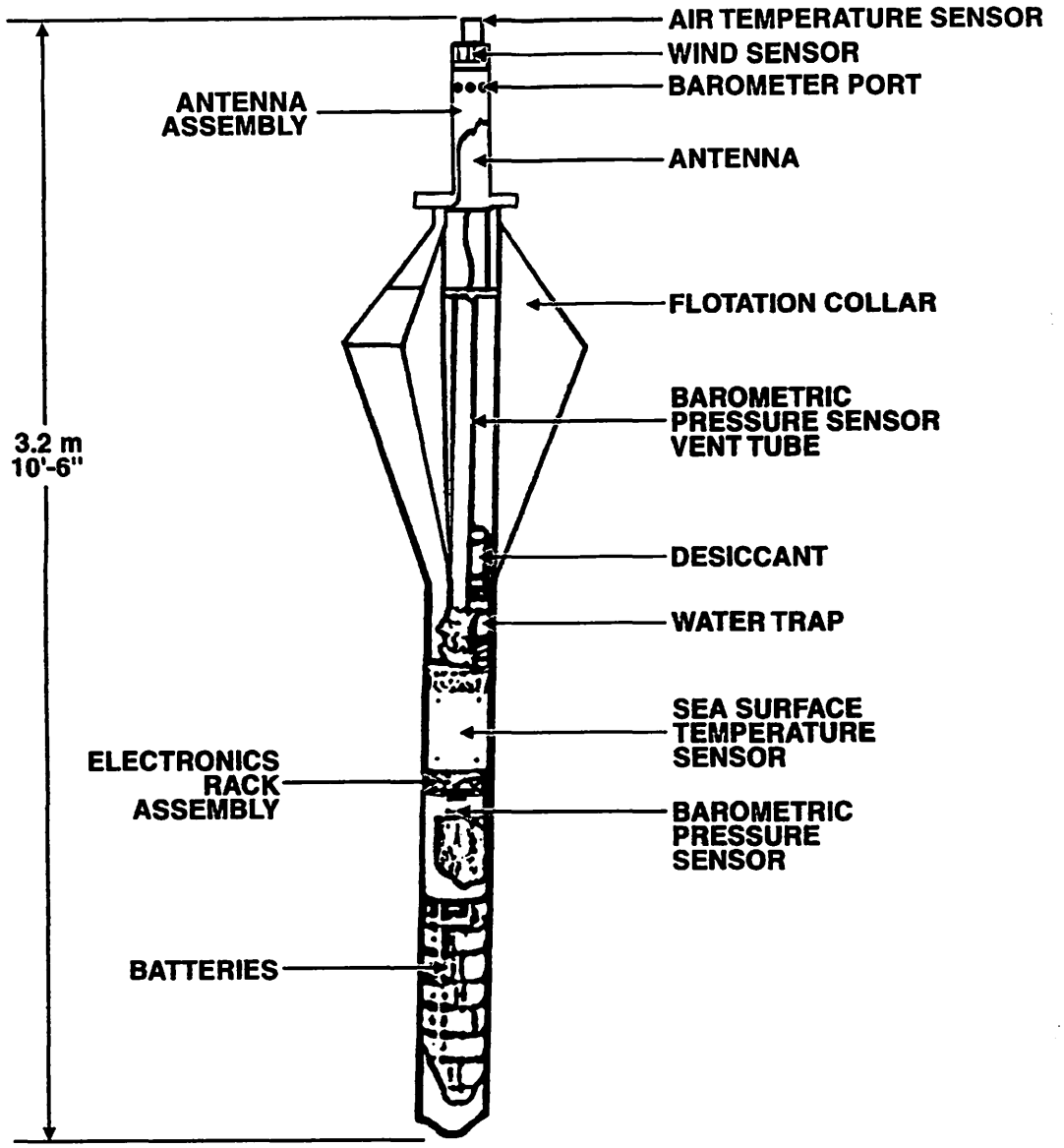

Figure 1. FGGE Drifting Buoy

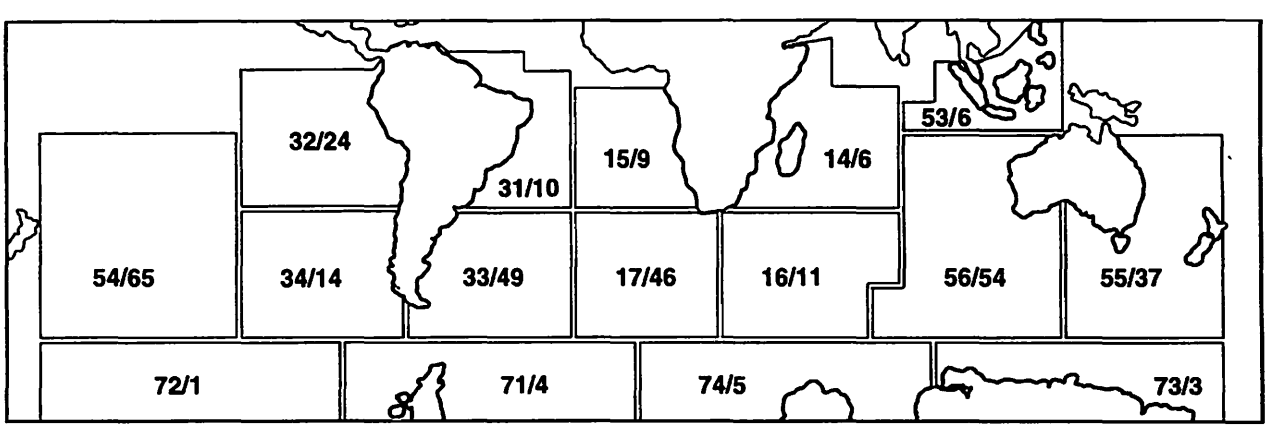

Figure 2. Buoys Deployed Between 1984 and 1995

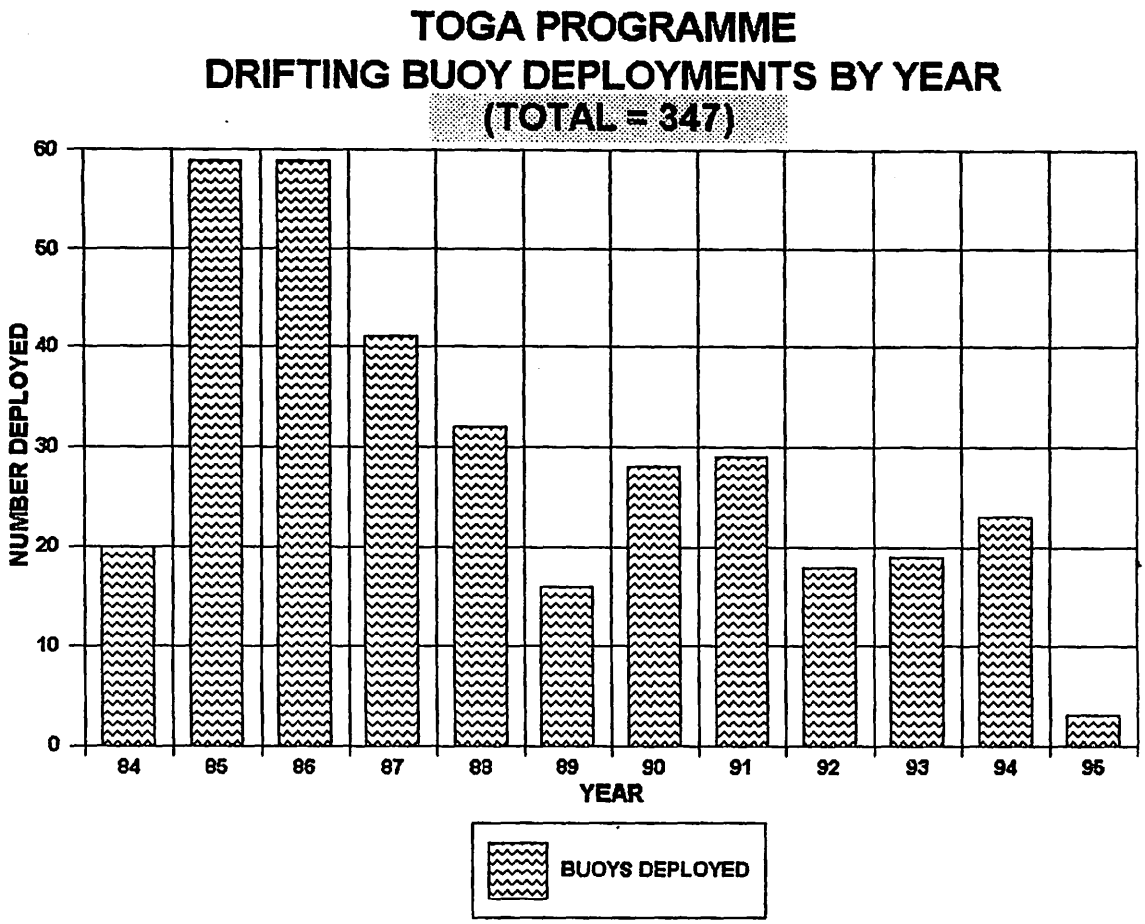

Figure 3. Buoys Deployed

Table 1. TOGA Drifting Buoys

		SENSOR MTTF* (DAYS)												
YEAR		84	85	86	87	88	89	90	91	92	93	94	95	AVG
NUMBER DEPLOYED		20	59	59	41	32	16	28	29	18	19	23	3	29
SENSOR	Tx	463	426	450	528	480	300	492	451	438	616	723	442	477
	P	463	414	427	528	480	300	491	426	423	616	719	442	468
	Ta	446	404	438	474	469	252	381	428	368	246	513	442	407
	To	449	409	440	484	459	285	472	421	376	575	609	442	447
	DROG	440	361	249										

*THROUGH 7/31/97

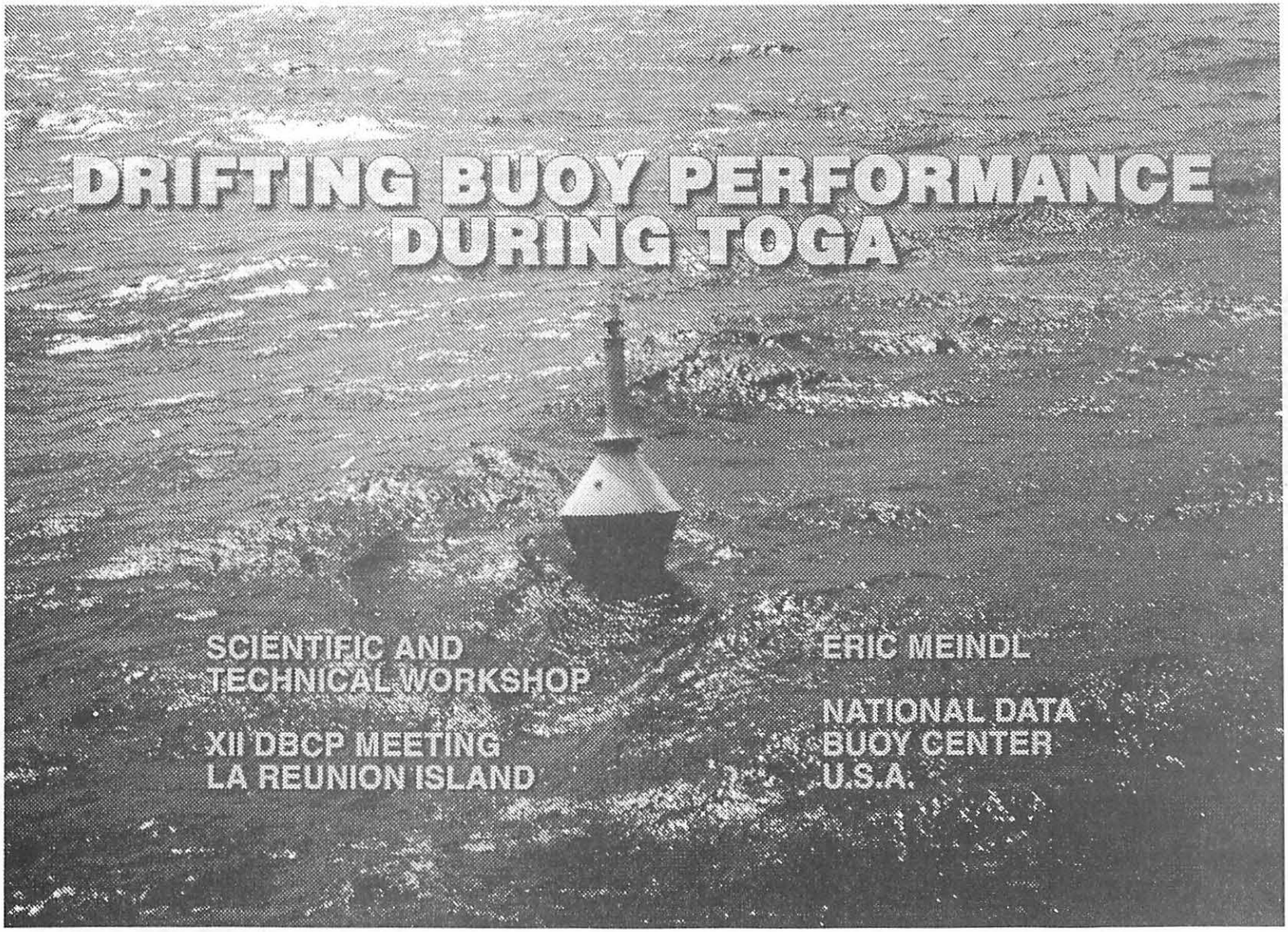
DRIFTING BUOY PERFORMANCE
DURING TOGA
SCIENTIFIC AND
TECHNICAL WORKSHOP
XII DBCP MEETING
LA REUNION ISLAND
ERIC MEINDL
NATIONAL DATA
BUOY CENTER
U.S.A.

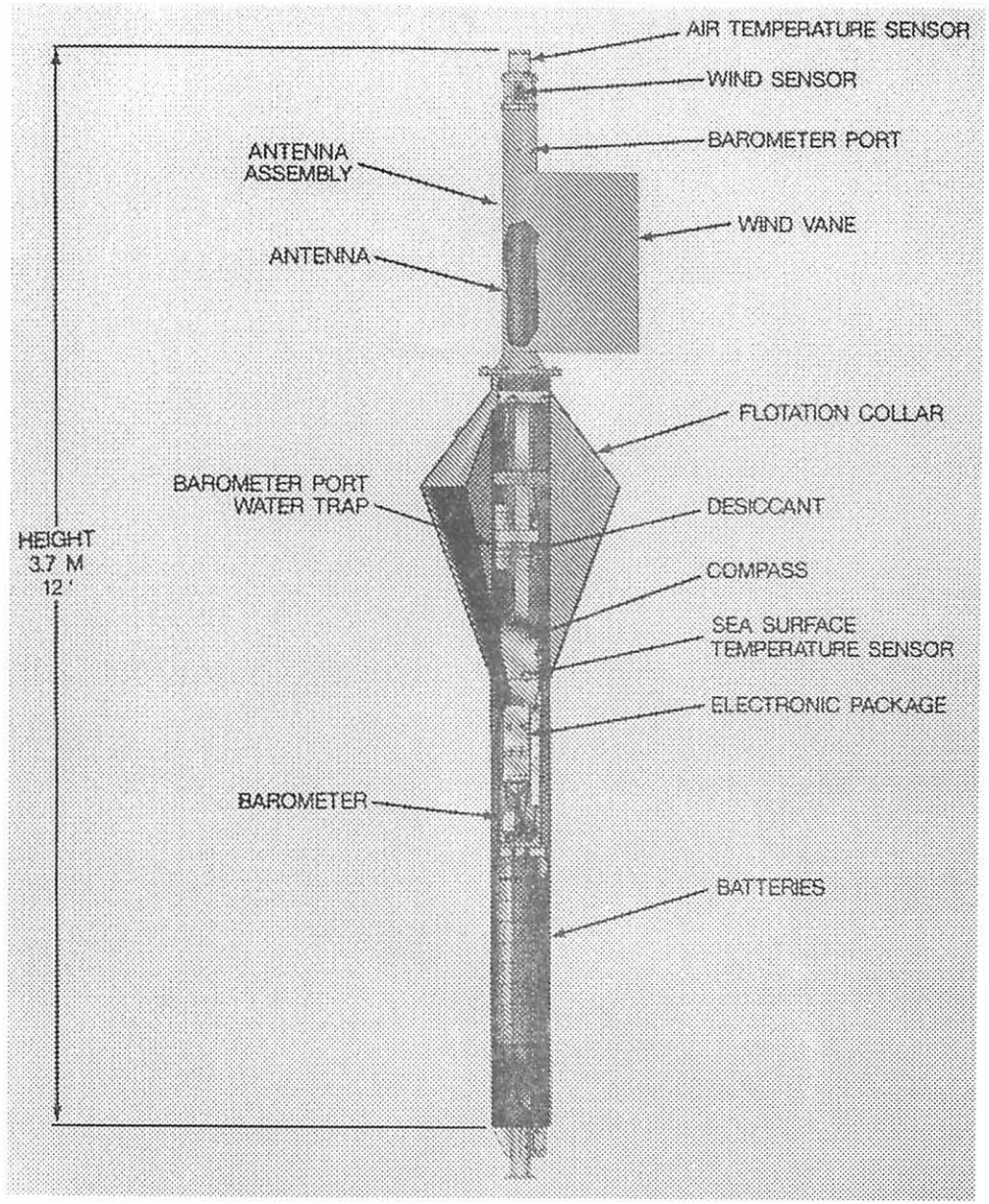
AIR TEMPERATURE SENSOR
WIND SENSOR
BAROMETER PORT
ANTENNA ASSEMBLY
WIND VANE
ANTENNA
FLOTATION COLLAR
BAROMETER PORT WATER TRAP
DESICCANT
HEIGHT 3.7 M 12'
COMPASS
SEA SURFACE TEMPERATURE SENSOR
ELECTRONIC PACKAGE
BAROMETER
BATTERIES

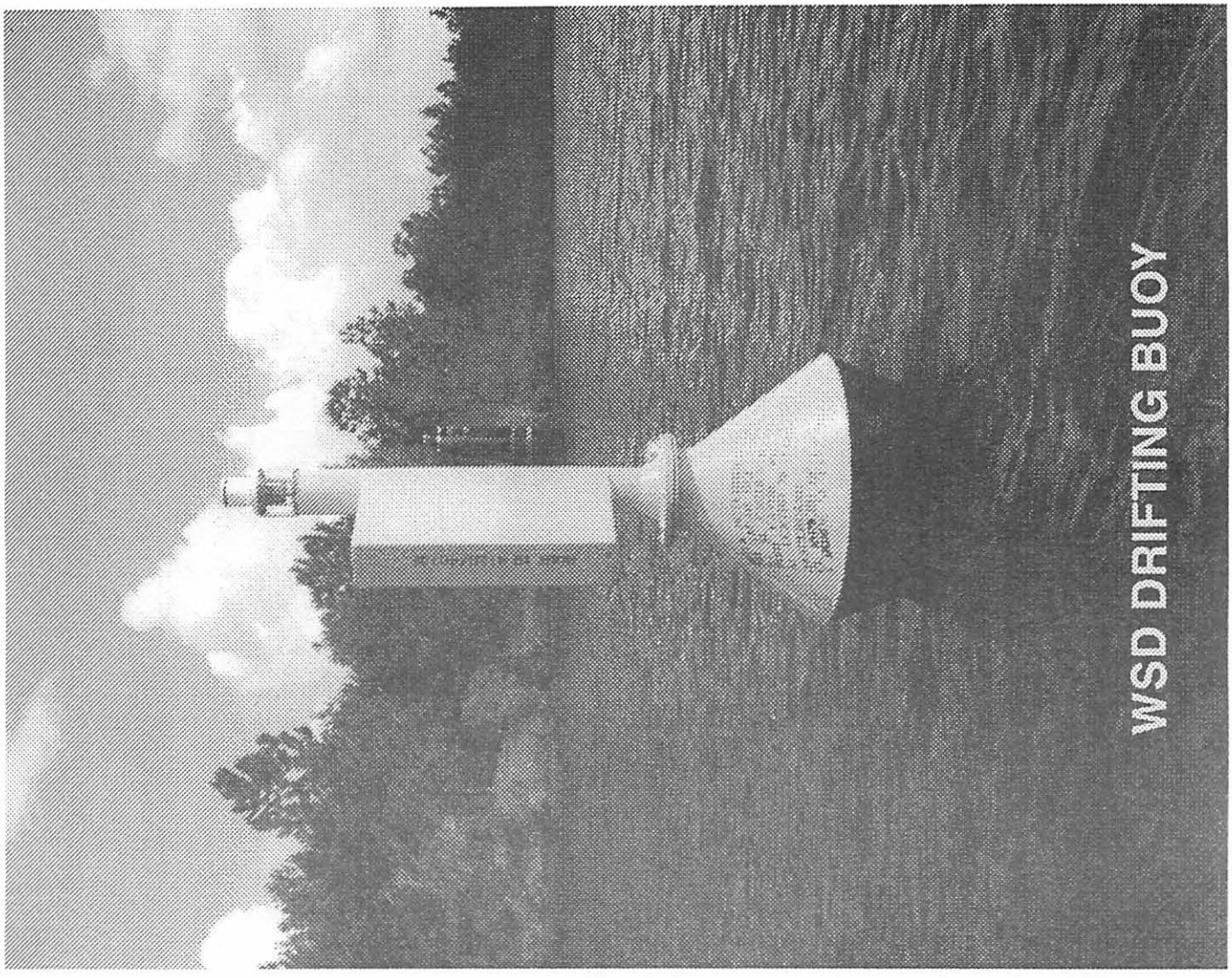
WSD DRIFTING BUOY

NDBC TOGA DRIFTING BUOY TRACKS 1988

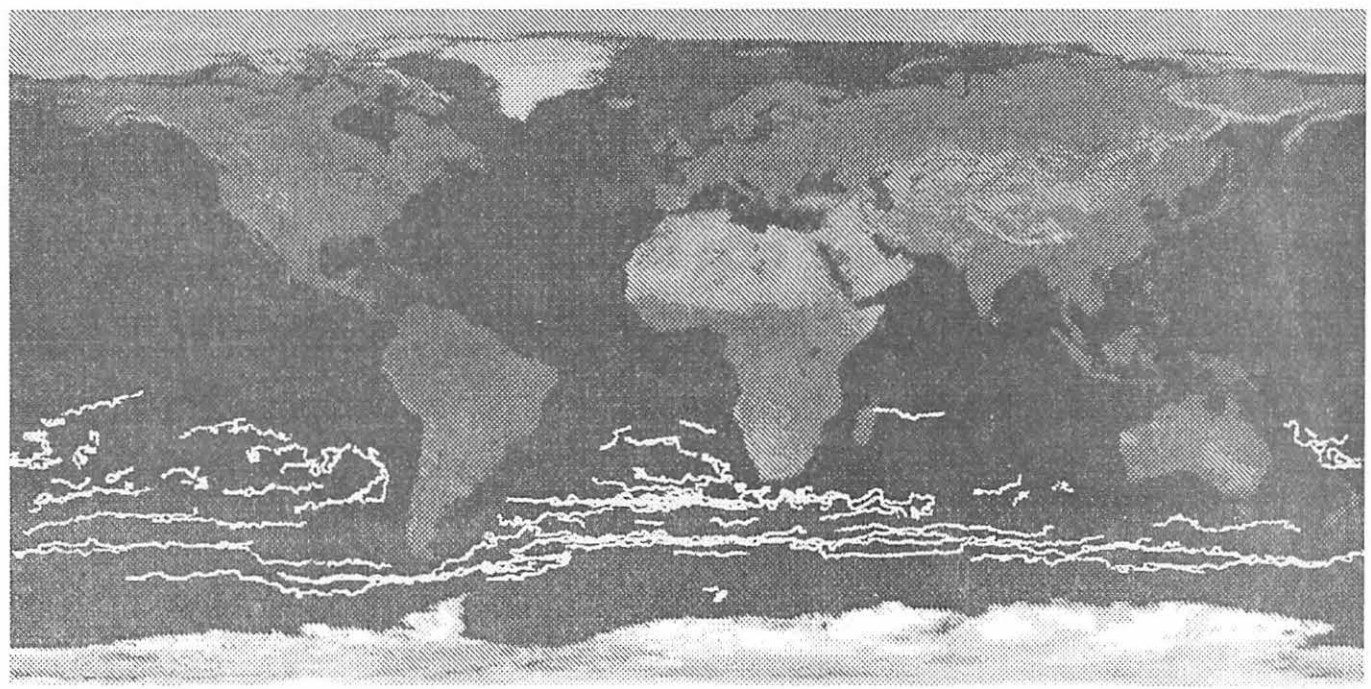

NDBC TOGA DRIFTING BUOY TRACKS 1994

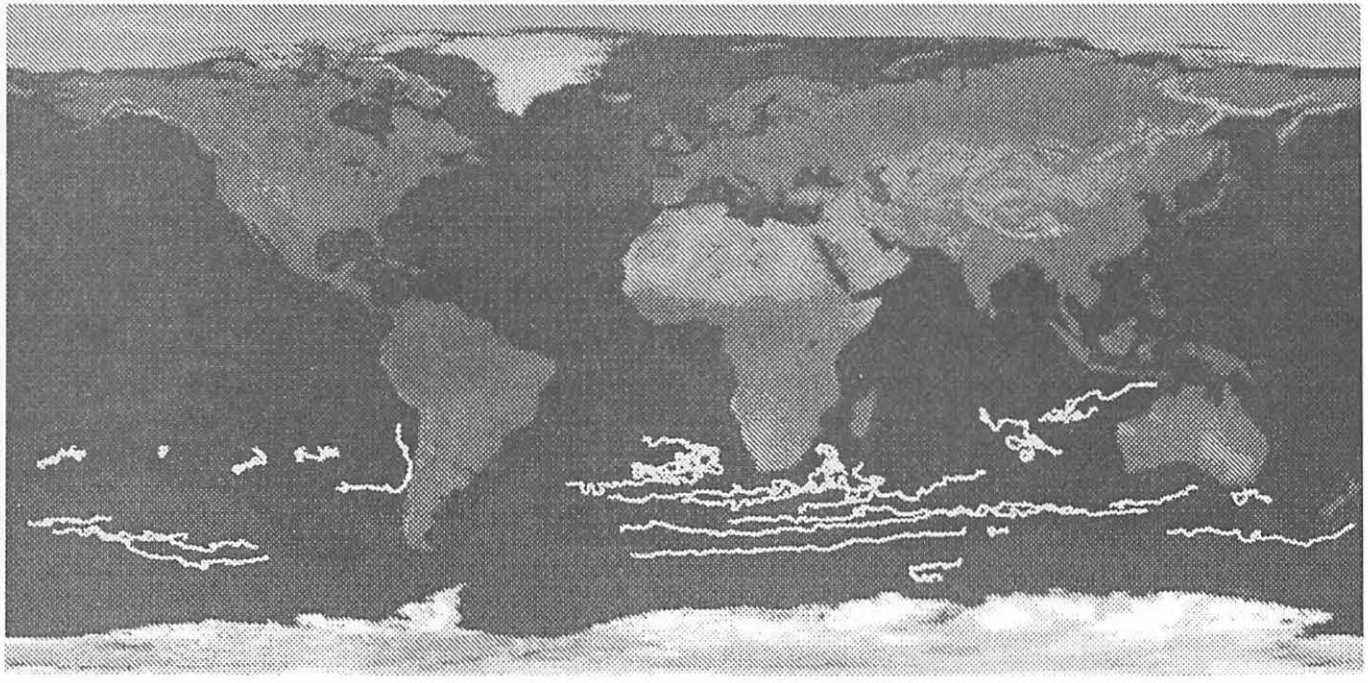

TOGA PROGRAMME
DRIFTING BUOY DEPLOYMENTS BY WMO AREA
(WMO AREA/NUMBER DEPLOYED)

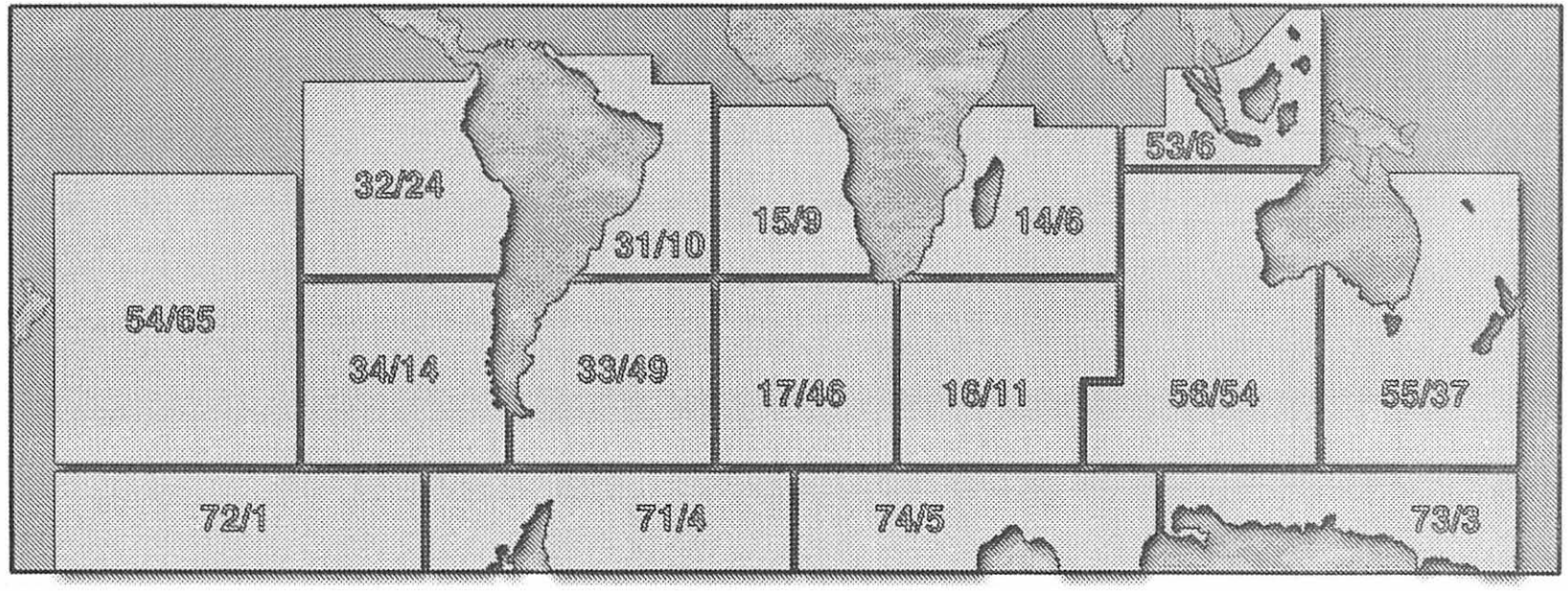

TOGA PROGRAMME
DRIFTING BUOY DEPLOYMENTS BY YEAR
(TOTAL = 347)

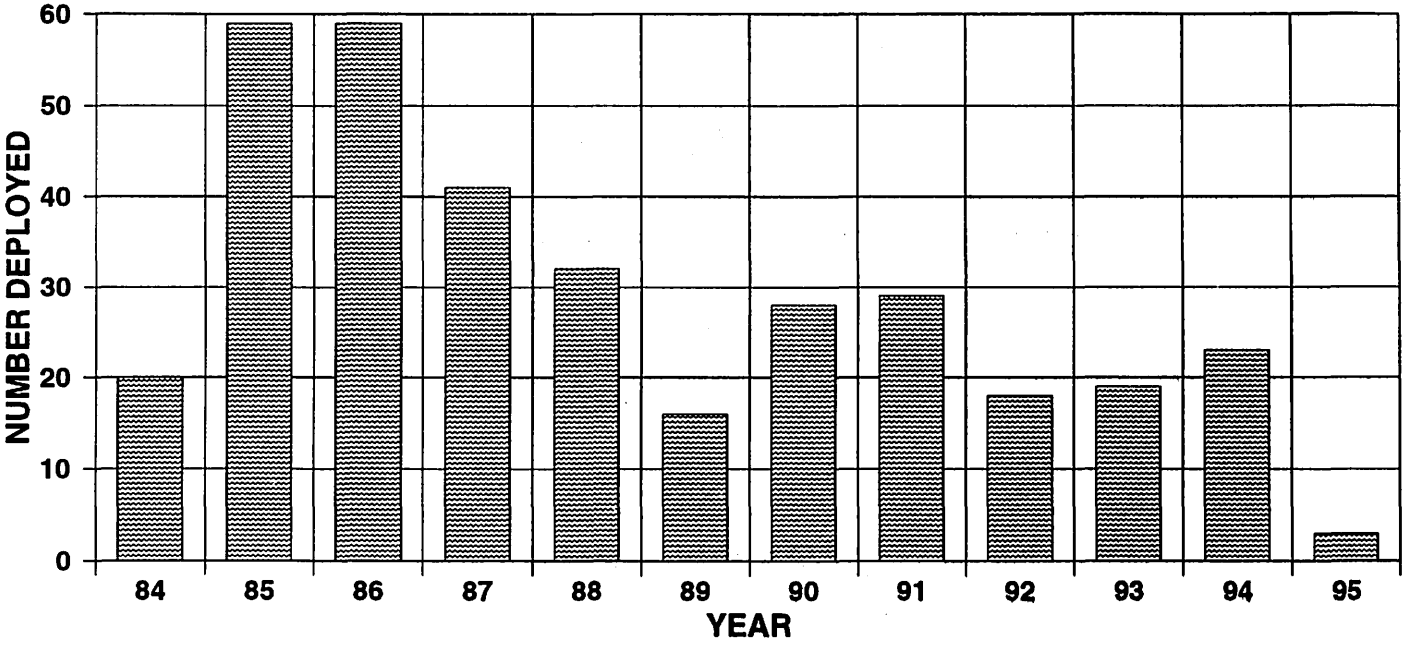

TOGA DRIFTING BUOYS
SENSOR MTTF* (DAYS)

YEAR		84	85	86	87	88	89	90	91	92	93	94	95	AVG
NUMBER DEPLOYED		20	59	59	41	32	16	28	29	18	19	23	3	29
SENSOR	Tx	463	426	450	528	480	300	492	451	438	616	723	442	477
	P	463	414	427	528	480	300	491	426	423	616	719	442	468
	Ta	446	404	438	474	469	252	381	428	368	246	513	442	407
	To	449	409	440	484	459	285	472	421	376	575	609	442	447
	DROG	440	361	249										

*THROUGH 7/31/97

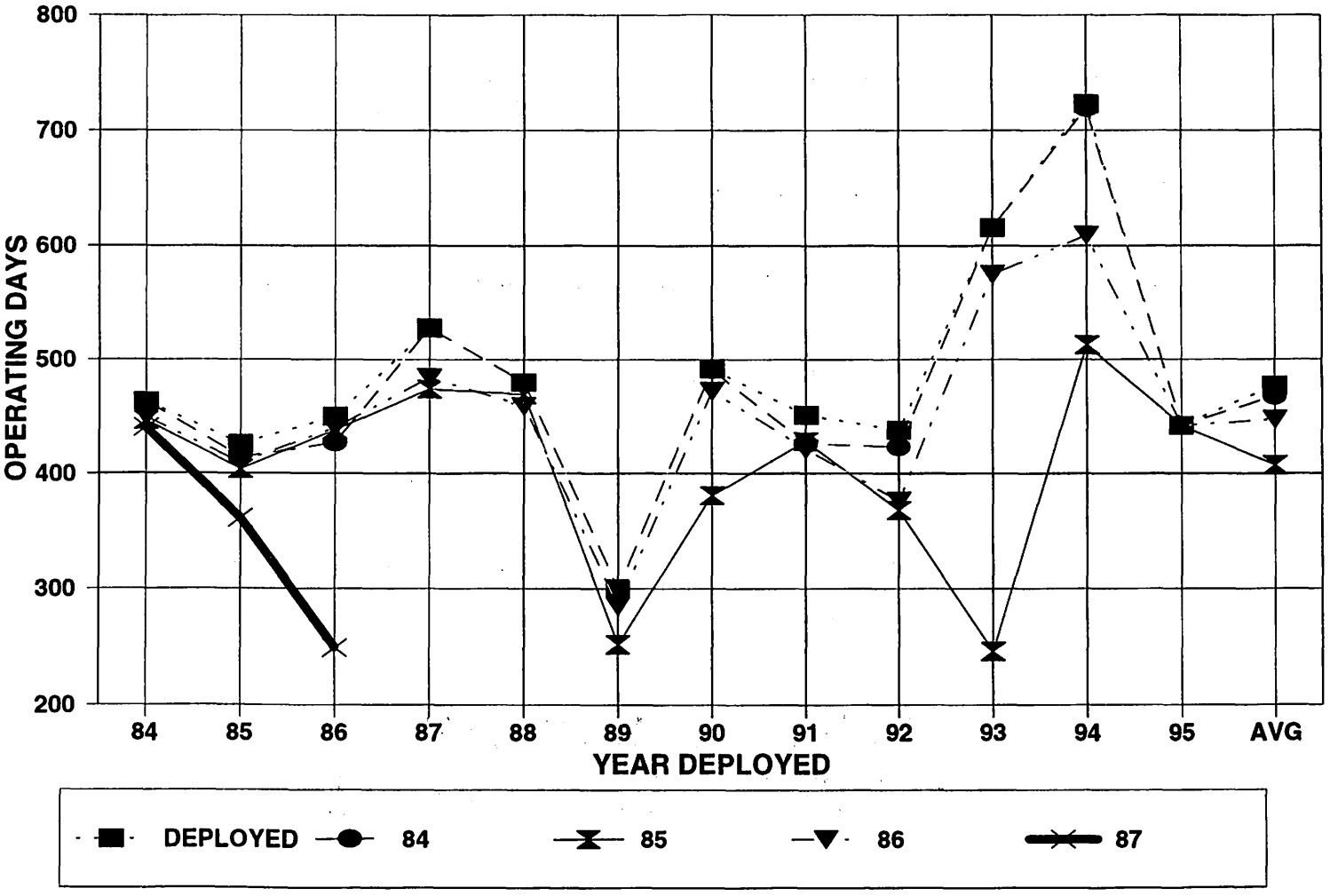

*THROUGH 7/31/97

TOGA DRIFTING BUOY PERFORMANCE
(347 BUOYS)

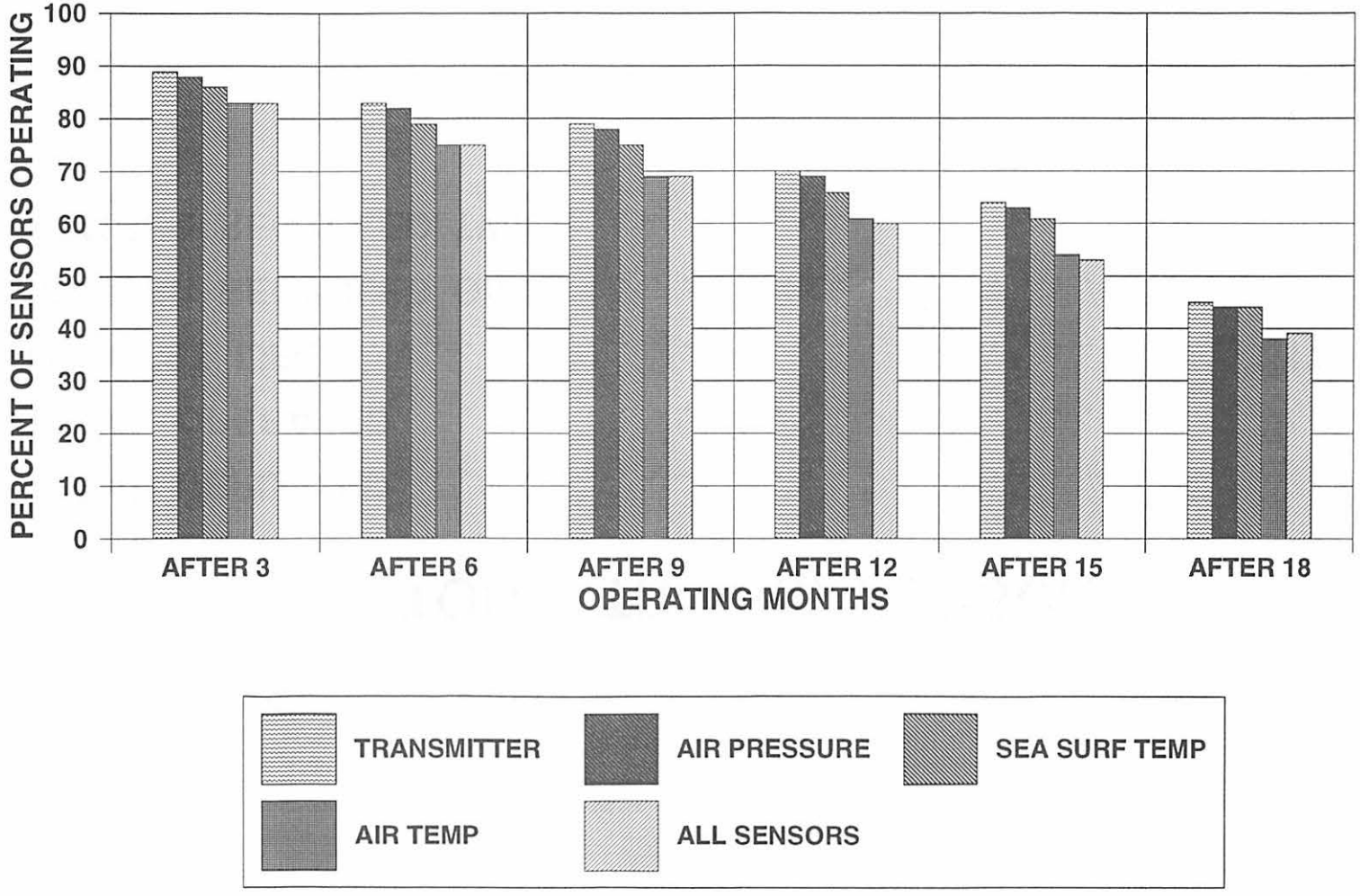

P29

TOGA TRIVIAL PURSUIT

TOTAL DEPLOYED	347
TOTAL OPERATED	337
LONGEST LIFE	1,171 DAYS
NUMBER RECYCLED ONCE	8
NUMBER RECYCLED TWICE	1

Evolution of the performances of air pressure measurement on the SVP-B drifter

Pierre Blouch & Jean Rolland
Centre de Météorologie Marine
Météo-France

December 1997

Abstract

The performances of air pressure measurement of almost the whole SVP-B drifters deployed in the World Ocean are continuously surveyed. The study, presented at the last DBCP Workshop was updated with inputs from more recent deployments. As foreseen last year, the number of buoys which fail quickly after their deployment increased significantly during the past months. Although this problem is probably not a specificity of the SVP-B drifters, it has an important consequence on their mean lifetimes. However there is a long delay between the manufacture of buoys and the results of their work. We hope the manufacturers took care to oppose the apparent falling quality of the drifters.

The study provides numerous tables and graphs on mean lifetimes and percentages of untimely ends according to different parameters such as manufacturer, mean of deployment and buoy characteristics.

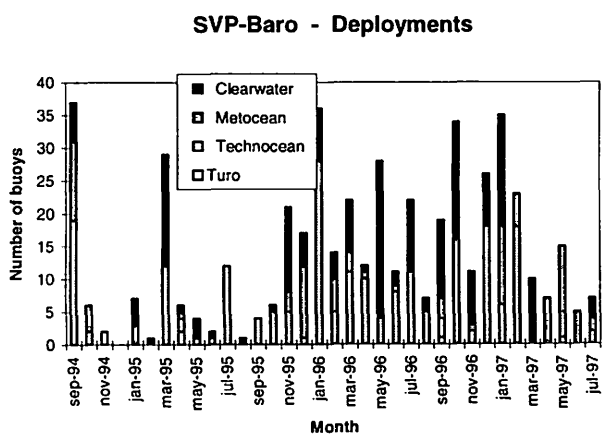

Figure 1 - SVP-Baro deployments from September 94 to July 97

About 450 SVP-B drifters from 4 different manufacturers were deployed over the world's oceans from September 1994 to July 1997 (figure 1). The quality of the barometric pressure values they report on the GTS[1] are continuously surveyed.

The method used to evaluate the performances, based on monthly statistics of differences with weather forecasting model outputs, was described last year by P. Blouch [1]. To determine the dates of air pressure measurement failures, the statistics provided by ECMWF[2] are used exclusively. The criteria to detect failures are: gross errors greater than 5% or bias greater than 5 hPa or standard deviation greater than 3 hPa.

Mean air pressure lifetimes

Figure 2 shows the Air Pressure (AP) measurement lifetimes for the 355 drifters deployed before March 1st, 1997 (sorted by decreasing lifetime) and which failed before October 1st, 1997. The mean lifetime is 165 days (instead of 168 computed last year on 165 drifters deployed before May 1st, 1996).

---

1 GTS : Global Telecommunication System of WMO (World Meteorological Organisation).
2 ECMWF : European Centre for Medium-range Weather Forecasts.

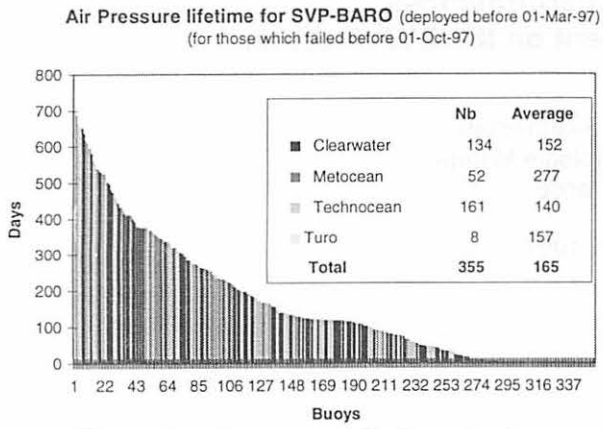

Figure 2 - Air pressure lifetimes for buoys which ceased to work before Oct. 97

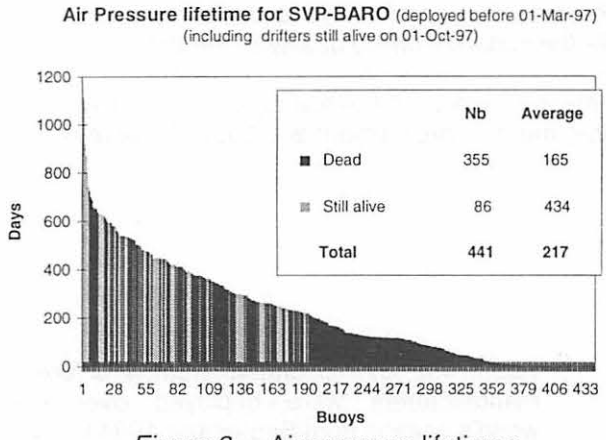

Figure 3 - Air pressure lifetimes according to buoy status in Oct. 97

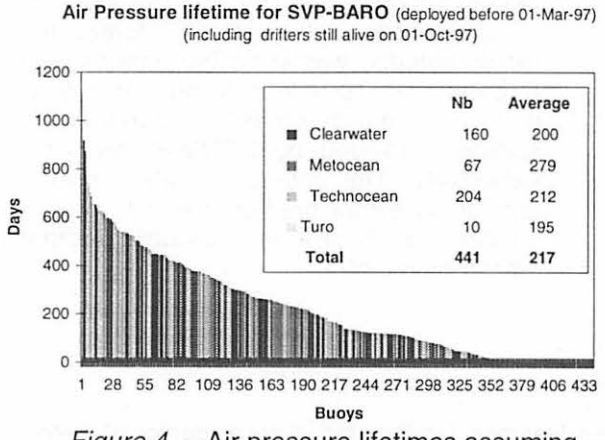

Figure 4 - Air pressure lifetimes assuming buoys still alive died on 1st Oct. 97

Figures 3 and 4 show the AP measurement lifetimes for the 441 drifters deployed before March 1st, 1997 including those still operating on October 1st, 1997. **The mean lifetime is 217 days** that is more than the value obtained with buoys which failed. This is due to some buoys deployed a long time ago which were still alive the 1st of October. A couple of buoys, built by Technocean, continued to provide reliable AP values in the southern seas, more than 3 years after their deployment !! This proves the concept is good. SVP-B drifters can have similar mean lifetimes than standard FGGE[3] buoys on condition they are conscientiously built.

Actually the performances of SVP-B drifters vary from a manufacturer to another and from a series to another. For instance, although the first drifters, built by Metocean Data System for the SAWB[4], had very good results, the following, purchased by Météo-France and the UKMO[5], failed rapidly in average. It seems the problems were corrected on the new series.

Theoretical buoy lifetimes

Of course, the theoretical lifetime of SVP-B drifters is related to various parameters such as:

- the length of the message Argos ;
- the acquisition scheme (duration and occurrence of measurements) ;
- the power energy and
- the duty cycle (full time or one third of the time).

Table 1 on the following page shows the theoretical lifetime of Metocean drifters equipped with 84 Ah batteries. We can see the lifetime is more related to the Argos message length than the occurrence of measurements.

Odd short lifetimes

During the 12 last months, several drifters built by Clearwater and Technocean stopped transmitting after 120 days only at sea. At least 50 drifters were concerned by this problem. Among the different possible causes, a programming error in the transmitters could explain this anomaly.

---

3 FGGE : First Global GARP (Global Atmosphere Research Programme) Experiment.
4 SAWB : South African Weather Bureau.
5 UKMO : United Kingdom Meteorological Office.

Argos mess length in bits	One obs. every hour	One obs. every 15 min.
64	514	425
96	462	388
128	419	358
224	328	290
256	306	272

Table 1 - Theoretical lifetime (in days) for Metocean SVP-B drifters with 84 Ah batteries.

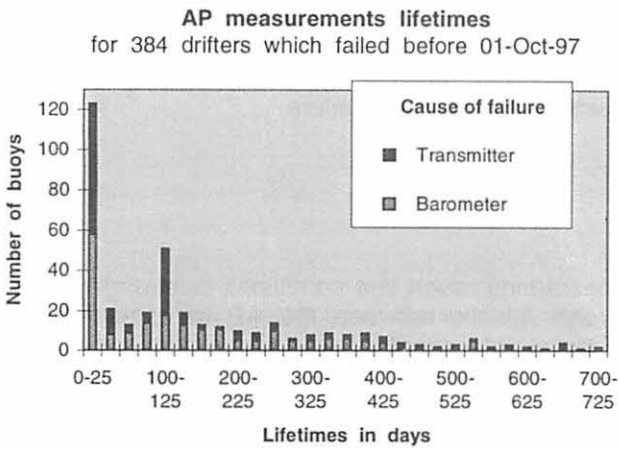

Figure 5 - Histogram of Air pressure measurement lifetimes

Although our study doesn't take in account the whole drifters affected by this problem - some of them were deployed after the 1st of March 1997 - we can see a step at approximately 120 days on figures 2, 3 and 4.

Figure 5 shows the lifetime histogram for 384 drifters which stopped to report reliable AP values before the 1st of October 1997 according to two causes: «transmitter» and «barometer». In the transmitter failure class, it's difficult to share the buoys which normally stopped transmitting after emptying their batteries from the rare buoys which were recovered or beached or those of which the transmitter failed. However, an abnormal peak at 100-125 days appears on the graph in addition to the peak observed at 0-25 days.

The «barometer» failure class contains the «AP measurement» failures indeed. Although it is difficult to detect what exactly the cause of failure for AP measurements are, it is assumed the most frequent failures comes from the system (port, pipe...) than from the barometer itself.

Quick failures

As shown in table 2, the percentage of buoys which fail quickly after their deployment is abnormally increasing. Around 10-15 % in 1995, it was nearing 25-30 % in 1997. This should have an effect on lifetime statistics in the next months. It is foreseen the mean lifetime will decrease when buoys recently deployed will be took in account. During the period Oct-96/Feb-97, one third of the buoys failed less than 20 days after their deployment.

The percentage of quick failures is a little higher for air deployments but the difference with ship deployments is not significant (excepted during the period Mar-97/Jul-97).

	All buoys			Deployed by Air		
	Deployed	< 20 days	Percentage	Deployed	<20 days	Percentage
Sep 94 - Jan 95	52	7	13 %	19	4	21 %
Feb 95 - Jun 95	41	4	10 %	19	2	11 %
Jul 95 - Nov 95	44	3	7 %			
Dec 95 - Apr 96	99	16	16 %	23	8	35 %
May 96 - Sep 96	86	22	26 %	40	9	23 %
Oct 96 - Feb 97	117	38	33 %	28	6	21 %
Mar 97 - Jul 97	40	9	23 %	13	7	54 %
Total	482	98	20 %	142	36	25 %

Table 2 - Percentage of drifters for which AP measurements failed quickly - historical record according to deployment type

Table 3 presents the same figures shared by manufacturers. Although the main cause of quick failure seems to be the «transmitter» for Technocean, it seems the «barometer» for Clearwater. The use of transmitter emitting with too low power, and/or antenna having a bad ground plan, can explain «transmitter» failures. At sea, the conditions to emit are worse than ashore.

		Total		Transmitter		Barometer	
Manufacturer	**Nb deploy.**	**<20 days**	**Percent.**	**<20 days**	**Percent.**	**<20 days**	**Percent.**
Clearwater	170	37	22 %	13	8 %	24	14 %
Metocean	91	8	9 %	6	7 %	2	2 %
Technocean	210	52	25 %	34	16 %	18	9 %
Turo	11	1	9 %	0		1	
Total	482	98	20 %	53	11 %	45	9 %

Table 3 - Percentage of drifters for which AP measurements failed quickly according to manufacturer and cause of failure

Quality of AP measurements

No particular study was carried out on the performances during rough sea conditions or strong wind. Statistically, there is no significant differences in North Atlantic between the AP measurements provided by SVP drifters and those provided by FGGE buoys (Marisondes or Metocean): the standard deviations of differences between observations and model outputs is comparable as shown on table 4.

Area	Owner	Buoy type	Manufact.	Format	Numb.	Jan-97	Feb-97	Mar-97	Apr-97
54°N	UKMO	FGGE	Metocean	EGOS	4	1.8	2.5	1.7	1.1
44°-50°N	UKMO	FGGE	Metocean	EGOS	3	1.6	2.4	1.3	0.9
44°-50°N	UKMO	SVP-B	Metocean	SAWB	1	1.0	2.6	1.9	1.1
44°-50°N	UKMO	SVP-B	Metocean	EGOS	2	1.6	2.5	2.0	1.3
44°-50°N	Météo-France	SVP-B	Metocean	Old GDC	4	1.5	2.6	2.1	1.2

Table 5 - RMS differences in hPa between observations and background field from UKMO model, gross errors were excluded

Conclusion

Although the quality of AP measurement on SVP-B drifters is similar to this of FGGE buoys, lifetimes are fewer. This is mainly due to a high percentage of buoys which fail quickly for various reasons. It is unacceptable to note this percentage increased during the past months. We couldn't help thinking the first series had better results than the following because the manufacture and the deployments were done with more caution than later.

Although these difficulties, Météo-France continues to rely on these drifters and on its next generation equipped to measure the wind speed and wind direction. The results obtained with the first series of this new drifter are full of promises.

Reference

[1] Blouch P., 1997: The quality control of buoy data transmitted on the GTS and its use in evaluating the SVP-B drifter, Developments in buoy and communication technologies, *Data Buoy Co-operation Panel Technical Document*, **10**, 17-22.

UPDATE ON THE KIWI BUOY RECYCLING BUSINESS

By: Julie Fletcher Marine Meteorological Officer and
John Burman Calibration Engineer
Meteorological Service of New Zealand Limited

Date: 1 September 1997

Abstract:
MetService New Zealand continues to deploy standard FGGE/TOGA style Drifting Buoys with very good results. A rigorous pre-deployment testing programme and the ability to verify sensor performance on recovered buoys lies behind the success of this operation. This paper will look at the lifetimes achieved by NZ buoys and will examine pre and post deployment sensor calibrations.

Buoy Network

MetService maintains an operational network of seven Meteorological Drifting Buoys in the Tasman Sea to provide real-time weather data for its forecasting activities. All buoys have been of the FGGE/TOGA design and since 1988 buoys have been manufactured by DSI/CTA Space Systems. The last procurement of buoys was for basic buoys with air pressure, sea and air temperature sensors only, but previously WSD buoys have been purchased. All buoys use the Paroscientific Barometer and are drogued with a 100 metre, weighted line.

Recovery and Redeployment Programme

All MetService Drifting Buoys are deployed in the Tasman Sea. The prevailing westerly and south-westerly currents carry the buoys from their deployment positions back towards New Zealand allowing approximately 80% of all buoys to be recovered. The positions of all operational buoys are monitored and attempts are made to recover them when they are in close proximity to the coast. Buoys that are no longer active and whose positions are not known are sometimes recovered from beaches after reported sightings. MetService offers a reward incentive to encourage buoy finders to report beached buoys. All buoys are marked "reward may be payable" and have a collect phone number for buoy finders to call MetService. This has worked well and buoys have been recovered long after their battery life has finished. Where practicable buoys are recovered and returned to the MetService laboratory for examination and assessment for refurbishment. Particular attention is paid to any sensors which were flagged as defective during the buoy's operational life. Post recovery all sensors are calibrated and compared with pre-deployment calibrations to find out how the buoy has performed. Buoys are then refurbished for redeployment as required. Replacement of sensors is rarely required, but new battery packs, and new drogues are always fitted.

MSNZ Buoy Lifetimes

The recovery and refurbishment programme has been very successful. Since December 1988, MetService has recycled 20 Buoys through 39 deployments, while maintaining an operational network of 7 buoys. Of the five buoys operational at 1 September 1997, two buoys are on their first deployment, two are on their second deployment and one buoy is on its third deployment.

The high number of recoveries shortens individual buoy lifetimes. Thus in MetService's case it is more representative to look at cumulative lifetimes achieved by buoys over several deployments. Lifetime is counted until barometer failure, transmission failure or recovery. (See Figs 1 & 2) The Average Cumulative Lifetime of the 5 buoys operational at 1 September 1997 is 26.4 months. Buoy #6439 has achieved a cumulative lifetime of 80 months over three deployments.

Co-operative International Buoy Programmes
TOGA Buoy Lifetimes
Between 1985 and 1995 MetService tested and deployed 56 TOGA buoys for NDBC in the Southern Pacific Ocean. The last batch of ten TOGA buoys were deployed in the period July 1994 to February 1995. Nine of the ten buoys were manufactured by METOCEAN, these were the first buoys that MetService had worked on from this supplier. The remaining buoy was a DSI TOGA buoy that had first been deployed in February 1991 in the South Atlantic. The buoy had failed due to a positioning problem after one month. The buoy was recovered from the NZ coast in December 1993 and was refurbished for redeployment. All buoys were equipped with the Paroscientific barometer, and with the exception of one buoy, were deployed in the Southern Pacific Ocean. NDBC suggested that the remaining buoy (#20721) be deployed in the Tasman Sea so that its performance could be compared with nearby MetService buoys, and that it might possibly be recovered at a later date. The ten TOGA buoys produced very good results. The Average Lifetime achieved by the 10 buoys to 1 September 1997 is 25.8 months, this includes two buoys which are still operational. (see figs 3 & 4) Three of the ten buoys beached, shortening their operational lifetime. Buoy #20721 was recovered after 22 months, see details of its calibration later in this paper.

SVP-B Buoy Lifetimes
1996 was MetService's first involvement with the WOCE/SVP Programme. AOML sent 8 SVP-B buoys for deployment in Southern Pacific Ocean and these buoys were deployed in the period January to May 1996. The buoys had been manufactured by Technocean.
Predeployment testing identified a problem with the non-alignment of the breathing holes in the pressure port. Two buoys were returned to USA because their barometers were out of specification. Six buoys were deployed. The barometers failed within five months on four of the six buoys. The remaining two buoys are still operational. (see figs 5 & 6) All SVP-B buoys are on 1/3 duty cycle.

Recovered Buoys - Pre and Post Deployment Calibrations
Since 1 September 1995, MetService has recovered 7 buoys. The following notes describe the history of six of these buoys. The seventh buoy has only just been returned from Queensland, Australia and has not yet been examined.

CTA WSD #8584
Recovered 10 November 1995 at Bundaberg, Australia after 12 months, on its 2nd deployment, cumulative lifetime 21 months.
History
1st deployment - 25 September 1992. The buoy was still operational when recovered from 90 Mile Beach, NZ after nine months.
2nd deployment - 12 November 1994.
All sensors (except WS) operational until recovery
WS sensor output went to base data after eight months
Examination post recovery:
AP within 0.15 hPa of pre deploy calibration (see fig 7)
ST & AT within spec
WS pick-off coil had gone open circuit
WD calibration unchanged

Buoy suitable for refurbishment and redeployment

METOCEAN TOGA #20721
Recovered 10 May 1996 at French Pass, NZ after 22 months, on its 1st deployment.
History

This buoy was one of the first of a batch of TOGA buoys manufactured by METOCEAN. NDBC was keen to see how METOCEAN buoys performed and suggested that one buoy be deployed in the Tasman Sea so that its data could be compared with MSNZ buoys. It was also hoped that it might be recovered at a later date so its sensor performance could be examined.
After deployment on 26 July 1994 the AT sensor failed. The YSI thermistor was suspected.
Examination post recovery:
AP within 0.4 hPa of pre deploy calibration (see fig 8)
ST within spec
AT housing & sensor smashed off
AT failure due to early water ingress onto the temp PCB in the antenna. Water had capillaried down the AT sensor cable into the antenna. Although the YSI thermistor was not present, it had not caused the failure.

Redeployed February 1997, with a Gill AT sensor housing (RM Young). Buoy still operational.

CTA WSD #8583
Recovered 10 August 1996 at Te Kopuru, NZ after 16 months, on its 3rd deployment, cumulative lifetime 30 months.
History
1st deployment - 24 September 1992. Following deployment the onboard processor had a complete failure and transmitted only base data from all sensors. After two months the buoy was successfully recovered from the central Tasman Sea by a container ship.
2nd deployment - 24 December 1993. The buoy was recovered, still fully operational after thirteen months from the Bay of Plenty, NZ.
3rd deployment - 11 April 1995.
WSD output locked up 10 days after deployment
AP, ST & AT operational when recovered
Examination post recovery:
AP within 0.1 hPa of pre deploy calibration (see fig 9)
ST & AT within spec
WSD failure caused by eeprom failure on winds board

Suitable for refurbishment and redeployment.

CTA WSD #8586
Recovered 26 August 1996 at Raglan, NZ after 20 months, on its 2nd deployment, cumulative lifetime 34 months.
History
1st deployment - 26 September 1992. Buoy was fully operational until it struck the Great Barrier Reef, Australia, 14 months later. The base of the spar was ripped open exposing the battery pack. The buoy was recovered by a fisherman and delivered to the Bureau of Meteorology in Brisbane. The antenna and electronics rack were salvaged and returned to NZ. The PTT had been salt damaged, so was replaced, all other components were reused.
2nd deployment - 24 December 1994.
March 1996 - AT & WS output went to base values, WS was restored after one week.
Recovered by a fishing vessel using the Argos position supplied by MSNZ.
Examination post recovery:
AP within 0.15 hPa of pre deploy calibration (see fig 10)
ST & WD within spec
Pillar carrying AT cable had been severed, explaining the AT failure.
It is suspected that the broken pillar temporarily obstructed the anemometer rotor causing base value WS output for one week.

Redeployed October 1996. The WS output stuck on 26m/s after deployment. All other sensors are still operational.

CTA BASIC #22189
Recovered 30 November 1996 at Waitarere Beach, NZ after 10 months, on first deployment.
History
Deployed 25 January 1996. AP, ST, AT sensors all operational when recovered
Examination post recovery:
AP within 0.15 hPa of pre deploy calibration (see fig 11)
ST & AT within spec

Redeployed March 97
August 1997, all sensor outputs locked up, probably due to an onboard processor fault

CTA WSD #7176
Recovered 2 December 1996 from the sea approximately 400 miles north of NZ by GRV Tangaroa after 19 months, on 4th deployment. Cumulative Lifetime 47 months.
History
1st deployment - 28 July 1990. The buoy moved very rapidly in strong currents towards the NSW coast and became snagged in crayfish pots near Port Kembla. Despite being submerged for 4 days, the AP sensor was within 0.25 hPa when recovered.
2nd deployment - 29 March 1991. Buoy was still fully operational when recovered after 10 months from Stewart Island. New bearings were fitted to the anemometer rotor and a new heading sensor was fitted as examination found the old unit was not outputting any westerly headings.
3rd deployment - 18 January 1992. The WS and WD data was flagged on the BuoyQC board as being erratic in June 1992, and the sensors were removed from GTS. The buoy was reported ashore on Kadavu Island, Fiji in October 1994, and was recovered and sent back to NZ.
4th deployment - 9 May 1995.
WSD output locked up after 2 months
September 1995 ST rescaled +3.5 following BuoyQC board requests
ST returned to original calibration after 3 months following BuoyQC board requests
Examination post recovery:
AP within 0.15 hPa of pre deploy calibration (see fig 12)
ST & AT within spec
WSD failure caused by eeprom failure on winds board

Suitable for refurbishment and redeployment

Recovery Benefits
1. Cost Effective - Refurbishment produces a 'New' Buoy.
2. Data Verification - Post-recovery all sensors are calibrated and compared with pre-deployment calibrations. Special attention is paid to sensors 'flagged' defective during the buoy's operational life.
3. Product Improvement - Recovered buoys present the opportunity to examine component and sensor performance. This has revealed various faults and weaknesses and has led to modifications and improvements to Anemometer bearings, Drogue attachments and Power supply line reliability.

Cumulative Lifetimes MSNZ Buoys

ID	Deployment 1	Deployment 2	Deployment 3	Deployment 4	Cumulative Lifetimes	
6435	19	23			42	
6436	9				9	
6437	24	30			54	
6438	14				14	
6439	22	18	40		80	
7175	7	17			24	
7176	2	10	16	19	47	
7177	15	25			40	
7178	29				29	
7179	20	15	27		62	
8583	1	13	16		30	
8584	9	12			21	
8585	18	18			36	Operational
8586	14	20	11		45	Operational
8587	20				20	
22186	10				10	Operational
22187	12				12	
22189	10	5			15	
22190	12				12	Operational
20721	22	7			29	Operational

Buoy Lifetimes in months to 1 September 1997. Lifetime being until Barometer failure, Transmission failure, or Recovery.

Fig 1.

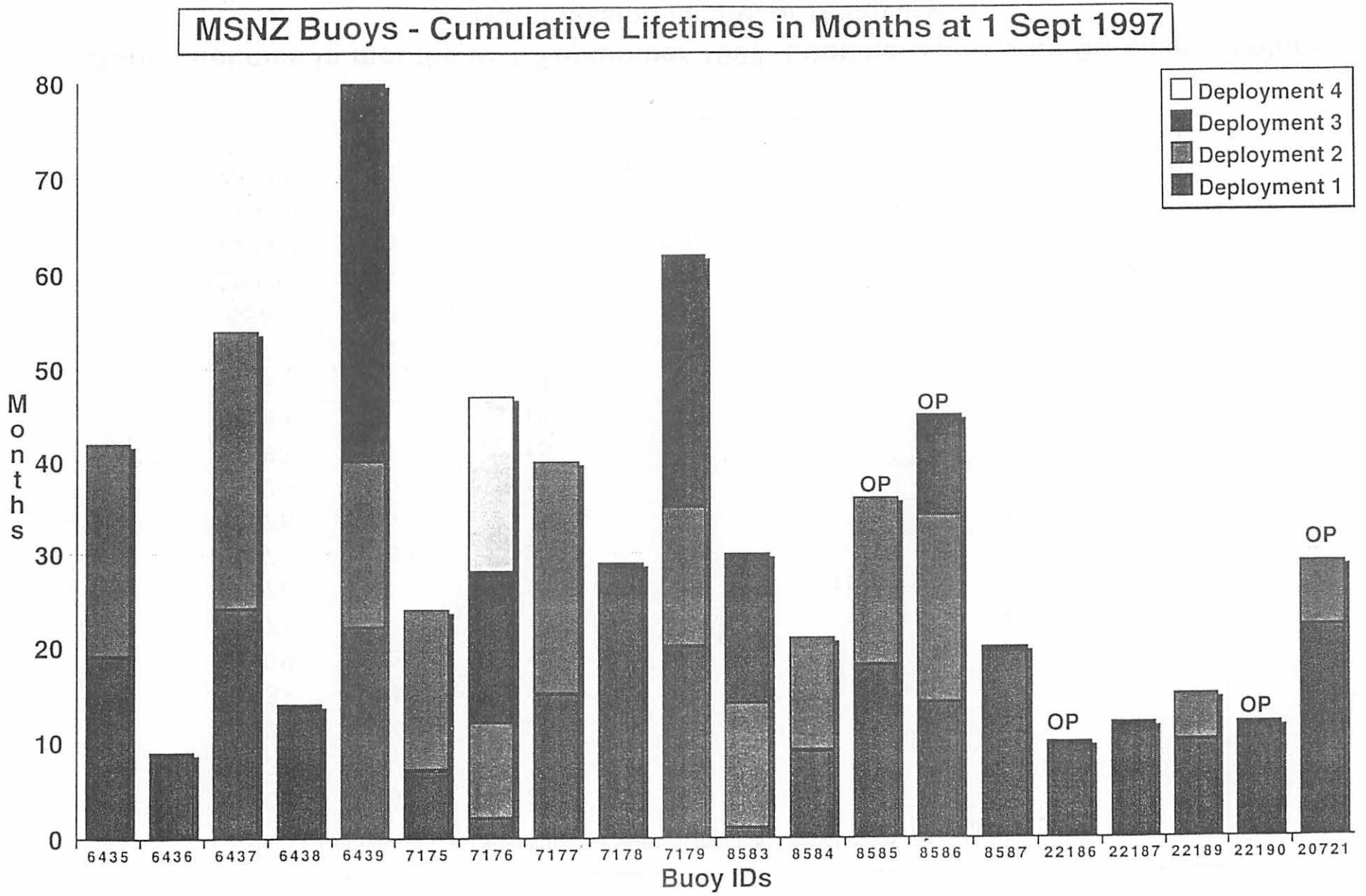
MSNZ Buoys - Cumulative Lifetimes in Months at 1 Sept 1997
Deployment 4
Deployment 3
Deployment 2
Deployment 1
Months
0
10
20
30
40
50
60
70
80
OP
OP
OP
OP
6435
6436
6437
6438
6439
7175
7176
7177
7178
7179
8583
8584
8585
8586
8587
22186
22187
22189
22190
20721
Buoy IDs

Fig 2.

Lifetimes of METOCEAN TOGA Buoys deployed by MSNZ July 1994 - Feb 1995

ID	Lifetime in Months	Reason For Failure
20721	22	Recovered on NZ coast, Redeployed
20718	23	Beached - Chile
20722	21	Transmission Finished
20719	32	Transmission Finished
17181	16	Beached - Fiji Islands
20713	32	Transmission Finished
20717	32	Transmission Finished
17162	12	Transmission Finished
17178	35	Operational
5127	33	Operational

Buoy Lifetimes in months to 1 September 1997. Lifetime being until Barometer failure, Transmission failure, or Beaching.

Fig 3.

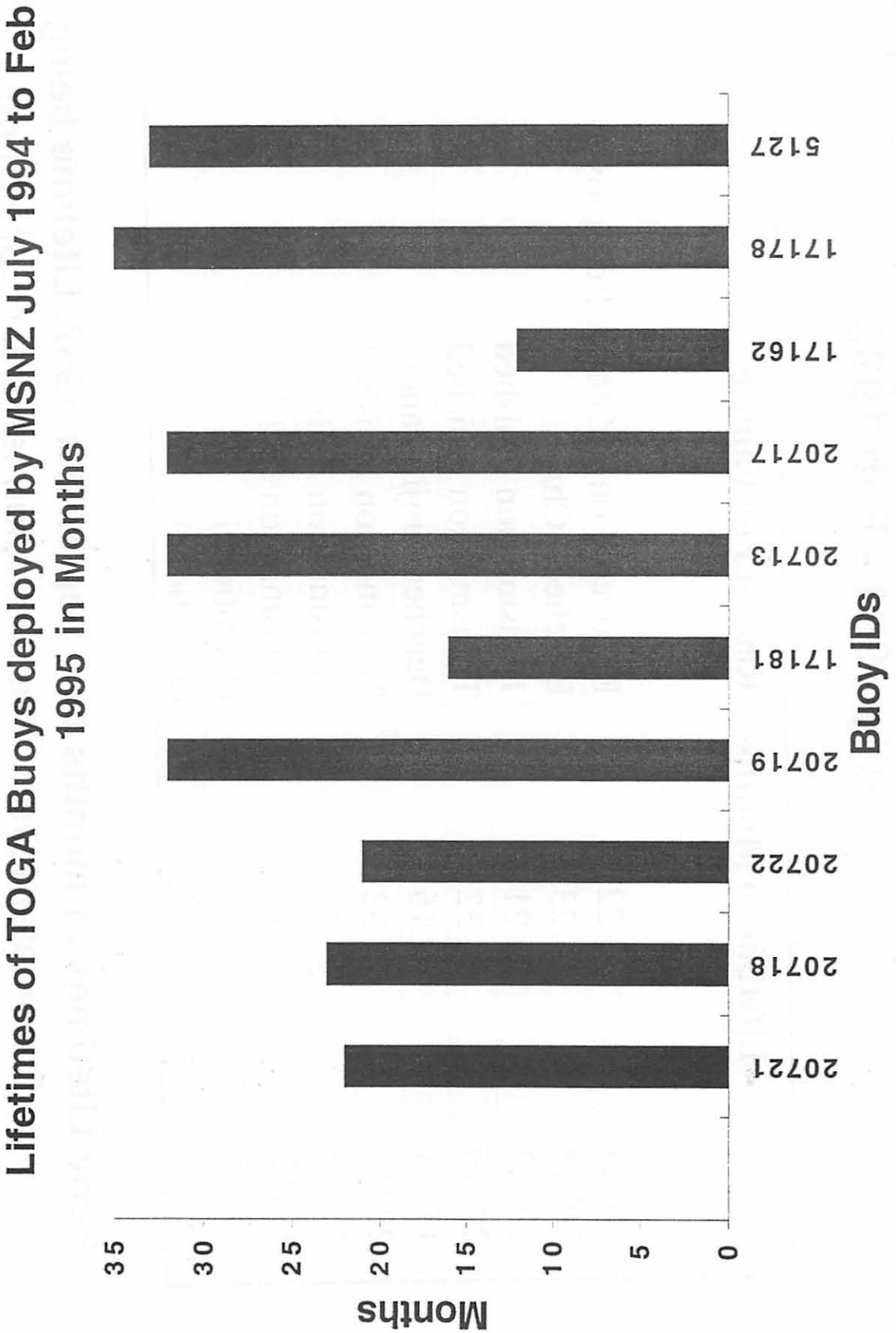
Lifetimes of TOGA Buoys deployed by MSNZ July 1994 to Feb 1995 in Months
Months
0
5
10
15
20
25
30
35
Buoy IDs
20721
20718
20722
20719
17181
20713
20717
17162
17178
5127

Fig 4.

Lifetimes of SVP-B Buoys deployed by MSNZ Jan 1996 - May 1996

ID	Lifetime in Months	Reason For Failure
25784	20	Operational
25786	5	Barometer Failure
25798	3	Barometer Failure
25800	4	Barometer Failure
25797	5	Barometer Failure
25785	15	Operational

Buoy Lifetimes in months to 1 September 1997. Lifetime being until Barometer failure, Transmission failure, or Beaching.

Fig 5.

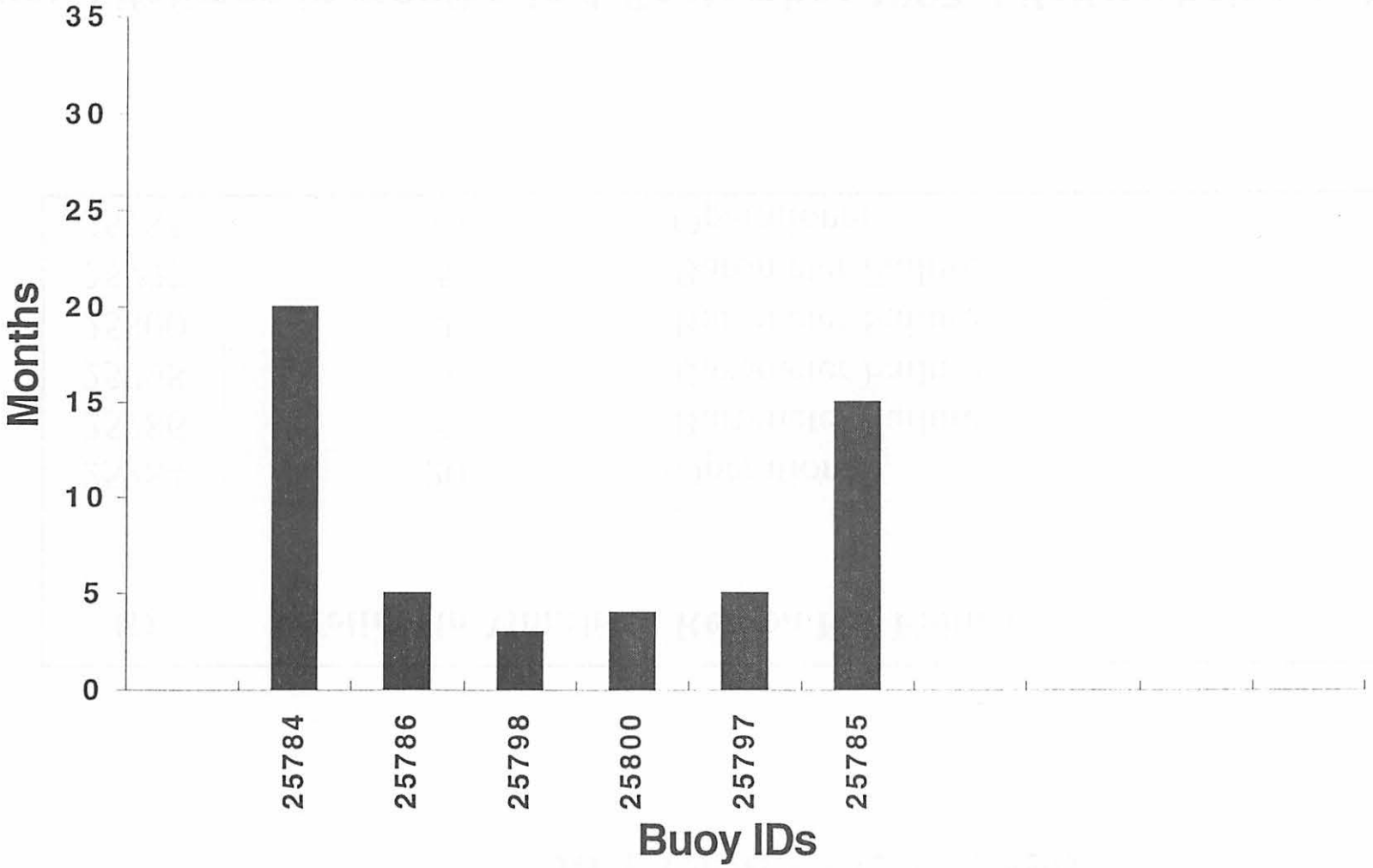
Lifetimes of SVP-B Buoys deployed by MSNZ
Jan - May 1996 in Months
Months
35
30
25
20
15
10
5
0
25784
25786
25798
25800
25797
25785
Buoy IDs

Fig 6.

CTA BUOY #8584

Calibration History for Paroscientific Barometer

Serial Number 35739

REF PRESS (hPa)	#1PRE DEPLOY CAL 11 SEP 92	POST RECOVERY CAL 3 MAR 94	#2PRE-DEPLOY CAL 19 OCT 94	POST RECOVERY CAL 27 AUG 97
1050.00	1050.15	1050.00	1050.00	
1040.00	1039.95	1040.10	1039.95	1039.95
1030.00	1030.05	1030.05	1030.05	
1020.00	1020.00	1020.15	1020.15	1020.15
1010.00	1010.25		1009.95	
1000.00	999.90	999.90	1000.05	999.90
990.00	990.00		990.00	
980.00	979.95	979.95	979.95	979.95
970.00	969.90		970.05	
960.00	960.00	960.00	960.00	
950.00	949.95		950.10	
940.00	939.90	940.05	940.05	939.90
930.00	930.00		930.00	
920.00	919.95	920.10	920.10	
910.00	909.90		910.05	
901.00	900.90		901.05	901.05

Fig. 7 1 Sept 97

METOCEAN BUOY #20721

Calibration History for Paroscientific Barometer

Serial Number 52506

REF PRESS (hPa)	#1 PRE - DEPLOY CAL 16 JUN 94	POST RECOVERY CAL 6 JUN 96	#2 PRE - DEPLOY CAL 14 JAN 97
1053.00	1053.40	1053.20	
1050.00	1050.40	1050.00	1050.20
1040.00	1040.40	1040.20	1040.20
1030.00	1030.20	1030.40	1030.40
1025.00	1025.20	1024.80	
1020.00		1020.20	1020.20
1010.00		1009.80	1009.80
1000.00	1000.20	1000.00	1000.00
990.00			990.00
980.00			980.20
975.00	975.20	975.00	
970.00			970.00
960.00			960.00
950.00	950.20	950.00	950.00
940.00			940.20
930.00			930.20
925.00	925.20	925.00	
920.00			920.20
910.00			910.20
900.00	900.00	900.20	900.20
875.00	875.20	875.20	
850.00	850.20		

Fig 8 1 Sept 97

CTA BUOY #8583

Calibration History for Paroscientific Barometer

Serial Number 35726

REF PRESS (hPa)	#1PRE DEPLOY CAL 9 SEP 92	#2PRE DEPLOY CAL 13 DEC 93	#3PRE-DEPLOY CAL 24 MAR 95	POST RECOVERY CAL 27 AUG 96
1050.00	1050.00	1050.15	1050.00	1050.00
1040.00	1040.10	1040.1	1040.10	
1030.00	1029.90		1030.05	
1020.00	1020.00	1020.00	1020.00	
1025.00				1024.95
1010.00	1010.10		1009.95	
1000.00	1000.05	1000.05	1000.00	999.90
990.00	990.00		990.00	
980.00	980.10	980.10	980.10	
970.00	970.05		970.05	
960.00	960.15	960.15	960.00	
950.00	950.10		949.95	949.95
940.00	940.05	940.05	940.05	
930.00	930.00		930.00	
920.00	919.95	920.10	920.10	
910.00	910.05		910.05	
901.00	901.05		901.05	901.05
900.00		900.15		

CTA BUOY #8586

Calibration History for Paroscientific Barometer

Serial Number 49099

REF PRESS (hPa)	#1 PRE - DEPLOY CAL 14 SEP 92	#2 PRE - DEPLOY CAL 12 DEC 94	#3 PRE - DEPLOY CAL 17 SEP 96
1050.00	1050.00	1050.00	1049.85
1040.00	1039.95	1039.95	1039.95
1030.00	1030.05	1030.05	1029.90
1020.00	1020.00	1020.00	1019.85
1010.00	1010.10	1009.95	1009.95
1000.00	1000.05	1000.05	999.90
990.00	989.85	990.00	989.85
980.00	979.95	979.95	979.95
970.00	969.90	969.90	969.90
960.00	960.00	960.00	959.85
950.00	949.95	950.10	949.95
940.00	940.05	940.05	939.90
930.00	930.00	930.00	929.85
920.00	919.95	919.95	919.95
910.00	910.05	910.05	909.90
901.00	901.05	901.05	900.90

Fig 10 1 Sept 97

CTA BUOY #22189

Calibration History for Paroscientific Barometer

Serial Number 53788

REF PRESS (hPa)	#1 PRE - DEPLOY CAL 09 JAN 96	#2 PRE - DEPLOY CAL 17 FEB 97
1050.00	1050.00	1049.85
1040.00	1039.95	1039.95
1030.00	1029.90	1029.90
1020.00	1020.00	1020.00
1010.00	1009.95	1009.95
1000.00	999.90	999.90
990.00	990.00	990.00
980.00	979.95	979.95
970.00	970.05	969.90
960.00	960.00	959.85
950.00	949.95	949.95
940.00	939.90	939.90
930.00	930.00	929.85
920.00	919.95	919.95
910.00	909.90	909.90
901.00	901.05	900.90

Fig 11 1 Sept 97

CTA BUOY #7176

Calibration History for Paroscientific Barometer

Serial Number 38903

REF PRESS (hPa)	#2 PRE DEPLOY CAL 21 MAR 91	#3 PRE DEPLOY FIELD CAL 15 JAN 92	#4 PRE-DEPLOY CAL 3 APR 95	POST RECOVERY CAL 27 AUG 97
1050.00			1050.30	
1040.00	1040.10	1039.95	1040.25	1040.10
1030.00			1030.20	
1020.00		1020.15	1020.30	1020.15
1010.00	1010.10		1010.25	
1000.00	1000.20	1000.20	1000.20	1000.05
990.00			990.30	
980.00	980.10	980.10	980.25	980.10
960.00			960.30	
950.00	950.10	950.10	950.20	
940.00			940.20	940.20
920.00	920.10	920.10	920.25	
910.00			910.35	
901.00			901.50	901.20

PRE 1ST DEPLOYMENT CAL 11 JUL 90 REF PRESS 1014.63 BUOY 1014.75

POST RECOVERY CAL 24 OCT 90 REF PRESS 1027.55 BUOY 1027.50

Fig 12 1 Sept 97

METHOD OF CALCULATION OF CHARACTERISTICS OF DIVING DRIFTERS WITH SATELLITE COMMUNICATION FOR THE STUDY OF THE ACTIVE LAYER OF OCEANS AND SEAS

By Dr. S. V. Motyzhev
Marine Hydrophysical Institute
Of National Ukrainian Academy of Sciences

Introduction

Drifting buoys with satellite communication or drifters are today the most representative part of the satellite contact monitoring of the World ocean. They deliver the main part of information about variability of surface currents and temperature. The successful use of this class of the buoys has led to the problem of extension of their measuring capabilities, first of all, for the operative prognosis of variability of the weather. The new generation of the SVP-B drifters equipped with the atmospheric pressure sensor on the sea level was elaborated with this purpose [1]. Since 1995 the use of this class of the buoys completely predominates above all the other.

However, the measuring possibilities of the SVP-B drifting buoys are limited by the surface layer of water and near surface layer of the atmosphere. At the same time there is an interest to study hydrophysical and hydrochemical characteristics of water within the active layer from the space, first of all, for the purposes of ecology and fishery. The possible drifter technologies for the solution of this problems were proposed on the annual session of DBCP in 1995 [2].

The underwater buoys which are capable to move vertically and horizontally in the water layer are in the basis of the suggested engineering solution. The general feature of these buoys is that they use satellite communication channel for transfer of data. Depending on the method of the buoyancy control such buoys can be used for solution of various problems.

As any autonomous instrument, the diving drifters have a number of limitations which reduce their life-time and area of their application. Therefore it is obviously important to create such a method of calculation of the measuring characteristics of diving drifters, which would allow the optimum way to use their capabilities.

An attempt to create such method is made in the present article. With this purpose the analysis of measuring capabilities of a diving drifter is presented; the diving drifter is used here as a thermoprofilograf; with taking into consideration the limitation, which are put on such a system by the volume passage capability of the satellite communication channel, capacity of power batteries, depth of diving and number of diving cycles.

The accepted limitations on purpose and volume of transfer are not an axiom. This method can be used for the analysis of characteristics of diving drifters when they are used for the study of salinity, speed of the sound, optical density and other characteristics of water. The important detail of this analysis is that the results of measurements should be comparable to the results of measurements by other methods. The structure of the system and its main characteristics are clear from the Fig.1. The technical characteristics of the satellite communication system ARGOS are used for the analysis.

Areas of application of the drifting thermoprofilograf

The depth of diving up to 150 m is of interest, when the measurements cover the upper mixed layer (UML), whole or top layer of the seasonal thermos profile of main regions of the World ocean, cold intermediate layer (CIL) and partial (where the high bound of a hydrogen sulphide zone is located higher then 150 m) of the oxygen zone in the Black sea. Alongside with other means of data acquisition (ship thermoprofilograph XBT or STD-systems) diving drifters will allow to receive the information about UML heat contain, topography of the high bound of thermos profile in the ocean, boundaries of creation and distribution of the CIL, and also about dynamics of a high bound of the hydrogen sulphide zone in the Black sea. All this will help to put more correctly

and to resolve the problems of interaction of ocean and atmosphere, mechanisms of heat transfer and evaluation of the global circulation of water in the upper layer of the ocean with the purposes of further study of the climate variability of the Earth and increase of reliability of the long-term prognosis of the weather.

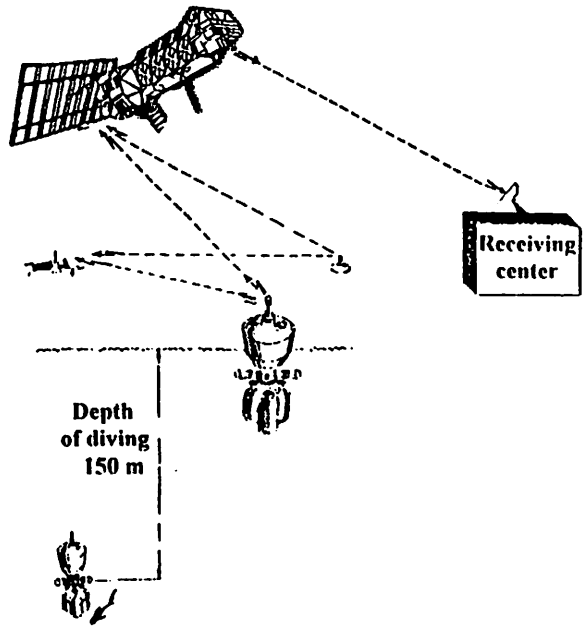

Fig. 1. The satellite automatic system of underwater monitoring for the study the active layer of ocean and sea

The entry conditions for the analysis

Taking into account the limitation of the energy search and volume of data transmitted via satellite, and also limitations superimposed on diving modes, it was accepted, that the buoy could supply the following modes of operation:

- Life-time of drifter - 3 months;
- Total number of explorations during the life-time - 15;
- Average time between diving - 6 days;
- Periodicity of communication sessions via satellite - each 3-5 days;
- Volume of transmitted data for one session no more than 256 bits;
- Optimum speed in a half-cycle of immersing V_{div} = 0,2 m/s;
- Maximum time of immersing up to depth of 150 m no more than 750 s;
- Main measured parameters: temperature of water T_w and depth Z_b..

The purpose of the analysis

As the result of the present analysis resolving ability and acceptable error of measurements should be determined. The obtained data would allow to answer on a problem: "Are the measuring characteristics of diving drifters the same as the ones of identical devices for example - thermoprofilograph XBT of a type T-4 [3], which have the following total error of measurement channels: temperature ±0,15°C and depth ± 5 m?"

The main contents

Error of measurement ΔX of any elements X while estimation of its distribution on depth Z and error of measurement of depth ΔZ are interconnected:

$$\Delta X = (dX/dZ)\ \Delta Z, \qquad (1)$$

where dX/dZ - vertical component of the element X gradient.

As it is clear from the expression (1) the error of measurement of depth Z for restoration of temperature structure or any other element is determined by the acceptable error of measurement of temperature ΔT or ΔX of any other element X and by the vertical gradient dT/dZ or dX/dZ:

$$\Delta Z = \Delta T/(dT/dZ); \qquad (2)$$

$$\Delta Z = \Delta X/(dX/dZ). \qquad (2a)$$

The vertical gradients of temperature are different depending both on depth and on region of the ocean. In the outer ocean dT/dZ rarely exceeds 1°C/m in layers of width 1m and more, however, in the mediterranean and internal seas (for example, in the Black sea) dT/dZ can reach (3-5)°C/m. In this case the calculated significance ΔZ can be within the following limits:

$$\Delta T/(dT/dZ)_{max} \leq \Delta Z \leq \Delta T/(dT/dZ)_{min}. \quad (3)$$

For the cases of explorations in the ocean and in the Black sea when ΔT = ± 0,15°C it will correspond to the following ratio:

$$0,03\ m \leq |\Delta Z| \leq 0,15\ m. \quad (4)$$

When the ratio (4) is realized the number of discernible gradations n_z along the depth can be calculated by the following formula (for the case of direct digitisation):

$$n_z = \frac{Z_{max} - Z_{min}}{2|\Delta Z|} \quad (5)$$

And, according to the ratio (4) it will be:

$$2500 \geq n_z \geq 500. \quad (6)$$

Total volume of the information N_Σ, received for one diving period when only two main parameters are measured (temperature and pressure), can be estimated by the following formula:

$$N_\Sigma = (\log_2 \frac{T_{max} - T_{min}}{2|\Delta T|} + \log_2 n_z) n_z \quad (7)$$

and for the above-stated conditions for T_{max} - T_{min} = 38°C, $|\Delta T|$ = 0,15°C it will be:

- for the ocean: N_Σ = (7 + 9) 500 = 8000 bits;
- for the Black sea: N_Σ = (7 + 12) 2500 = 47500 bits.

Such volume of information exceeds the limitations accepted in the present analysis. If the adaptive method of data, when the values of the counted temperature differ by intervals $2|\Delta T|$ is used instead of the direct digitisation on depth, the number of discernible gradation on temperature n_T will be:

$$n_T = \frac{T_{max} - T_{min}}{2|\Delta T|} = \frac{36 - (-2)}{2 \times 0,15} = 123 \quad (8)$$

and the number of data on depth will be equal to:

$$n_z = n_T = 123. \quad (9)$$

Then the maximum volume of the information received when diving up to 150 m under condition of (9) can be calculated on the ratio (7) and will be equal:

- in the ocean: N_Σ = (7 + 9) 123 = 1968 bits;
- in the Black sea: N_Σ = (7 + 12) 123 = 2337 bits.

Thus, it is impossible to transmit the information, which is obtained for one diving of drifter for the adaptive digitisation on depth and the acceptable error of registration of the temperature profile ΔT = 0,15°C even during 5-8 communication sessions. Taking all the above into account and not changing the selected error of measurement of temperature in the points of reference, we shall find such a value of the acceptable error of depth measurement ΔZ, that the condition:

$$(\log_2 \frac{T_{max} - T_{min}}{|\Delta T|} + \log_2 \frac{Z_{max} + Z_{min}}{|(\Delta Z)_{add}|}) \times (\frac{Z_{max} - Z_{min}}{2|(\Delta Z)_{add}|} = N_\Sigma \leq 256 \text{ bits} \quad (10)$$

will be true.

The condition (10) is true for $(\Delta Z)_{add} \approx \pm 4$m. It means that dot weight of water of temperature $(T_i \pm 0{,}15)$°C can be on depth $(Z_i \pm 4$m$)$ with the probability $\alpha = 0{,}95$. The installed discretization of the depth data should be equal to (8-10) m, and the number of data from the surface up to maximum depth will be equal to (19-20). If the number of measured parameters is increased by two elements, the number of data on the whole range of depth will decrease approximately twice, and the interval of the discretization on depth will be (16-20) m.

The total error $(\Delta T)_\Sigma$ of the temperature measurement channel is determined by the static $(\Delta T)_{st}$ and dynamic $(\Delta T)_{dyn}$ errors:

$$(\Delta T)_\Sigma = (\Delta T)_{st} + (\Delta T)_{dyn}. \quad (11)$$

Assuming the statistical independence of the error components in the general view, we can write down:

$$(\Delta T)^2_\Sigma = (\Delta T)^2_{st} + (\Delta T)^2_{dyn}. \quad (12)$$

If both component's influences are equal, we can find out:

$$(\Delta T)_{st} = (\Delta T)_{dyn} = (\Delta T)_\Sigma / \sqrt{2} = 0{,}1\,°C. \quad (13)$$

The parameter of inertia of the temperature measuring channel τ_T can be evaluated by the formula:

$$\tau_T = \frac{(\Delta T)_{dyn}}{(dT / dZ) V_{div}}, \quad (14)$$

where: dT/dZ - vertical component of the temperature gradient (°C/m); V_{div} - speed of diving (m/s).

The expression (14) is correct when drifter moves in the layer with a gradient dT/dZ for the time more than $3\tau_T$. Taking into account maximum gradients of temperature, as it was above said, for the ocean conditions $(dT/dZ)_0 = 1$°C/m, and for the Black sea $(dT/dZ)_{B.S} = (3\text{-}5)$°C/m, we can find, that for the ocean conditions the parameter of inertia for the speed of explorations $V_{div.} = 0{,}2$m/s should not exceed $(\tau_T)_o \leq 0{,}5$ s, and for the Black Sea conditions - $(\tau_T)_{B.S} \leq (0{,}2\text{-}0{,}1)$ s. In this case the shift on depth of the obtained structure of temperature regarding the actual on the value will appear:

$$\delta Z = V_{div}\, \tau_T = (0{,}1\text{-}0{,}02)m. \quad (15)$$

If the parameter of inertia of the sensors is settled in the bounds (0,2-0,1) s, then the error of instantaneous data of temperature will not exceed ± 0,15°C for the stipulated gradients.

For the discrete data on depth it is advisable to measure the average temperature of a layer between two adjacent horizons of count. In this case the structure restoration errors caused by the high-frequency pulsation of temperature or its variability within the limits of large wave numbers and by the final discretization of measurements in time or space, decrease considerably. The integrated sensors of temperature, represented as distributed resistor are the most convenient for this purpose. Such sensors can have length of 1-4 meters and the above defined heat inertia of sensor, which is the same as in the discrete sensor case. However, their application on the diving

drifters is connected to essential operational difficulties. The effect of space average for the moving sensor can be obtained by the increasing of the heat inertia parameter. The greatest significance of the time-constant of the temperature sensor can be achieved from the ratio:

$$\tau_T = \delta Z / V_{div}, \tag{16}$$

where δZ - interval between the depth data.

For δZ = (8 - 10) m, V_{div} = 0,2 m/s we shall receive:

$$\tau_T = (40 - 50)s. \tag{17}$$

The depth shift of the low-frequency component or the components located in the area of small wave numbers of the temperature structure can be compensated by the appropriate synchronous filtering of the pressure (depth) measurement data with the help of the first inertial filter with time-constant $\tau_p \approx \tau_T$ or by the space-inertial filter with the equivalent parameter τ_p =(8-10)m. The filtering of pressure can be made during the information processing at coastal centre of data collection.

The word length of the analogue-to-digital converter of the drifter sensors should make 8 bits on the temperature channel and 6 bits on the of depth (pressure) channel. The volume of the least bit will make γ_T= 0,15°C for the temperature and γ_Z = 2,5 m for the depth, and the quantization error will be accordingly ΔT_{qua} = ±0,075°C and ΔZ_{qua} = ±1,25 m.

The acceptable errors caused by the long-term instability of the prior temperature measuring converters $(\Delta T)_{nst}$ and of the depth sensor $(\Delta Z)_{nst}$ during three months term should not exceed:

- on the temperature:

$$(\Delta T)_{nst} \le \sqrt{(\Delta T)_{st}^2 - (\Delta T)_{qua}^2} = 0,066\,°C; \tag{18}$$

- on the depth

$$(\Delta Z)_{nst} \le \sqrt{(\Delta Z)_{add}^2 - \Delta Z_{qua}^2} \approx 3,7\ m. \tag{19}$$

The thermistor sensors of the temperature and also the potentiometer pressure sensors have such characteristics.

After determination of probable and acceptable errors on depth $(\Delta Z)_{add}$ and $(\Delta Z)_{qua}$, it is possible to evaluate the minimum volume of the temperature sensor inertia, which makes the optimum agreement of errors of temperature and depth data in the instantaneous single measurement:

$$(\tau_T)_{min} = (\Delta Z)_{qua} / V_{div} = 6,2\ s. \tag{20}$$

For the decreasing of error due to the shift of the structure, it is necessary to filter data of the pressure channel with the help of inertial filter of the first degree with the time-constant $\tau_p \approx (\tau_T)_{min}$=6,2 s, the same way as it was specified above. For the final choice of the best value of the inertial parameter of the temperature sensor with the good adaptation of correctness of single data (small inertia) and correctness of the temperature structure restoration on rare data (large inertia), it is necessary for the correct tests to have at least on three samples of the drifters the temperature sensors with parameter of inertia of 5s, 25s and 50s. Carrying out the synchronous diving for the near placed drifters, it is possible to receive the necessary information and to compare it with the data of the STD-probe. The criterion of choice regularity of the correct inertia

will be the least divergence of the restored temperature structure obtained from data of three drifters and the structure obtained by the STD-probe.

Summarising we'll make the evaluation of space shift of single data of the temperature structure, using the data of the diving drifter and one time use thermoprofilograph T-4 in the gradient layers. According to the expression (15) these shifts will be:

$$(\Delta Z)_{sh} = (\tau_T)_{min} \times V_{div} = 1,24\ m; \quad (21)$$

$$(\Delta Z)_{T\text{-}4} = (\tau_T)_{T\text{-}4} \times (V_3)_{T\text{-}4} = 0,9\ m, \quad (22)$$

where $(\tau_T)_{T\text{-}4}$=0,15s- is the parameter of inertia of one time use thermoprofilograph; $(V_{div})_{T\text{-}4}$=6 m/s - speed of the free falling.

Thus, in the points of reference the data from the diving drifter practically completely coincides with the data from the one time use thermoprofilograph Sippican T-4 for the temperature error (±0,15°C), and for the interval of the depth single measurement average both (1,2 m and 0,9 m correspondingly).

It is possible to increase the reliability of the temperature structure restoring on rare data by use of the adaptive digitisation of temperature together with the method of data of singular points of a structure (inflection point, extremum, etc.). The selection of the characteristic points requires the knowledge of the whole structure, that is possible in developed buoy, as it has big amount of inside memory and microprocessor for the preliminary analysis of the data and preparation of the 256-bit message for the transfer. In this case the spline approximation of a structure also can be tried with the consequent transfer of the spline's parameters on the various plots of depths.

The brief description of the diving drifter

For the buoyancy control of the diving buoy the pressed air is used, which is under pressure of 15 - 20 MPa. This value of pressure exceeds ten times the hydrostatic pressure on the maximum depth of diving, i.e. provides an appropriate energy potential for the operation against the forces of external hydrostatic pressure in the diving cycles. The value of pressure is limited by the characteristics of the widespread high pressure bottles. Choice of the pressed gas has defects and advantages, however for the low cost one time use buoys such solution seems preferable. As it was already noted the power aspect in this case is resolved, , by use of the potential energy of the pressed gas, and thus, the expensive high-power sources of power and electromechanical converters reducing at each stage efficiency of the used energy potential are not necessary.

The extension of the pressed gas is not also an ideal thermodynamic process, however, the decreasing of the gas internal energy is reimbursed by the background thermal energy, so that the final temperature of gas is always determined by the temperature of the outside water.

Fig. 2. Main view of the diving drifter

During the development of the diving buoy schematic, shown on the Fig.2, the former experience of creation and testing of similar devices is taken into account. The buoy has a new unified electronic instrumentation (adaptive to various systems of satellite communication) with the reduced energy consumption and dimensions, and there is also a possibility of programming of the buoy operational modes (type of the communication system, date and time of immersing, number of sensors etc.). Programming is made via the computer through the interface RS-232.

Main results

The obtained results can be generalised as follows:

- the tests of the diving drifter, which were carried out in the summer 1996, have confirmed serviceability of the developed device completely;

- during the interval between explorations the buoy can be used as the surface drifter for the measurement of the surface current characteristics and temperature in the surface layer;

- it was determined, that in the diving mode the diving drifter of such class is identical in the area of application to the low cost XBT probes, for example to the Sippican T-4 type;

- the selected method of the buoyancy control with the elastic working bodies more then other methods suites to the problem of the low cost one time use diving drifter creation;

- equipping of the buoy by the microprocessor controller and sufficient volume of the onboard memory for the data processing after the measurements allows to make the preliminary analysis and compression of data onboard of the buoy with the purpose of creation of the informatic message of the satellite communication system ARGOS;

- the possibility of programming of date and time of diving immediately before the buoy deployment allows to use the buoy resources rationally regarding to the solution of this or other problem;

- summarising the material and financial costs for the production and operation of the developed drifter it is possible to relate it to the devices of one time use, same as the SVP-B drifter and that makes the work realisation at oceans and seas essentially cheaper.

Resolution

On base of the network of the diving drifters the satellite automatic system of underwater monitoring can be created with small financial and material expenses for the study of the active layer with data transfer to the shore in the actual time scale. Such system can have wide practical application. With its help it will be possible to organise the monitoring of the biological efficiency in the Southern ocean, to measure the level of the high bound of hydrogen sulphite zone in the Black sea, to study of the thermos profile structure in the open ocean for the resolution of problems of fishery and etc.

References

1. Sybrandy A. L., Martin C., Niiler P. P., Charpentier E., Meldrum D. T., 1995. WOCE Surface Velocity Programme Barometer Drifter Construction Manual. WOCE Report No 134/95; SIO Report No 95/27. Published by the Data Buoy Co-operation Panel.

2. Motyzhev S. Marine, air and ground automatic observing station developed at the Marine hydrophysical institute. - Development in buoy technology and enabling methods. Technical presentations made in the eleventh session of the DBCP. DBCP Technical Document No. 7, 1996, p. 4 - 52.

3. Alexander Sy. XBT Measurements. WOCE operations manual. Volume 3: The observational Programme. WOCE report № 68/91. 1991, Woods Hole, Mass. USA.

Pekka Järvi, Vaisala, Finland

VAISALA

Sources of barometric pressure measurement uncertainty

Wind induced pressure measurement errors

Wave effects

Long term stability - drift with time

Accuracy of the barometer

Gravity errors

VAISALA

Requirements for a buoy barometer

Good long term stability (± 0.1 hPa / year)

Low power consumption

Ruggedness

Cost effectiveness

Fair or good accuracy (± 0.5 hPa or up to 0.1 hPa)

VAISALA

BAROCAP® pressure sensor

silicon capacitive absolute pressure sensor

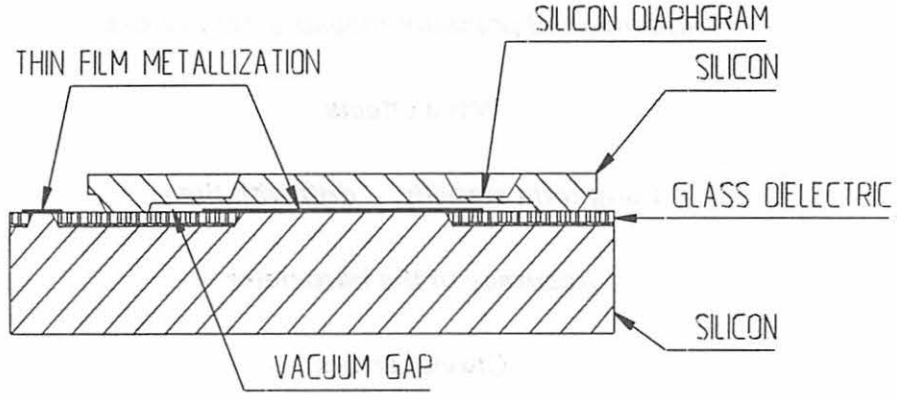

VAISALA

BAROCAP® pressure sensor

silicon capacitive absolute pressure sensor

BAROCAP® pressure sensors combine two well-proven techniques for barometric pressure measurement

- ***the use of single crystal silicon as pressure sensor spring material***
- ***the capacitive sensor principle***

VAISALA

BAROCAP® pressure sensor

silicon capacitive absolute pressure sensor

the advantages of silicon as pressure sensor spring material

- *perfect elasticity*
  - *low hysteresis*
  - *excellent repeatability*
- *stability*
  - *small temperature dependence*
  - *excellent long-term stability*
- *can be manufactured using microelectronic techniques*

the advantages of the capacitive pressure sensor structure

- *wide dynamic range*
- *built-in overpressure stop mechanism*
- *non-linearity results in good sensitivity at surface pressures*
- *no warming-up*

VAISALA

BAROCAP® pressure sensor

silicon capacitive absolute pressure sensor

Operating range	
• pressure range	50...1300 hPa
• temperature range	-55...+80 °C
• humidity range	non-condensing
• overpressure	10 MPa
Accuracy	
• hysteresis	±2 Pa
• repeatability	±2 Pa
• temperature dependence at 1000 hPa	typically ±5 Pa/°C
• sensitivity temperature dependence	- 80 ppm/°C ±50 ppm/°C
• long-term stability	±0.05 hPa / year or better

VAISALA

BAROCAP® pressure sensor

silicon capacitive absolute pressure sensor

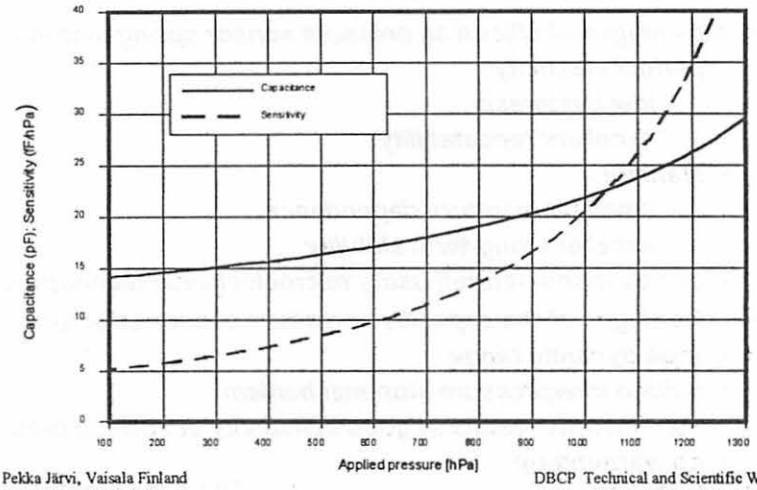

Pekka Järvi, Vaisala Finland DBCP Technical and Scientific Workshop 1997

VAISALA

BAROCAP® pressure sensor

silicon capacitive absolute pressure sensor

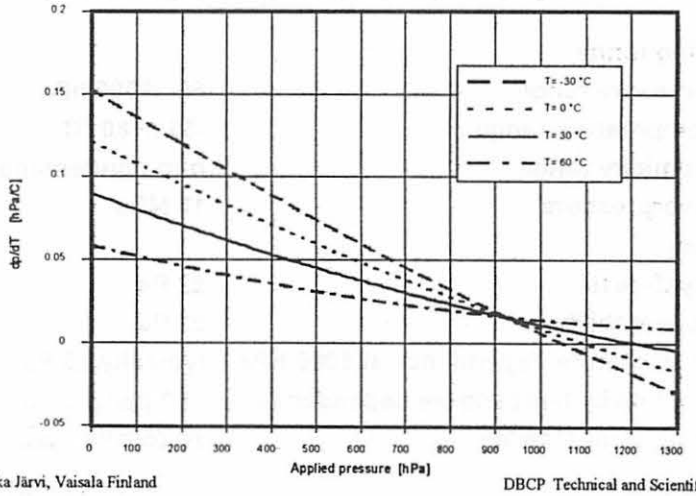

Pekka Järvi, Vaisala Finland DBCP Technical and Scientific Workshop 1997

VAISALA

Barometer electronics

Analogue

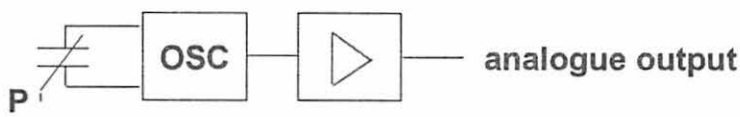

Digital

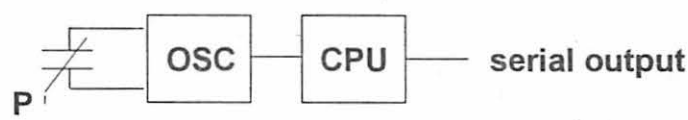

VAISALA

Analogue vrs. digital barometers

Analogue barometers	*Digital barometers*
+ low power consumption	*+ excellent pressure linearity*
+ small size	*+ small temperature dependence*
	+ good electronics stability
- poor electronics stability	*- power hungry*
- poor thermal dependence	*- bulky*
- quite expensive	*- expensive*

VAISALA

PTB101C analogue barometer

Accuracy at 900 to 1100 hPa / -40 to +60°C.

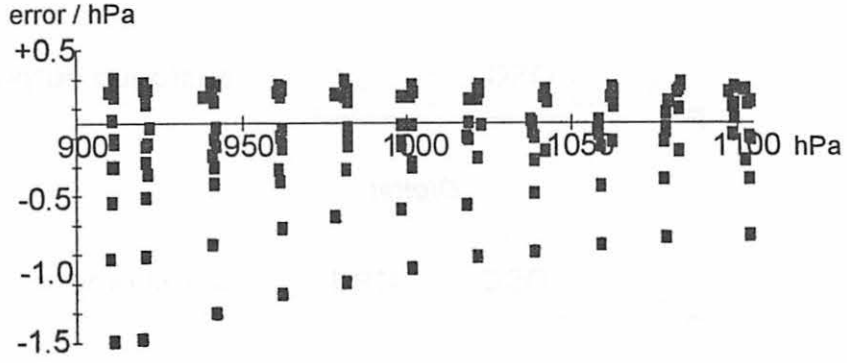

VAISALA

PTB200/220 series digital barometers

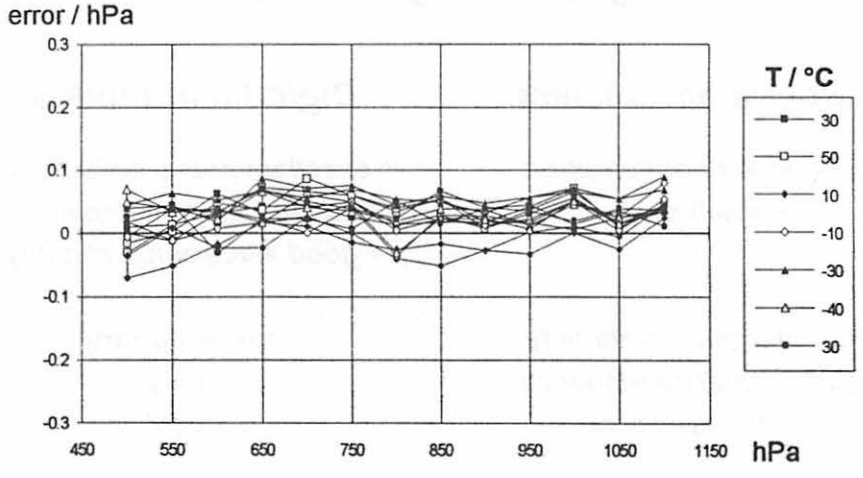

VAISALA

PMB100A Barometer Module

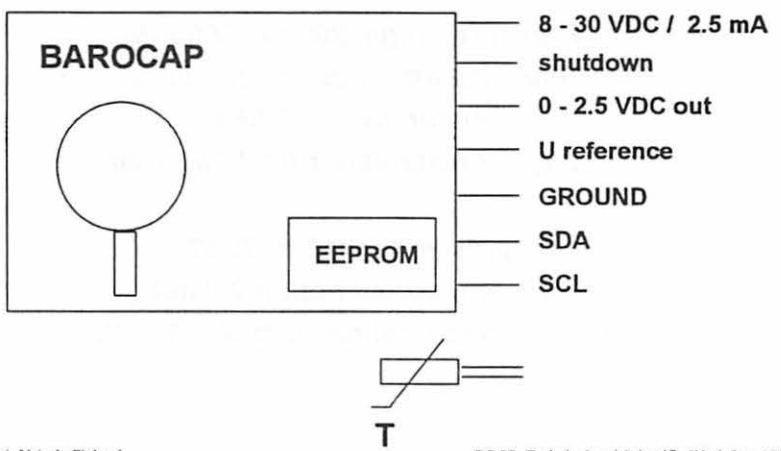

VAISALA

PMB100A Barometer Module

CIRCUIT BOARD MOUNTABLE

50 mm (2") x 25 mm (1") size

FOR INTEGRATED SYSTEMS WITH CPU

ALL COMPENSATIONS PERFORMED BY SOFTWARE OF THE HOST SYSTEM

VAISALA

PMB100A Barometer Module

Pressure range 900 to 1100 hPa
Temperature range -40 to +60 °C
Accuracy ± 0.5 hPa
Long term stability ± 0.1 hPa / year

Supply voltage 8 to 30 VDC
Current consumption 2.5 mA
Power consumption 30 mW / 12 VDC

Pekka Järvi, Vaisala Finland

Promising results of the WOTAN technique to provide wind measurements on SVP-BW drifters

Pierre Blouch & Jean Rolland
Centre de Météorologie Marine
Météo-France

January 1998

Abstract

A prototype of SVP-BW drifter, built by Metocean, was tested by Météo-France in North Atlantic during four months of winter conditions. The WOTAN technique (Wind Observation Through Ambient Noise) was used to measure the wind speed thanks to an hydrophone located at about 10 metres under the sea surface. The wind force is related to the energy contained in a frequency band of the ambient noise. A fixed vane rotates the float under the wind influence. So, the wind direction is obtained by an inbuilt compass sensor reading. Less than 2 weeks after the deployment, the wind measurements appeared so satisfactory, it was decided to transmit them on the GTS. The buoy was recovered in working order for expertise.

Several institutions, of which Météo-France, plan to deploy about 25 drifters of that type during the next few months, some of them in the Southern Ocean. The most recent results as well as their implications in case of success are discussed.

Introduction

Wind measurements are not easy to carry out automatically at sea particularly when a long-term reliability at low cost is required. Moored buoys are usually equipped with conventional vanes and anemometers. The sensors, being located high enough above the sea level (5-10 metres), don't suffer from the waves too much. However, moored buoys are expensive to built and maintain. The idea to measure wind speed and wind direction on drifting buoys for operational purposes isn't recent. By the beginning of 80's, the buoys used during the FGGE[1] experiment were modified to measure this parameter. The most simple way was to fit a profiled mast to them. Then the mast rotates the buoy under the wind influence and the wind direction can be assessed through a compass reading. The mast is topped with a standard anemometer to provide the wind speed.

By the end of 80's, within the framework of TOGA[2] and WOCE[3], the SVP[4] lagrangian drifter was fully developed for observation of in situ ocean currents. In the early 1990's, efforts were made to add more measurements than sea surface temperature. The idea was to have a common buoy for meteorologists and oceanographers needs. The first step was to try to measure the atmospheric pressure with SVP-B drifter; a challenging task because the SVP drifter spends a lot of time under the water. More than 500 SVP-B has been deployed since 1994, and two of them have been providing good surface pressure data for more than 1000 days.

It was difficult to imagine conventional anemometers on SVP buoys. The chosen method was to make use of the Wind Observation Through Ambient Noise (WOTAN) technique. The system is sturdy because the sensor, an hydrophone submerged at 10 metres depth, has no moving parts.

---

1 FGGE: First Global GARP Experiment. GARP: Global Atmosphere Research Programme
2 TOGA: Tropical Ocean and Global Atmosphere
3 WOCE: World Ocean Climate Experiment
4 SVP: Surface Velocity Program

The WOTAN Technique

The technique which consists to retrieve the wind speed by sampling the underwater ambient noise has been known for a long time. In 1964, Piggot showed the sound intensity at certain frequencies is related to the logarithm of the wind speed. Most of the noise between 500 Hz to 50 kHz is due to wind action on the ocean surface. Although a lot of acoustic sources exist under the water (ships, animals, rain, etc.), the spectral characteristics of sounds allow to differentiate them, or to consider them as disturbing ones.

In 1990, Vagle et al. proposed an algorithm to obtain wind speed from the spectral analysis of the ambient noise. Their study was based on the FASINEX[5] (North Atlantic - 1986) data. The maximum wind speed during this experiment (3.5 months) was about 15 ms^{-1}. Later, the proposed formulae was successfully verified with 4 instruments deployed during the OCEAN STORMS experiment (Pacific Ocean - 1987). The comparison with conventional surface measurements up to 15 ms^{-1} showed an accuracy of ± 0.5 ms^{-1}.

In shallow coastal waters, the relationship between ambient noise and wind speed is not well established. This is probably due to abnormal propagation and to the presence of many disturbing noises in these areas. For winds higher than 15 ms^{-1}, the presence of more and more microbubbles in the water could affect the wind measurements by absorbing and scattering the sound at frequencies above about 8 kHz. Lower frequencies are mostly unaffected by bubbles but it seems no comparisons with conventional sensors were carried out for winds higher than 15 ms^{-1}.

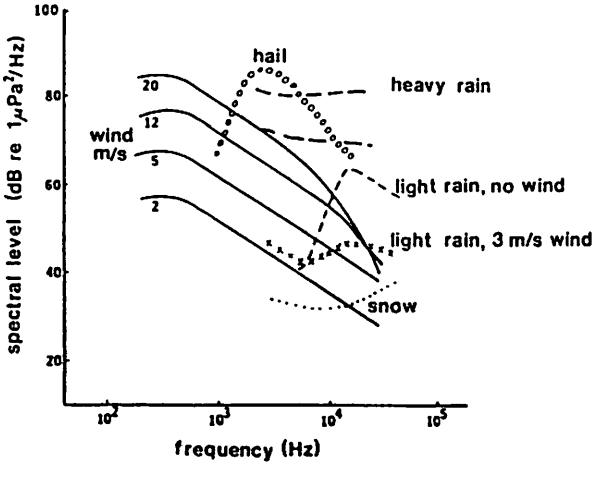

Figure 1 - Generic underwater sound spectra for different air-sea physical processes (Nystuen and Selsor, 1997)

The sound intensity SL is computed in dB relatively to 1μPa^2/Hz at various frequencies. The shape of the sound spectra allows to identify the presence of disturbing noises (ships, heavy or light rains...). Figure 1, proposed by Nystuen and Selsor in 1997, summarises the effects of different sound generators on the spectrum shape.

V being the wind speed in ms^{-1} at 10 m above the sea level, we have the following formula :

$$V = (10^{(SL/20)} - b) / a$$

where a and b are two empirical parameters determined by Vagle et al. thanks to the FASINEX data. These parameters depend on the chosen frequency for wind estimation.

The SVP-BW drifter

The SVP-BW float (photo 1) is derived from the SVP-B drifter. It consists of a spherical surface float (40 cm diameter) with a holey-sock drogue (diameter 0.92 m, length 6.7 meters) centred at a depth of 15 m. Its weight is about 30 kg. The float is equipped with a pressure measurement system (port + sensor + signal conditioning).

The hydrophone (photo 2) is submerged at 10 metres depth. To measure the wind direction, the technique which consists in rotating the buoy under the wind influence thanks to a fixed vane was retained. A swivel, located at the top of the drogue, allows to the float to rotate freely.

---

[5] FASINEX: Frontal Air-Sea Interaction Experiment

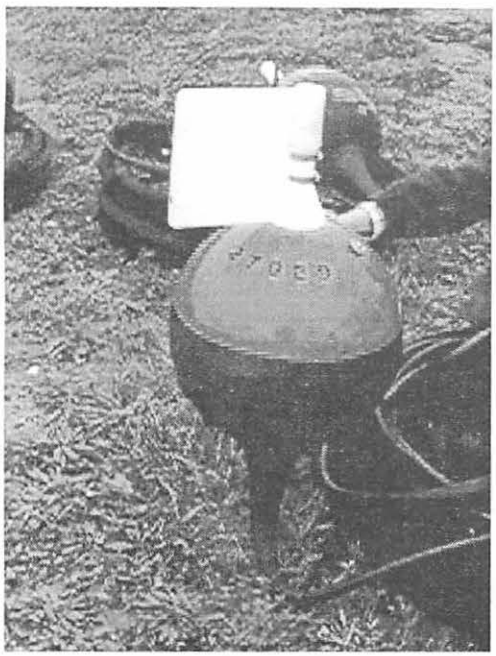

Photo 1 - Metocean SVP-BW drifter

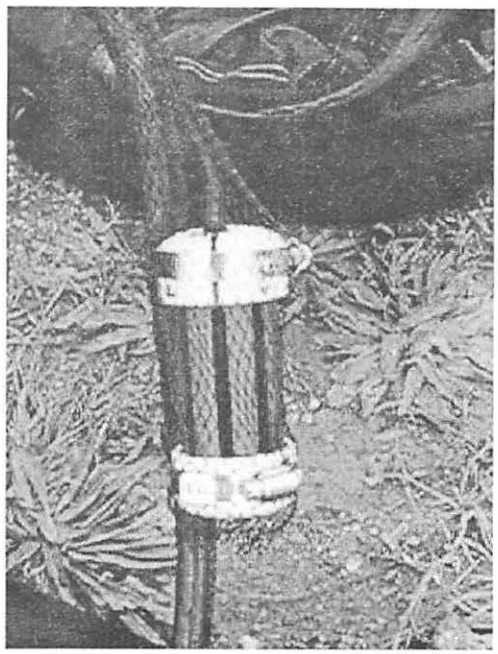

Photo 2 - Hydrophone

In 1996, Météo-France purchased a SVP-BW to Metocean Data System Ltd. and tested it off Biscay Bay during the winter 96/97. Hourly observations were done by sampling the ambient noise during a 210 s period (three periods of 35 s separated by a pause of 55 s). The algorithm (Vagle et al.) used the noise level at 8 kHz. Metocean estimates an accuracy of ± 2 ms^{-1} in the 2-15 ms^{-1} range and no indication beyond.

The compass, a TCM2 fluxgate, provides instantaneous buoy rotational positions with respect to the earth's magnetic field and other indications such as roll and pitch. The data were processed on board the drifter, then transmitted ashore via the Argos system. They comprised barometric pressure, sea temperature, wind speed and direction, pitch and roll indicators, sound spectrum shape indicator (also called «weather classification»), battery voltage and submergence count.

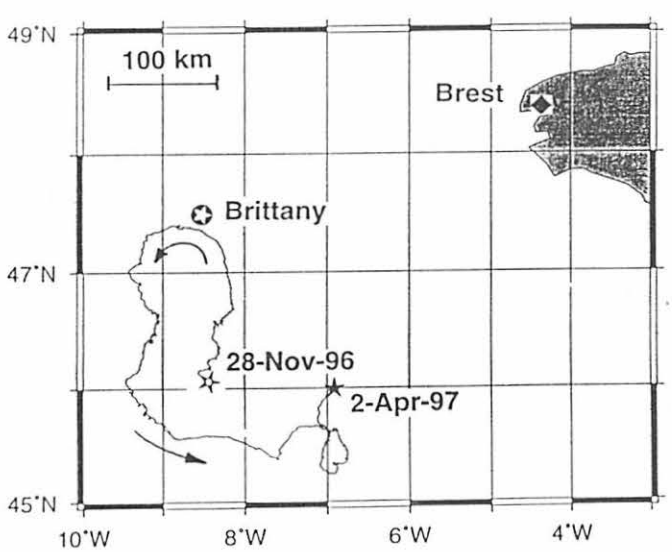

Figure 2 - SVP-BW #27939 - Buoy track from 28-Nov-96 to 2-Apr-97

Results obtained by Météo-France

Drifter id. 27939 (WMO 62551) was launched the 28 of November 1996 in position 46°N - 8°30'W. It provided reliable data until its recovery the 2 of April 1997 (fig. 2). In the middle of its trip, it passed at less than 8 nautical miles from the open ocean moored buoy Brittany. Barometric pressure and sea surface temperature were transmitted onto the GTS[6] as soon as the buoy was deployed. Two weeks later, the amount of wind data was sufficient to carried out comparisons with the moored buoy and the weather forecast model outputs. Measurements were declared satisfactory and wind data were transmitted on the GTS too.

The maximum mean wind speed observed by the drifter was about 20 ms^{-1}, similar to the Brittany mooring observations (fig. 3 and 4). Despite wave heights of about 10-11 meters

[6] GTS: Global Telecommunication System of WMO. WMO: World Meteorological Organisation

(observed in mid-February in the area), there appeared to be no significant disturbance in the wind measurements. The buoy was in a very good state when retrieved in April. It was sent back to Metocean for expertise.

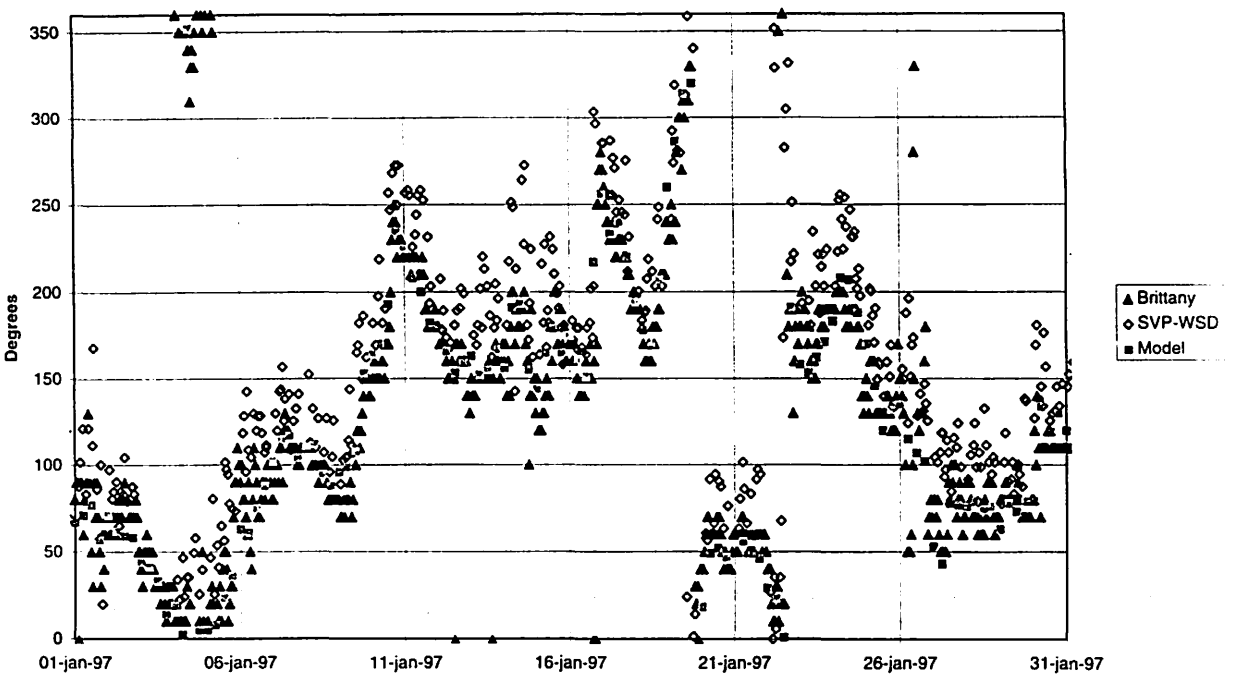

Figure 3 - SVP-BW #27939 - Wind direction (January 1997)
Comparisons with Brittany observations and model outputs

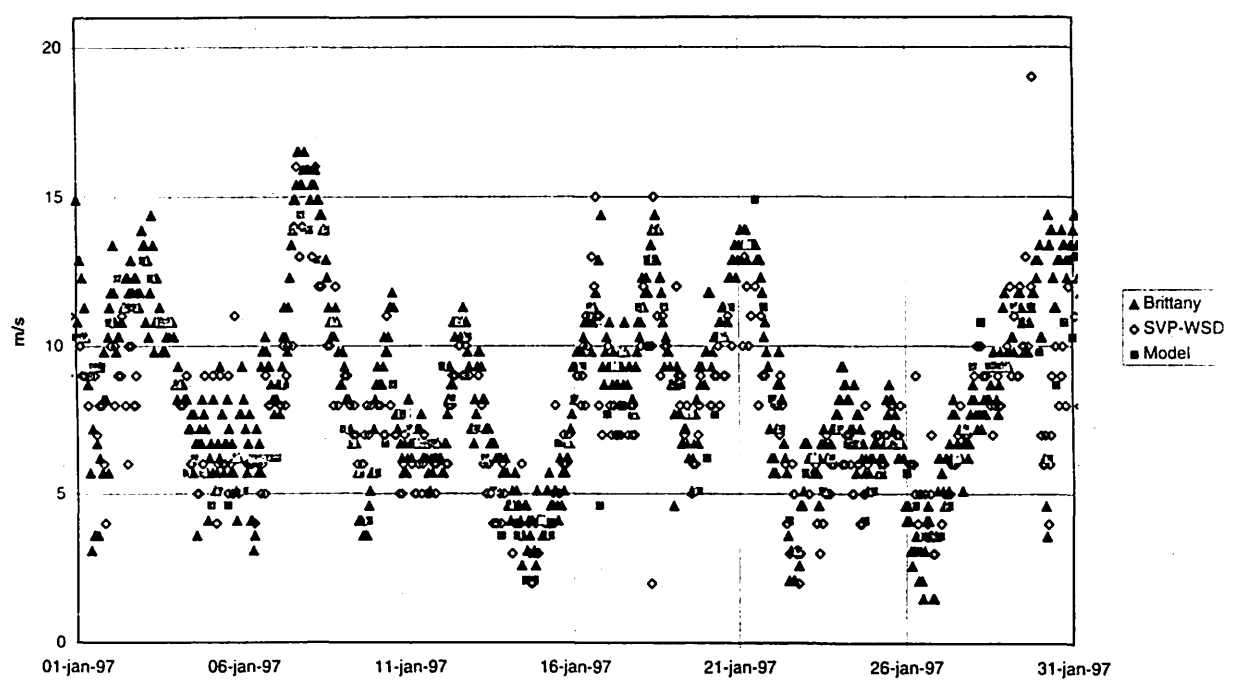

Figure 4 - SVP-BW #27939 - Wind speed (January 1997)
Comparisons with Brittany observations and model outputs

Three main problems were encountered during this test:

1. a systematic bias of 20 degrees was seen in wind direction data after the correction for magnetic deviation was applied. Soon detected, this bias was corrected before transmission on the GTS.

2. the «weather classification» indicator was almost constantly equal to 5 (meaning "shipping or other contamination noise present - wind speed estimate unreliable"). Despite this, the wind speed data were fully satisfactory.

3. the submergence sensor drifted from 60% to 100% by February 1997. Despite this, the flotation appeared unchanged when the buoy was recovered.

Figures 3 and 4 show the consistency of measurements carried out by the drifter and the Brittany moored buoy. During its four-month drift, the drifter was never further than 150 nautical miles from the moored buoy. Comparisons were done with the French model Arpege (analysis outputs interpolated at the location of the drifter). On figure 3, neither the magnetic deviation (about -5°), nor the systematic bias (+20°) were corrected.

Table 1 and 2 show some extracts from the monthly QC[7] statistics for wind data transmitted on the GTS for the Brittany moored buoy and the SVP-BW drifter. Comparisons are done with model outputs. «Rate» is the mean rate of wind speed measurements divided by model outputs. «Err» is the root square of differences (observed speed divided per «rate» minus model speed). It is expressed in ms^{-1} and constitutes a good relative indicator for the accuracy of wind speed measurements. More «err» is small, more the observations are close to the model outputs after applying a correction (multiplication by «rate»).

	December 96			January 97			February 97			March 97		
	Nobs	Bias	σ	Nobs	Bias	σ	Nobs	Bias	σ	Nobs	Bias	σ
SVP-BW	191	-1	25	306	3	28	207	0	32	235	6	27
Brittany	667	-3	18	733	2	25	399	-6	26			

Table 1. - Monthly QC statistics for wind direction in degrees (ECMWF model)

	December 96			January 97			February 97			March 97		
	Nobs	Rate	Err	Nobs	Rate	Err	Nobs	Rate	Err	Nobs	Rate	Err
SVP-BW	185	1.0	2.2	312	1.1	2.2	242	1.1	2.9	327	1.3	1.9
Brittany	712	1.1	1.6	737	1.2	1.6	352	1.2	2.3			

Table 2. - Monthly QC statistics for wind speed (err in ms^{-1} - Arpege model)

Here also the results are satisfactory. The biases for direction and the wind speed rates are similar for both buoys. However, we note the SVP-BW drifter has higher standard deviations for direction differences and higher accuracy indicators for wind speed observations than the moored buoy.

Next steps

Based upon these promising results a co-operative agreement between NOAA/AOML, Navoceano and Météo-France resulted in a large-scale air deployment in August 1997. An array of 12 SVP-BW drifters in the tropical Atlantic Ocean assisted in storm forecasts in the region. Since, several organisations have been ordering or plan to order such drifters. For its part, Meteo-France purchased 7 new drifters. Two of them were deployed in North Atlantic (EGOS network) and two others are devoted to the tropical Indian Ocean (IBPIO). All of these new drifters are still considered as prototypes. They provide the energy contained in 15 frequency bands between 0.5 and 40 kHz. Presently, the noise level at 8 kHz is used only for the data sent on the GTS. However, the amount of data collected in various

[7] QC: Quality Control

regions, at different latitudes, should serve to improve the algorithm. The possibility to use the noise level at 2 kHz for strong winds and a better detection of disturbing noises constitutes the two urgent concerns of the moment.

Taking into account the lifetime of pressure measurements, we believe that the SVP-B drifters advantageously replace the standard FGGE type buoys. Similarly, we can assume the SVP-BW could replace soon the FGGE type buoys which measure the wind. Presently, the cost price of observations is 1.5 times lower for SVP-B drifters than for standard FGGE buoys and the rate seems the same for wind buoys. But SVP drifters have other advantages. Because they are lagrangian drifters, they provide surface current measurements in addition to meteorological observations and, because of their small size, they are easier to store, to handle and to deploy.

References

Metocean, 1997: WOCE BP/WSD Drifting Buoy Technical Description. Dartmouth, Nova Scotia, 33 p.

Nystuen, J. A. and H. D. Selsor, 1997: Weather classification using passive acoustic drifters, *J. Atmos. Oceanic Technol.*, **14**, 656-666.

Piggott, C. L., 1964: Ambient sea noise at low frequencies in shallow water of the Scotian shelf, *J. Acoust. Soc. Am.*, **36**, 2152-2153.

Vagle, S., W. G. Large and D. M. Farmer, 1990: An evaluation of the WOTAN Technique of Inferring Oceanic Winds from Underwater Ambient Sound. *J. Atmos. Oceanic Technol.*, **7**, 576-595.

Impact of the Number of Drifting Buoys on Sea Surface Temperature (SST) Satellite Retrievals and Analyses

Richard W. Reynolds and Diane C. Stokes (National Centers for Environmental Prediction, Camp Springs, MD, 20746, USA) and Douglas May (Naval Research Laboratory, Stennis Space Center, MS, USA)

The number of drifting buoys decreased during the first half of 1997. This occurred partly from normal attrition and partly because some buoys were dropped prematurely to reduce transmission costs. Because these buoys produce observations of sea surface temperatures (SST) which are an important source of in situ data, we examined the importance of this change for two major uses of buoy SST data.

The first use is to tune the satellite SST retrieval algorithm. The algorithm is a function of two or three infrared satellite brightness temperatures with several unknown coefficients. The coefficients are determined by a global regression of the SST algorithm with SSTs from moored and drifting buoys (see, Barton, 1995). The regression is done globally, typically over a two week to one month period, when new satellites become operational or when operational differences between the satellite retrievals and the buoy SSTs become too large. Large differences occurred following strong volcanic eruptions such as Mount Pinatubo when the aerosols interfered with the retrievals. As discussed in Reynolds (1993), a different algorithm with new coefficients was needed during the period following the Mount Pinatubo eruptions.

To examine the sensitivity of the algorithm, we determined the coefficients for January 1997 using all available buoys (575) in the normal way. When these observations were used to tune the satellite algorithm, the residual RMS and bias were 0.47°C and 0.00°C, respectively. However, when only half of the number of buoys were used, the RMS and bias using the entire data set (both dependent and independent data) were almost unchanged at 0.47°C and 0.02°C. In this example, less than half the buoys (233) were in water colder than 20°C. The RMS and bias statistics increased to 0.60° and 0.16°C when these buoys were not used. In this case the largest differences came from SSTs with values less than 20°C. Thus, although the statistics for the tuning are not very sensitive to a random reduction in the buoys, a systematic loss of buoys in a particular temperature range can have a large negative impact on satellite retrieval accuracy.

The second use of buoy SST data is found in the National Centers for Environmental Prediction (NCEP) SST analysis. The analysis uses both satellite and in situ SST observations and is done by an optimum interpolation (OI) method with a preliminary satellite bias correction (see Reynolds and Smith, 1994). These SST fields are widely used for climate monitoring, prediction and research as well as specifying the surface boundary condition for numerical weather prediction

The distribution of the real-time in situ data for the week of 31 August to 6 September 1997 is shown in Figure 1. The upper panel shows the distribution of observations from ships. The lower panel shows the observations from drifting and moored buoys. The deployment of the buoys has partially been designed to fill in some areas with little ship data. This process has been most successful in the tropical Pacific and Southern Hemisphere.

Because in situ observations have a strong impact on bias correction of the satellite data, a simulation was devised to determine the minimum distribution of in situ data needed to correct any satellite biases. In this simulation, we used the actual distribution of in situ and satellite data but set the SSTs to a simple value or a function. For the in situ, using the distribution in Figure 1, the SST anomalies were set to zero. For the satellite distribution for the same week, not shown, the satellite SSTs were set to the $\cos(4\phi-\alpha)$ where ϕ is latitude and values of α vary.

To demonstrate the importance of drifting buoys, we show an example of the simulation with $\alpha=0$ along 45°S between 180° and 70°W. This region was selected, see Figure 1, because drifting buoys are the only source of in situ data there. Along 45°S with $\alpha=0$, the satellite SSTs are -1. If the in situ data were adequate, the analysis should be 0 everywhere, if not the analysis should be closer to -1. The results are shown in Figure 2 with the drifting buoys reduced by a percentage of the total. When all buoys are used, the simulated bias in the satellite data is almost completely removed from 180° to 110°W and partially removed from 110°W to 70°W. However, the ability to correct the biases decreases as the buoys are reduced. When no drifting buoys are used, there is no or very little correction between 160°W and 90°W. The impact of one isolated buoy can be seen at 125°W in the result using only 10% of the buoys.

Comparisons of the simulations for different values of α showed that a correction of satellite biases requires that in situ observations be available at least every 10°. Because of the availability of SSTs from ships, the required coverage by drifting buoys varies by ocean basin (see Figure 1). Drifting buoys on a 10° grid are needed south of 30°S in the Atlantic Ocean, south of the equator in the Indian Ocean, and south of 10°S in Pacific Ocean. If the mooring data in the equatorial Pacific were no longer available, than drifting buoys would be needed south of 10°N in the Pacific.

Figure Captions:

Figure 1. Number of in situ SST observations for the week of 31 August to 6 September 1997. The top panel shows the ship observations; the lower panel shows the buoy observations and the ice simulated SSTs. The moored buoys are indicated by a circle, the drifting buoys by a dot, the ice SSTs by a plus.

Figure 2. Analyzed SSTs with simulated satellite biases along 45°S. The number of drifting buoys is reduced by a percentage of the total. The satellite SST data are set to -1; the in situ SST data are set to 0. As the number of buoys is reduced, the bias correction becomes less effective and the analyzed SSTs become closer to the satellite data.

References:

Barton, I., 1995: Satellite-derived sea surface temperatures, current status, *J. Geophys., Res.*, **100**, 8777-8790.

Reynolds, R.W., 1993: Impact of Mount Pinatubo aerosols on satellite-derived sea surface temperatures. *J. Climate*, **6**, 768-774.

Reynolds, R. W. and T. M. Smith, 1994: Improved global sea surface temperature analyses. *J. Climate*, **7**, 929-948.

Figure 1

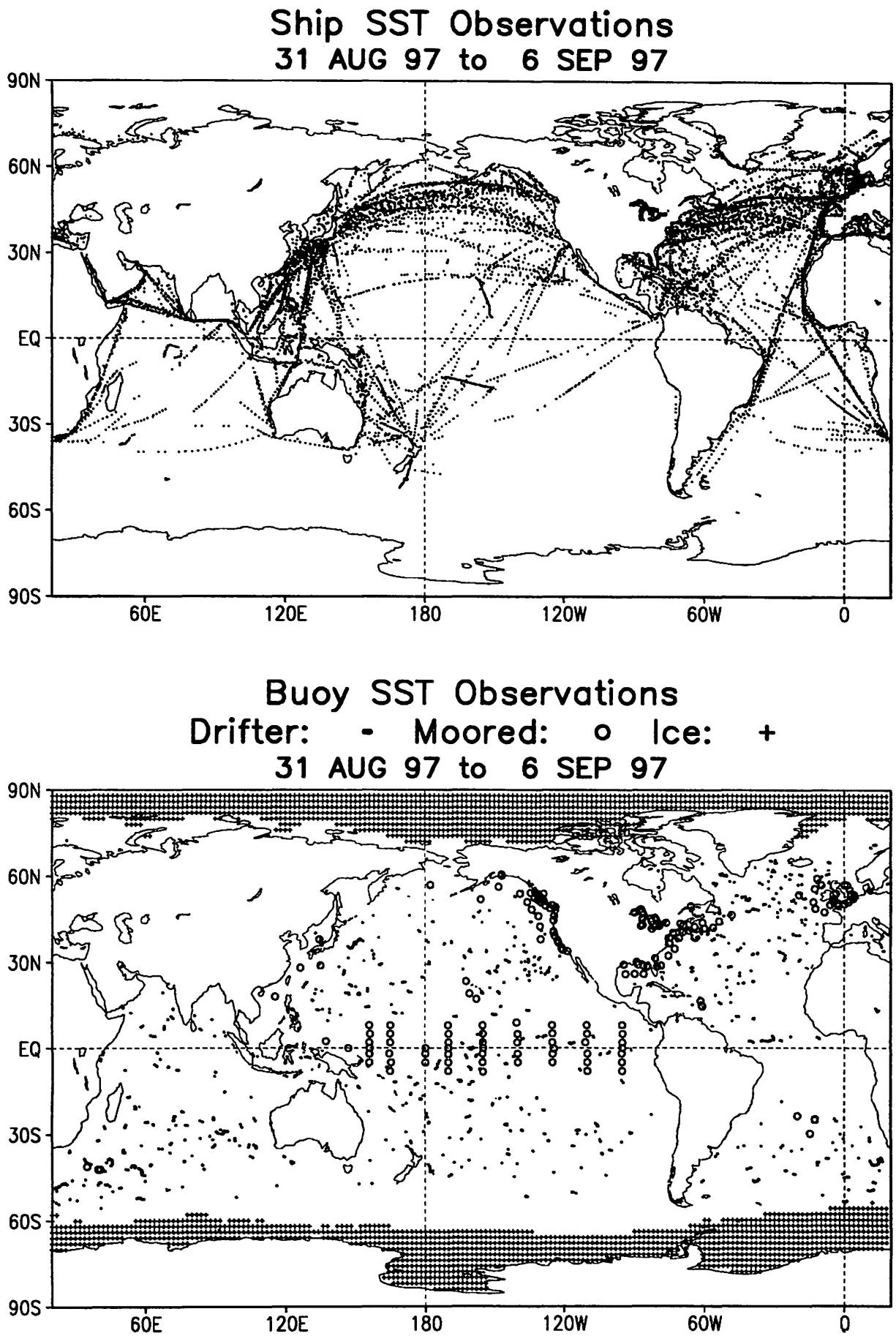
Ship SST Observations
31 AUG 97 to 6 SEP 97
90N
60N
30N
EQ
30S
60S
90S
60E
120E
180
120W
60W
0
Buoy SST Observations
Drifter: - Moored: o Ice: +
31 AUG 97 to 6 SEP 97
90N
60N
30N
EQ
30S
60S
90S
60E
120E
180
120W
60W
0

Figure 2

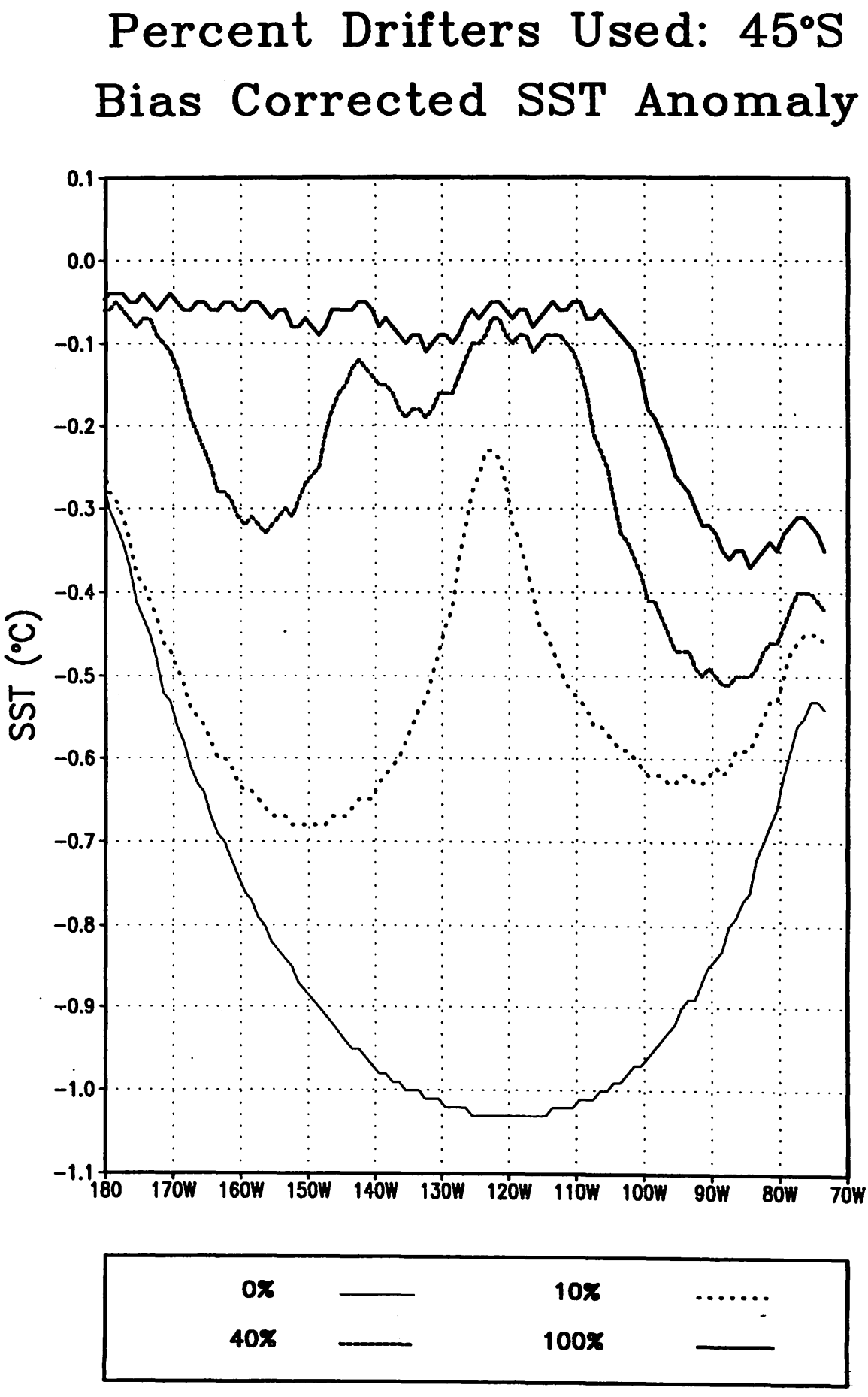
Percent Drifters Used: 45°S
Bias Corrected SST Anomaly
SST (°C)
0.1
0.0
-0.1
-0.2
-0.3
-0.4
-0.5
-0.6
-0.7
-0.8
-0.9
-1.0
-1.1
180
170W
160W
150W
140W
130W
120W
110W
100W
90W
80W
70W
0%
10%
40%
100%

On Ocean-Atmosphere Coupling in the North Atlantic Ocean

Mark Swenson
NOAA/AOML

We explore the geographical variability of the structure of the cross correlation function of sea surface temperature anomalies (SSTA) and anomalies of the sum of the latent and sensible heat fluxes (LSHFA) in the North Atlantic based on summaries from the Comprehensive Ocean Atmosphere Data Set (COADS) summaries from 1947-1990. Two distinct cross correlation structures emerge, one of which dominates in the open ocean at midlatitudes and the other of which dominates in the western boundary current and in the tropics. The former is characterized by a strong antisymmetric aspect, while the latter is one-sided with a peak at zero-lag. A simple stochastic model (vector first-order auto-regressive model) is proposed to account for the observed structure. This is the simplest auto-regressive model that can produce the antisymmetric aspect in the cross correlation found in the open ocean midlatitude region. The model reproduces the results with great fidelity, but requires essential mutual coupling between SSTA and LSHFA to reproduce the open ocean midlatitude result. The residuals from the fit contain low-frequency behaviour with decadal time scales.

A methodology for case studies of impact of buoy data upon numerical weather prediction using adjoint model technique.

Etienne Charpentier
Technical Co-ordinator of the
Data Buoy Co-operation Panel

Introduction

This methodology is to identify cases where buoy data inserted into Météo France numerical weather prediction model Arpège had a substantial impact upon the quality of the forecast of a particular meteorological event (e.g. a storm). To validate the methodology, we used the case of 29 September 1995 at 12H, where Grant[1] and Graham showed that a few buoys in the Atlantic Ocean had a significant impact upon quality of rain forecast over southern England.

The adjoint model of the linear tangent model, abusively called adjoint model, permits to move backwards from the forecast time to the analysis time, the gradient of any chosen cost function with respect to all historical variables of the model[2]. For example, Ps being surface air pressure (i.e. ground level over land, and sea level over the oceans), by using the mean surface pressure over a given area (e.g. a depression) at H+48 hours as a cost function J, running the adjoint model, and then extracting $\partial J/\partial P_s$ from the computed gradient of J at H we obtain the sensibility field of J with respect to initial surface pressure field. This sensitivity field permits to estimate the impact of a modification of the initial surface pressure field over the cost function.

Hence sensitivity area can be identified with respect to initial surface pressure field. If those sensitive area are over the ocean and include buoys reporting air pressure, we can expect that those buoys would have a higher impact upon the cost function than buoys in other area. The version of the adjoint model used did not permit to obtain normalised gradients of J. Only the sign of each of the components of the gradient was reliable. So sensitive area could be identified but the level of sensibility could not be estimated. By removing from the analysis "sensitive buoys" reporting air pressure from "sensitive area" we could estimate with precision the impact of the buoy data upon the H+48 forecast of the event we are interested in.

Discussion

The adjoint model of the linear tangent model used is a spectral model of truncation T63 with 19 levels. Adjoint model is adiabatic. Arpège Model of Météo France permits stretching, however no stretching was used for the purpose of this study (C=1). Limited T63 resolution was used to save computer power and memory resources. Model used for the impact study was also a T63/19L/C1 model (for example, operational model of Météo France is presently a T149/27L/C=3.5 model).

Tools have been developed for:

- Running adjoint model for sensibility studies. "Cost" function is the averaged 48 hours forecast surface pressure over an area of interest (e.g. a storm). For drifting buoys, we are mostly interested in how the cost function is sensitive to surface pressure (analysis).
- Running model initially in T63/19L/C1 mode for computing the 48 hour forecast for comparison with the operational forecast to make sure that the lower resolution model used gives similar results at least in the area of interest.
- Drawing verification analysis for final validation.
- Plotting buoys providing pressure observations in found sensitive area.
- In case buoys reporting air pressure do exist in those sensitive area, re-building an analysis by removing these "sensitive" buoys.
- Re-running 48 hour forecast (initially in T63/19L/C1 and later in T149/27L/C1).
- Comparing the two forecasts with and without the "sensitive" buoys.

Study was based on the UKMO case[1] of 29 September 1995 where Grant, Graham, and Bader showed that a few buoys reporting from the Atlantic Ocean had a significant impact upon the quality of rain forecast over southern England. However, since it was not possible to chose rain or even air relative humidity as a cost function (the

adjoint model does not include physics), mean air pressure over southern England on the 29 September 1995 at 12 UTC was chosen. It was assumed that meteorological situation over southern England on the 29 September 1995 at 12h00 UTC was quite sensitive to atmospheric surface conditions in certain area of the Atlantic Ocean. Hence, the forecasting period chosen was different than in the case studied by Grant, Graham, and Bader who worked on a bad 36 hour weather forecast starting on the 28 September at 06h00 UTC, and a good 24H weather forecast starting on the 28 September at 12h00 UTC both valid for the 29 September at 12h00 UTC. The difference between the quality of those two forecast was explained mainly by the fact that because of the data assimilation schemes, the first one did not assimilate a few drifting buoy data while the second one did.

Instead a 48 hour weather forecast starting on the 27 September at 12h00 UTC (see figure 1 for the analysis of the surface air pressure field) valid for the 29 September at 12h00 UTC (see figure 2 for the forecast of the surface air pressure field) was chosen. Cost function chosen was the average surface pressure in the box [54N,10W, 48N, 5E]. Actual situation on the 29 September at 12h00 (i.e. verification analysis) and box is shown on figure 3.

Sensitivity study conducted using proposed methodology showed that (i) a "sensitive" area was approximately located in a box [70N, 40W, 50N, 20W] (see figure 4 showing un-normalised field of $\partial J/\partial P_s$), and (ii) that 9 buoys were actually located in this area (figure 5), i.e. forecast mean sea level pressure over southern England is sensitive to sea level pressure in an area where the 9 buoys are reporting from.

Positive "sensitivity" field in that box suggests that an increase [a decrease] of the surface air pressure field in the area would imply an increase [a decrease] of the mean surface pressure over southern England (cost function). All 9 buoys reporting air pressure from the "sensitive" area reported values above the analysis in the order of 1hPa to 2 hPa (figures 3 and 5). Hence removing those 9 buoys from the analysis would result in a decrease in the surface air pressure field in that area. We can therefore expect that removing the 9 buoys from the analysis and then running the forecast again would result in a lower pressure field over southern England than with the original forecast.

This is what actually happens: Figure 2 shows the forecast surface air pressure field when actually using the 9 buoy data from the sensitive area in the analysis (original run); figure 6 shows the forecast air pressure field when removing the 9 buoy data from the analysis; figure 7 shows the difference between those two fields (in Pa). Figure 7 shows that pressure field was decreased of some 3hPa to 4 hPa over southern England. Interestingly, impact was not substantial over other area, except the area centred 62N, 30W (south west of Iceland).

By comparing the two forecasts with the verification analysis (figure 3), it also appears that the original run (i.e. with the buoy data) is of better quality than the run that did not use the buoy data. Attention, a better resolution is used for the verification analysis since it comes directly from the operational scheme of Météo France (T149 versus T63). Hence small features that appear in the verification analysis do not appear on the two forecasts.

The study showed that removing the 9 buoys from the analysis deteriorated the air pressure field forecast in southern England hence validating the methodology.

Some 10 FASTEX cases (January and February 1997) have then been studied but it was not possible to find any where removing the buoy data had a negative impact upon the quality of the weather forecast. This could be due to the following causes:

- Upper air conditions are predominant.
- First guess field in the North Atlantic is good and the buoy observations are very close to it hence having minor impact on the analysis.
- Presence of other surface observations (e.g. ships) does not permit to modify analysis substantially by removing buoy observations.
- Quality of forecast produced (both with and without the buoy data) was not always good enough because a low model resolution (63 spectral truncation versus 149 for the operational model) was used.

To avoid those sorts of problems the following approaches can be tentatively realised:

- Selecting cases where upper air conditions are not a priori predominant. Météo France is running the adjoint model on a routine basis based on a cost function using average surface pressure over France. These products can be useful to select those situations but limits us to meteorological events over France.

- Identifying drifting buoys producing good quality data and showing higher deviations from the first guess field in certain meteorological situations. It can be expected that these buoys during these situations may have a greater impact on the analysis.
- Removing ship reports as well from the data assimilation scheme while running the impact study. Impact of surface air pressure reports is aimed as opposed to impact of air pressure reports from drifting buoys. At least if such an impact can be proven, it would mean that buoys can have a positive impact in area where no ship reports are available.
- Studying area where the first guess field is not as good as in the North Atlantic. South Atlantic, Indian Ocean, Southern Ocean can be studied in that regard.
- Running the impact study using a higher resolution (e.g. T119 or T149). The adjoint model would still use a lower resolution because of a lack of computer resources (T63).

Conclusion

The UKMO case of 29 September 1995 permitted to validate a methodology based on the adjoint model technique and showed that in certain meteorological situation, removing from the analysis data of a limited number of buoys reporting from "sensitive" area could substantially deteriorate 48H weather forecast over a given area. However, identifying such cases remains difficult. Improvements are being proposed to strengthen the methodology and hopefully make it possible to identify other cases more easily.

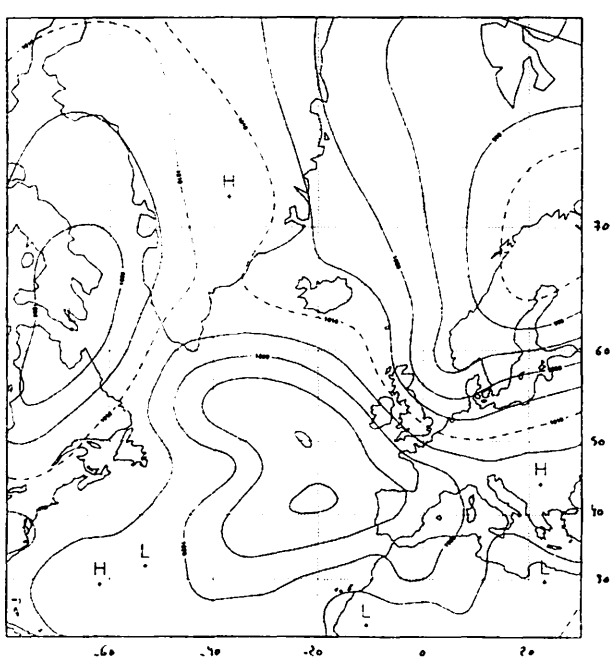

Figure 1: T63 resolution analysis of surface air pressure field on the 27 September 1995 at 12h00 UTC.

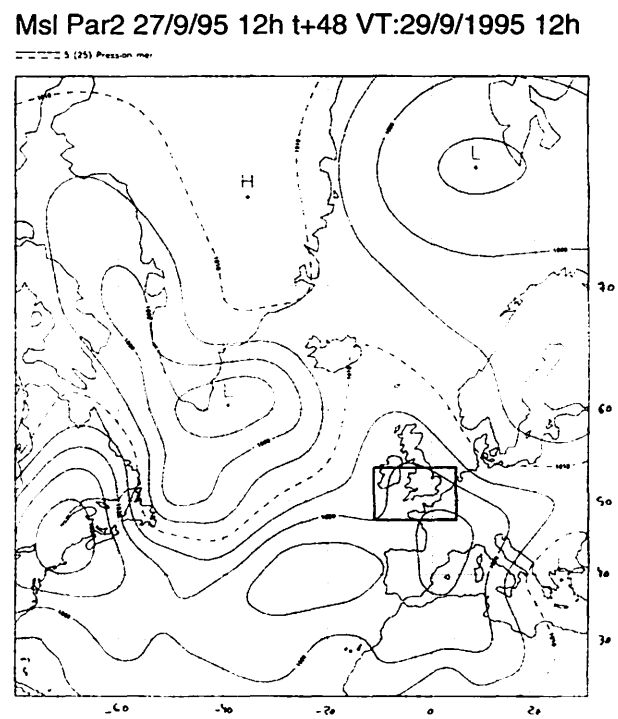

Figure 2: Surface air pressure field 48H forecast valid for the 29 September 1995 at 12h00 with the 9 buoy data assimilated. Box indicates area chosen for the cost function J.

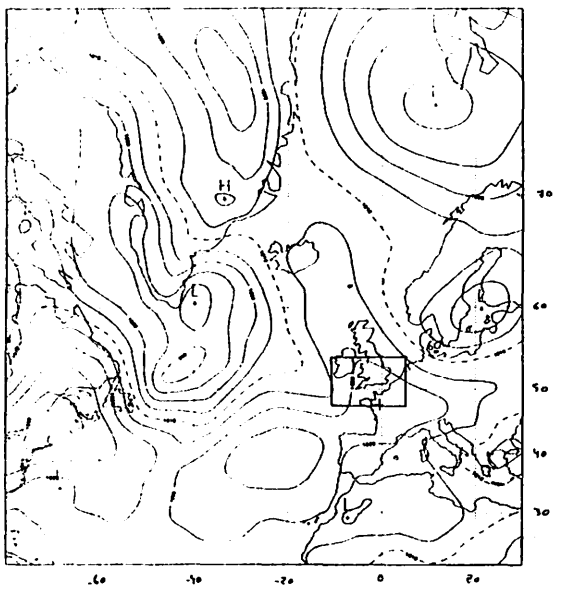

Figure 3: T149 resolution analysis of surface air pressure field on the 29 September 1995 at 12h00 UTC. Box indicates area chosen for the cost function J (mean surface air pressure over the area).

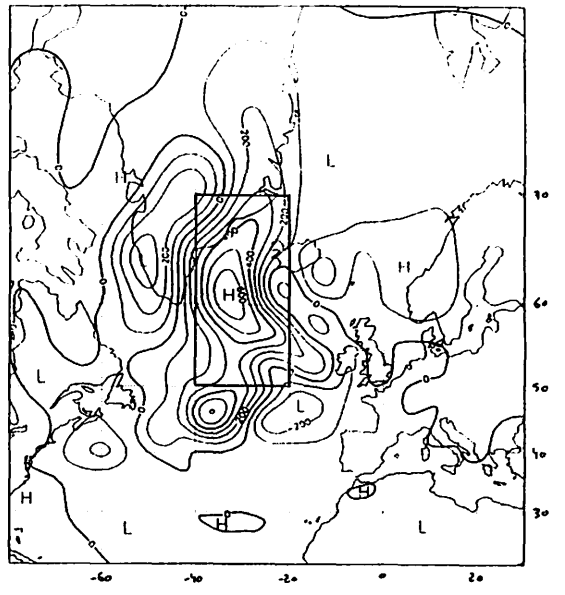

Figure 4: Un-normalised sensibility field $\partial J/\partial P_s$ on the 27 September 1995 at 12h00 UTC. Box indicates selected "sensitive" area.

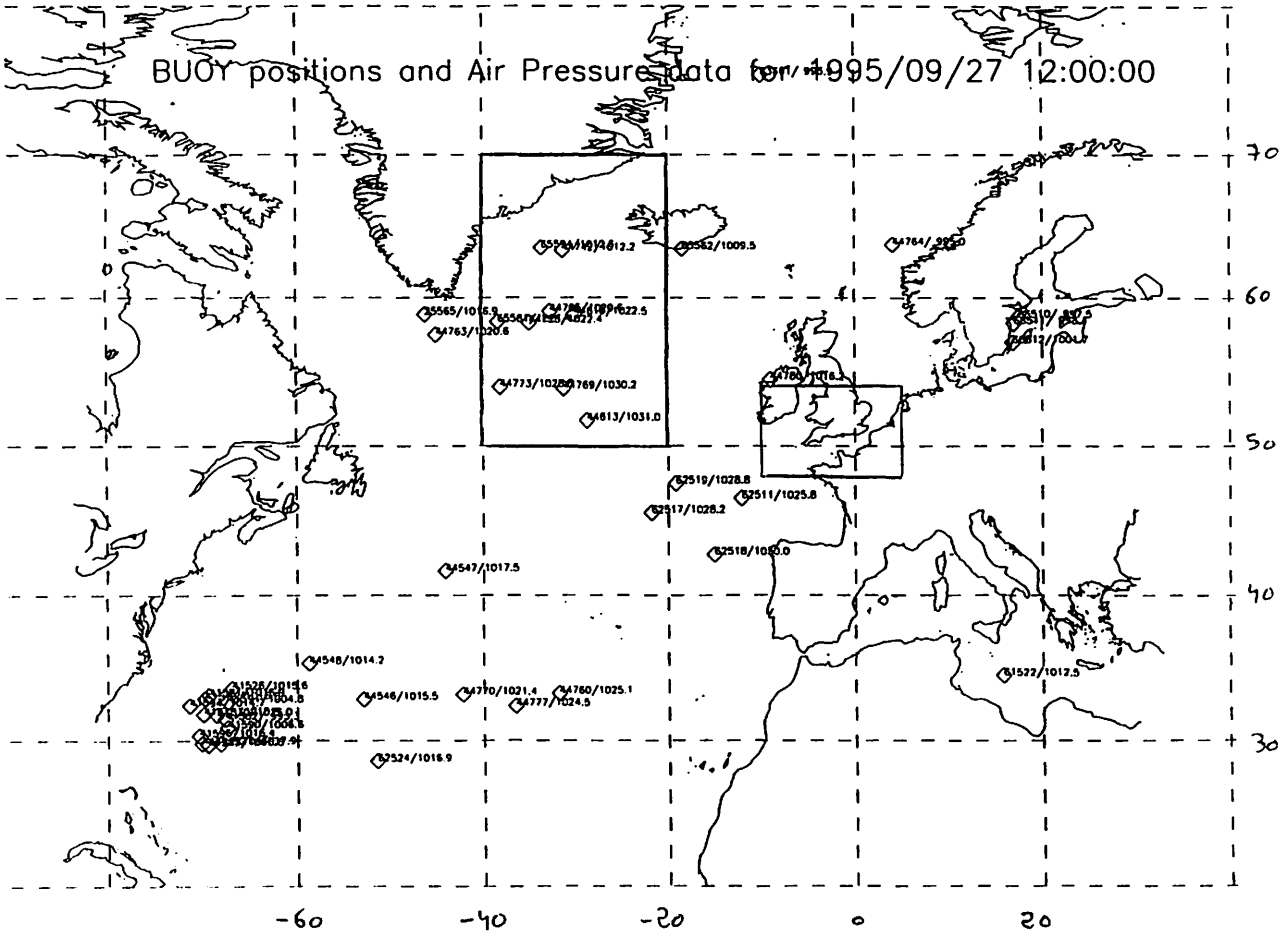

Figure 5: Plot of buoys reporting air pressure from the North Atlantic Ocean on the 27 September 1995 at 12h00 UTC. Big box indicates selected "sensitive" area. Small box indicates area chosen for the cost function J.

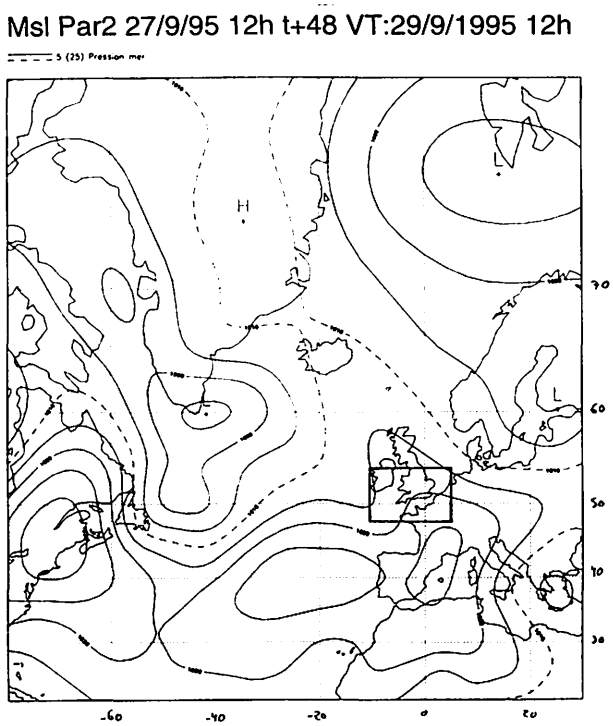

Figure 6: Surface air pressure field 48H forecast valid for the 29 September 1995 at 12h00 with the 9 buoy data removed from the analysis. Box indicates area chosen for the cost function J.

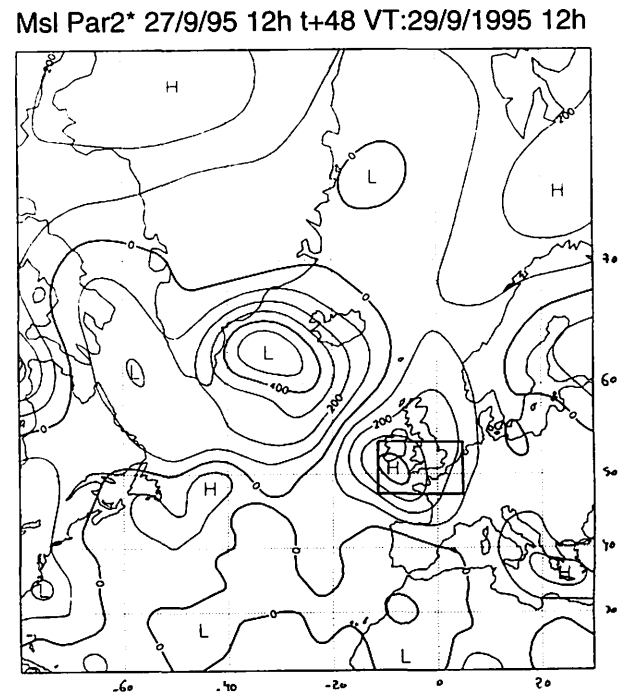

Figure 7: Difference in Pa between pressures fields shown in figures 2 and 6, i.e. P(with buoys) – P(without buoys).

References

1. DBCP Technical document No. 10, Developments in buoy and communication technologies; Impact of Drifting Buoy Observation on NWP model evolution – a case study – by J Roger Grant, Richard J Graham, and Michael J Bader, Observation Evaluation Group, NWP Division, UK Meteorological Office, Bracknell.

2. F. Delode, J. Pailleux, F. Bouttier, Météo France/CNRM, Note de travail du Groupe de modélisation pour l'assimilation et la prévision, No. 4, Etude de la sensibilité de la prévision aux conditions initiales à l'aide du modèle Arpège et de son modèle adjoint.

SVP drifters in Icelandic waters 1995-1997. Preliminary Results.

Hedinn Valdimarsson , Svend-Aage Malmberg and Mark Bushnell

Introduction

a. Iceland is situated at the meeting place or fronts of warm and cold ocean currents, which meet at this point because of the geographical position and the submarine ridges (Greenland-Scotland, Reykjanes and Kolbeinsey Ridges) which form a natural barrier against the main ocean currents around the country (Fig.1). To the south is the warm Irminger Current which is a branch of the North Atlantic Current (6-8 C) and to the north are the cold East-Greenland and East Icelandic Currents (<0 to 2 C). The different and variable hydrographic conditions in Icelandic waters are also reflected in the atmosphere or climatic conditions in and over the country and the surrounding seas (Iceland Basin, Irminger, Iceland and Norwegian Seas), mainly through the Iceland Low and Greenland High. These conditions in the sea and air have their impact on biological conditions, expressed through the food chain in the waters including recruitment and catches of commercial fish stocks.

b. For further studies on environment and recruitment along with general hydro-biological surveys in Icelandic waters a co-operative drifter programme between the Marine Research Institute in ReykjavÝk and Scripps Institution of Oceanography started in spring 1995. The project was as well supported by the Icelandic Research Council. Seasonally 10 drifters were deployed 4 times a year at selected locations (Fig. 1) or 40 drifters a year. The deployments were carried out in May/June, August and November 1995. February, May/June, August and November 1996, and in February, May/June and August 1997. Two more deployments are still planned or in November/December 1997 and February 1998. Thus totally 120 drifters will be deployed in this programme at least for the time being. The drifters used were Clearwater (SIO) and Technocean (MRI) Woce surface drifters with a drogue at 15 m depth. An Argos Limited Use 1/3 duty cycle was used throughout the programme. The aim of the programme was thus the following:

a) to obtain information on the flow of North-Atlantic Water from the south into Icelandic waters.

b) to obtain information on the coastal current from the spawning grounds of cod south of Iceland via waters west of Iceland into the main feeding grounds of cod in North Icelandic waters, with emphasis on drift of eggs and larvae through these waters. The result of this drift may again influence the recruitment of the cod stock in Icelandic waters.

Lifetime

The drifters last for very different time periods, a few fail from the beginning, some last just a few weeks or months, other up to a couple of years. (Fig.2). In Icelandic waters the drifters last shorter than in many other areas and the main reason for this seems to be the drift-ice conditions in the Denmark Strait between Iceland and Greenland and off Greenland in the Irminger and Labrador Seas, but also a few strand on the Icelandic coast (Fig.3). Drifters not captured by drift-ice or not stranding travel over long time periods (years) into remote areas. Some drift to the east into Faroes and Norwegian waters, other to the west into Greenland waters and even into the Labrador Sea and Newfoundland waters (Fig.4).

Results

The long distance drift mentioned above is in accordance with the general knowledge about the ocean current system in these areas. Some drifters travel to the east into Faroes and Norwegian waters. These drifters are all bound to the Atlantic inflow into the Norwegian Sea SE of Iceland, north of the Faroes (Faroes Current), and west off Norway (Norwegian Current with its different branches) even as far north as west of Spitzbergen (August 1995 - November 1997). No drifters along these routes drift into the area south of 62 N in the eastern part of the Iceland Basin. Other drifters drift westwards towards Greenland, follow the East- and West Greenland Currents into the Labrador Sea were most of them die out most probably due to drift-ice conditions, but one drifter deployed on the shelf west of Iceland in August 1995 took the course southwards with the Labrador Current to 42 N where it bent eastwards again across the Mid-Atlantic Ridge just south of the Charlie-Gibbs Fracture Zone at about 52 N and into the Iceland Basin to 56 N in November 1997. This drifter thus followed the lines of the so-called Sub-Arctic Gyre of the northern North Atlantic in 27 months.

Some seasonal differences in the drift may be seen. Those drifters deployed south of Iceland in winter have a tendency to drift SW-wards along the Reykjanes Ridge, indicating the influence of the bottom topography to a higher degree than expected, whereas in summer they cross the Ridge and drift into the waters west of Iceland. The increased stability of the surface layers in summer and consequently an increased geostrophic anticyclonic coastal flow around Iceland might be the reason. Also it is noteworthy (Fig. 5) that in 1995 no drift was observed from the waters south of Iceland east to Faroes waters and just one drifter deployed in 1997 went that way but several drifters did so again in 1996. In general the observed drift in the Iceland Basin is different from what expected for these region. Certainly the warm North-Atlantic water from the south reaches Icelandic waters (Irminger Current) but seemingly not as a continuous flow but just relatively slowly through eddies, variable in size. Also notable are the areas along the continental slope south and west of Iceland which are avoided by drifters (Fig. 3). This reveals upwelling or divergence zones from where deep nutrient rich water is distributed or advected into the surrounding surface layers. At last those drifters deployed south of Iceland which cross the Reykjanes Ridge as well as those deployed west of Iceland follow the shallow waters south and west of Iceland and even into the western part of the North Icelandic waters. Farther to the east the bottom topography (Kolbeinsey Ridge) again influences the drift of the North Icelandic Irminger Current, thus only a few drifters drift farther eastwards and than along the continental slope and farther eastwards into the Norwegian Sea.

At last, a few words about mean velocities of the drift from the first two years (Fig 6). It is in general relatively weak in Icelandic waters as well as in the Iceland Basin proper (<20 cm sec-1), but stronger (>40 cm sec-1) along topographic features like the Reykjanes Ridge and fronts in the Denmark Strait and at the East Greenland continental slope as well as in Faroes and Norwegian waters.

At the very last it must be stated that the results presented in this report are just an overview of preliminary results.

Figure 1 :
Topography and locations of deployments of SVP drifters in Icelandic Waters.

Figure 2 :
Lifetime (days) of SVP drifters in Icelandic Waters, 1995-1997.

Figure 3 :
Observed drift of SVP drifters in Icelandic Waters 1995-1997.

Figure 4 :
Observed drift of SVP drifters from Icelandic Waters into adjacent seas 1995-1997.

Figure 5a :
Observed drift of SVP drifters in 1995.

Figure 5b :
Observed drift of SVP drifters in 1996.

Figure 6 :
Mean velocity vectors, 1 x 2 degree bin. Scale in Iceland, 10 cm/s.

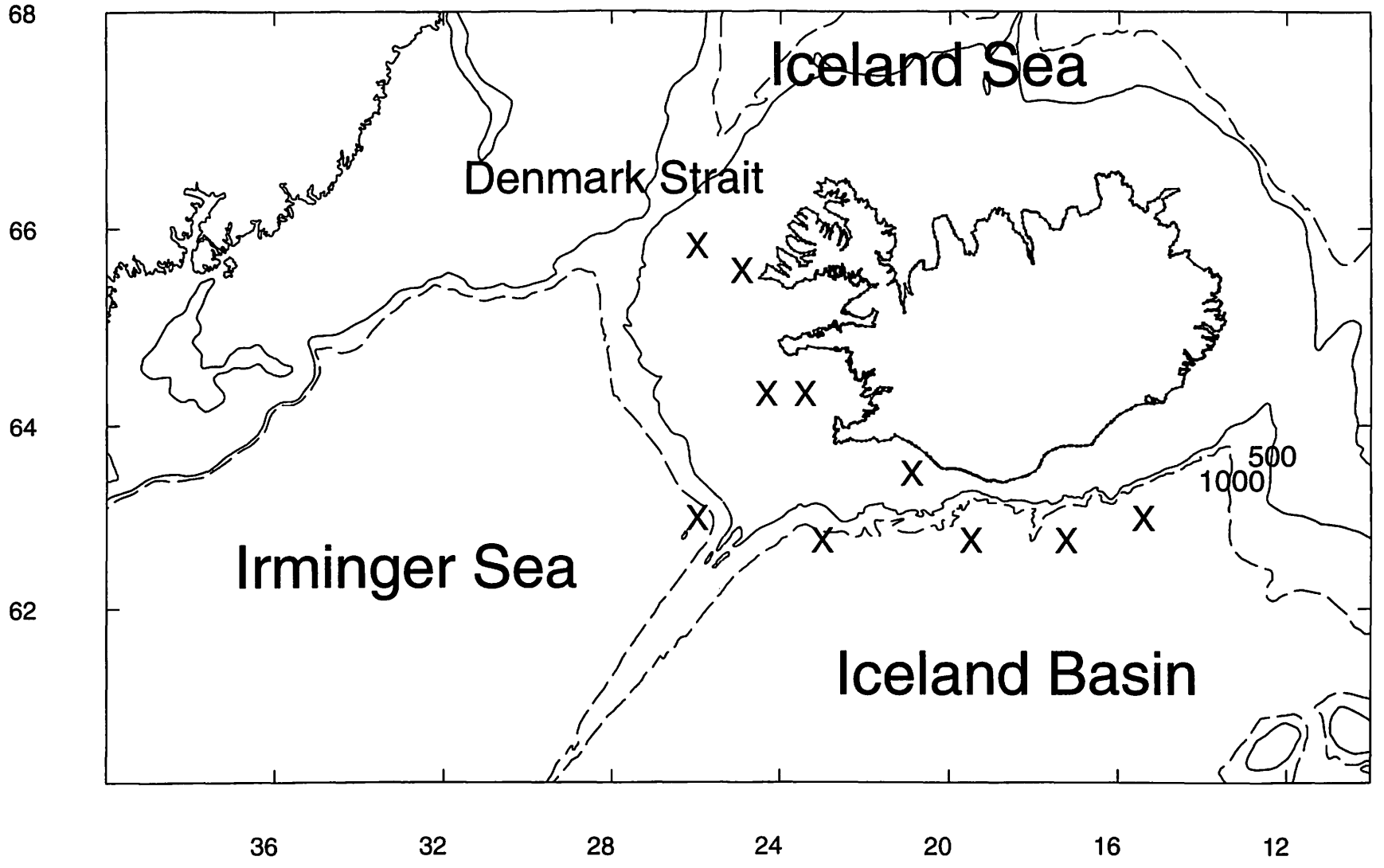

Figure 1: Topography and locations of deployments of SVP drifters in Icelandic Waters.

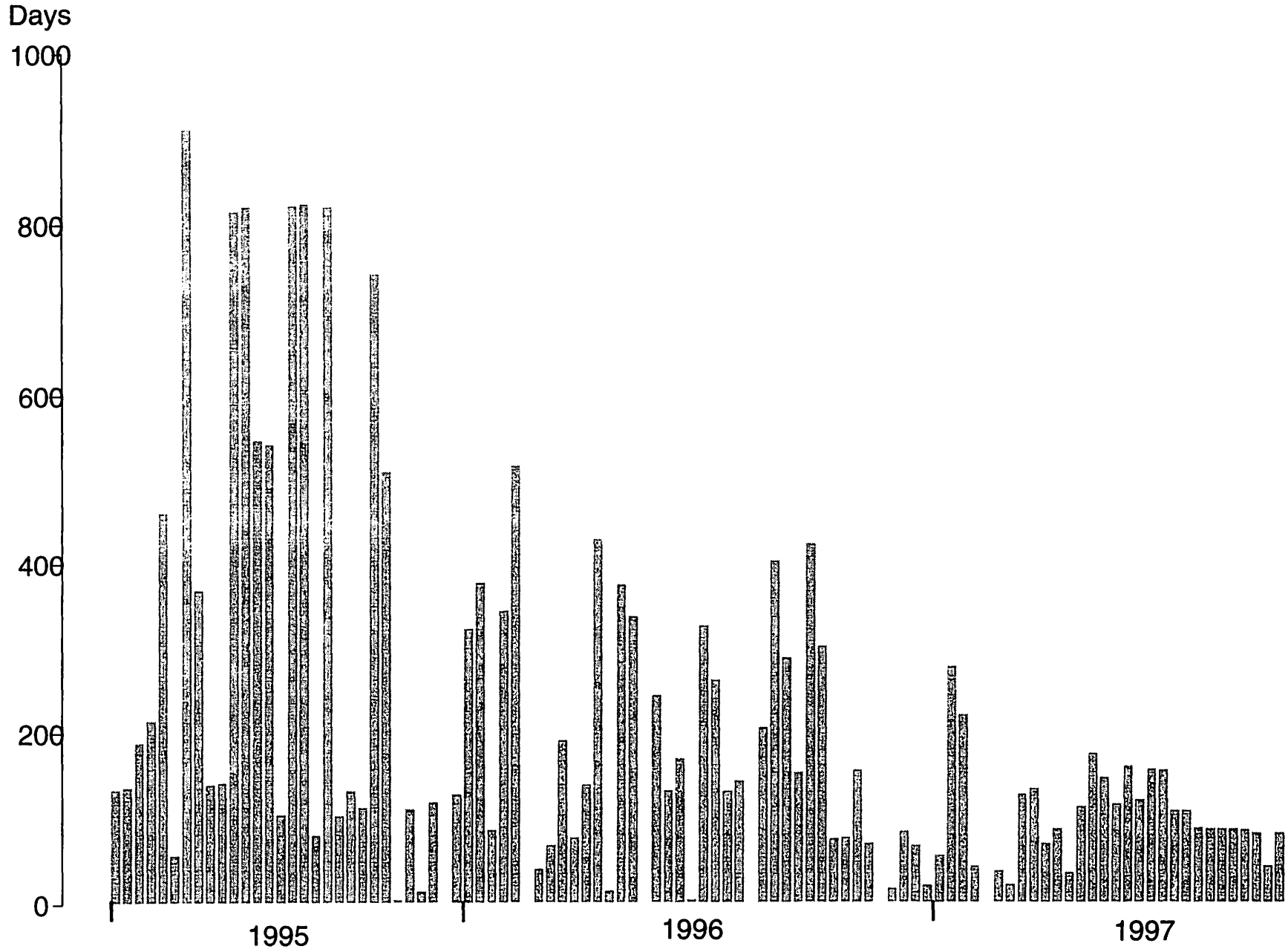

Figure 2: Lifetime (days) of SVP drifters in Icelandic Waters, 1995-1997.

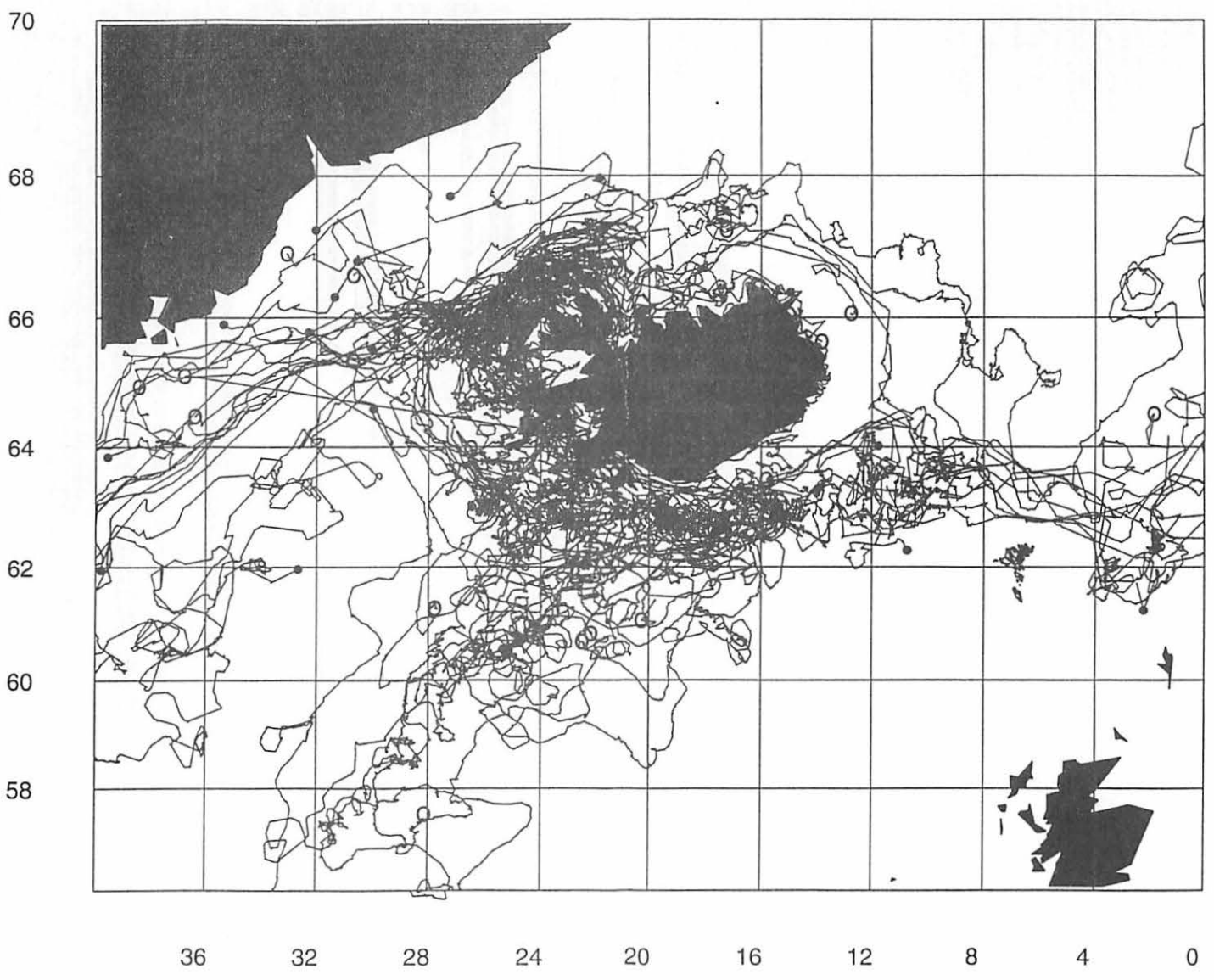

Figure 3: Observed drift of SVP drifters in Icelandic Waters 1995-1997

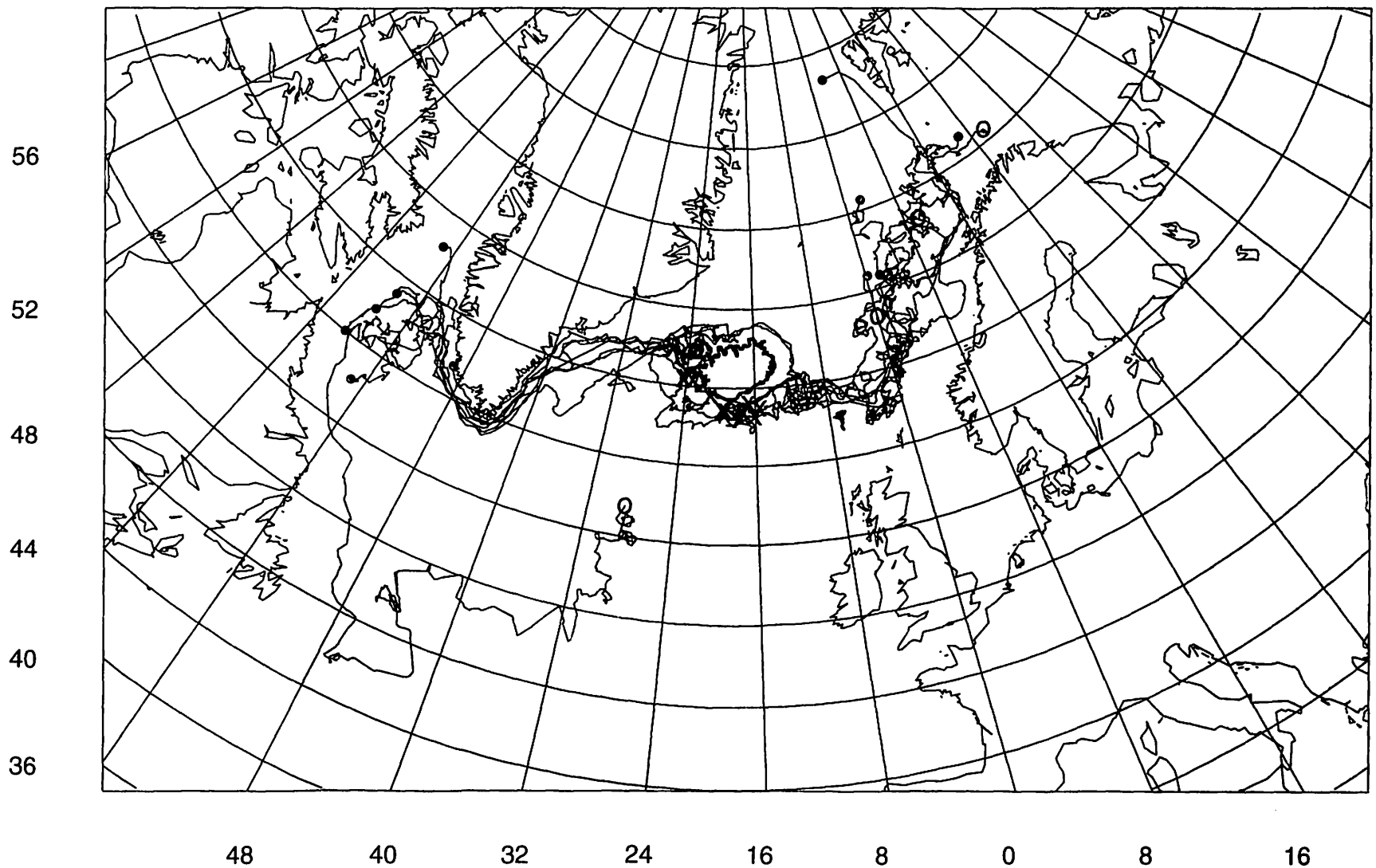

Figure 4: Observed drift of SVP drifters from Icelandic Waters into adjacent seas 1995-1997.

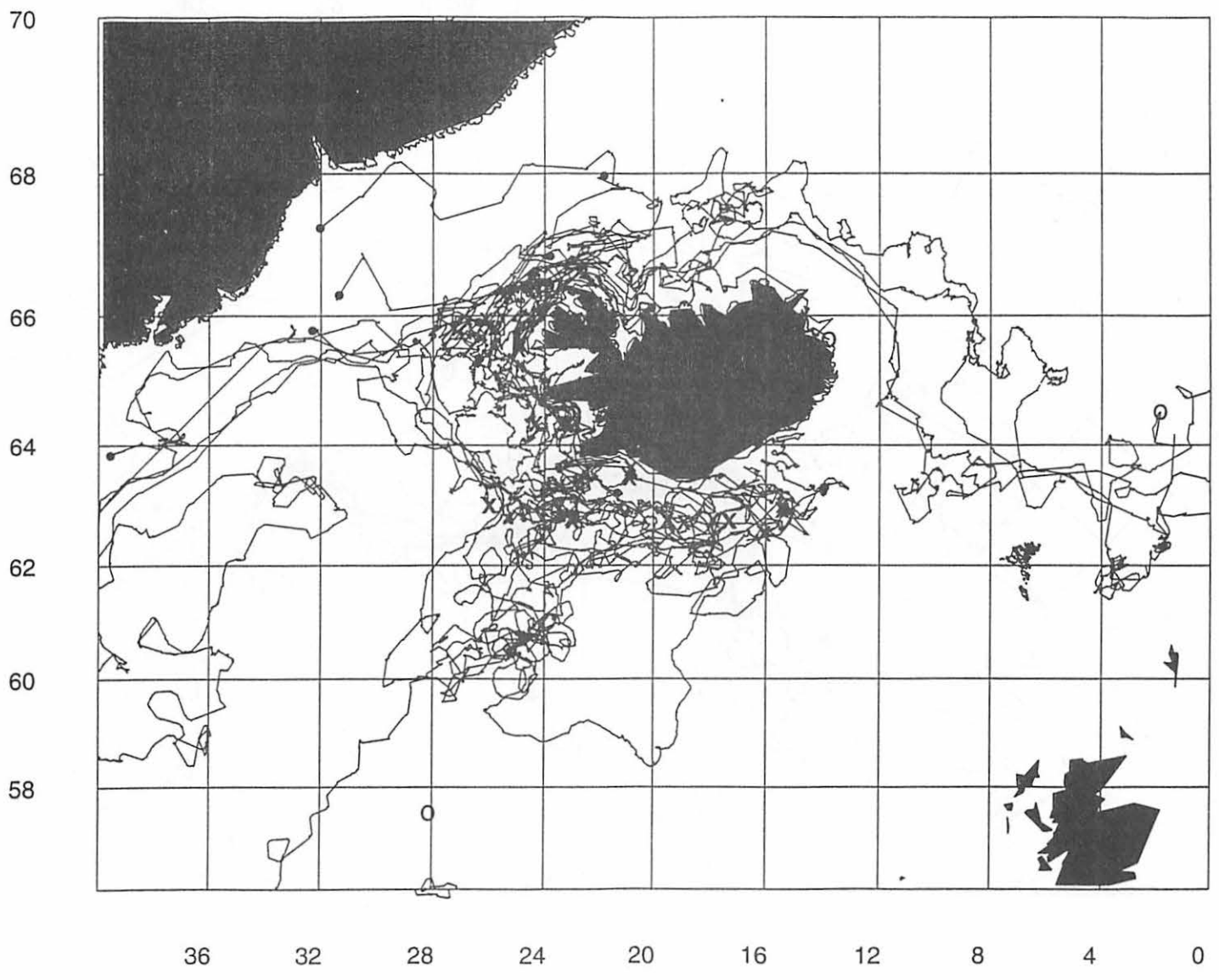

Figure 5a: Observed drift of SVP drifters in 1995.

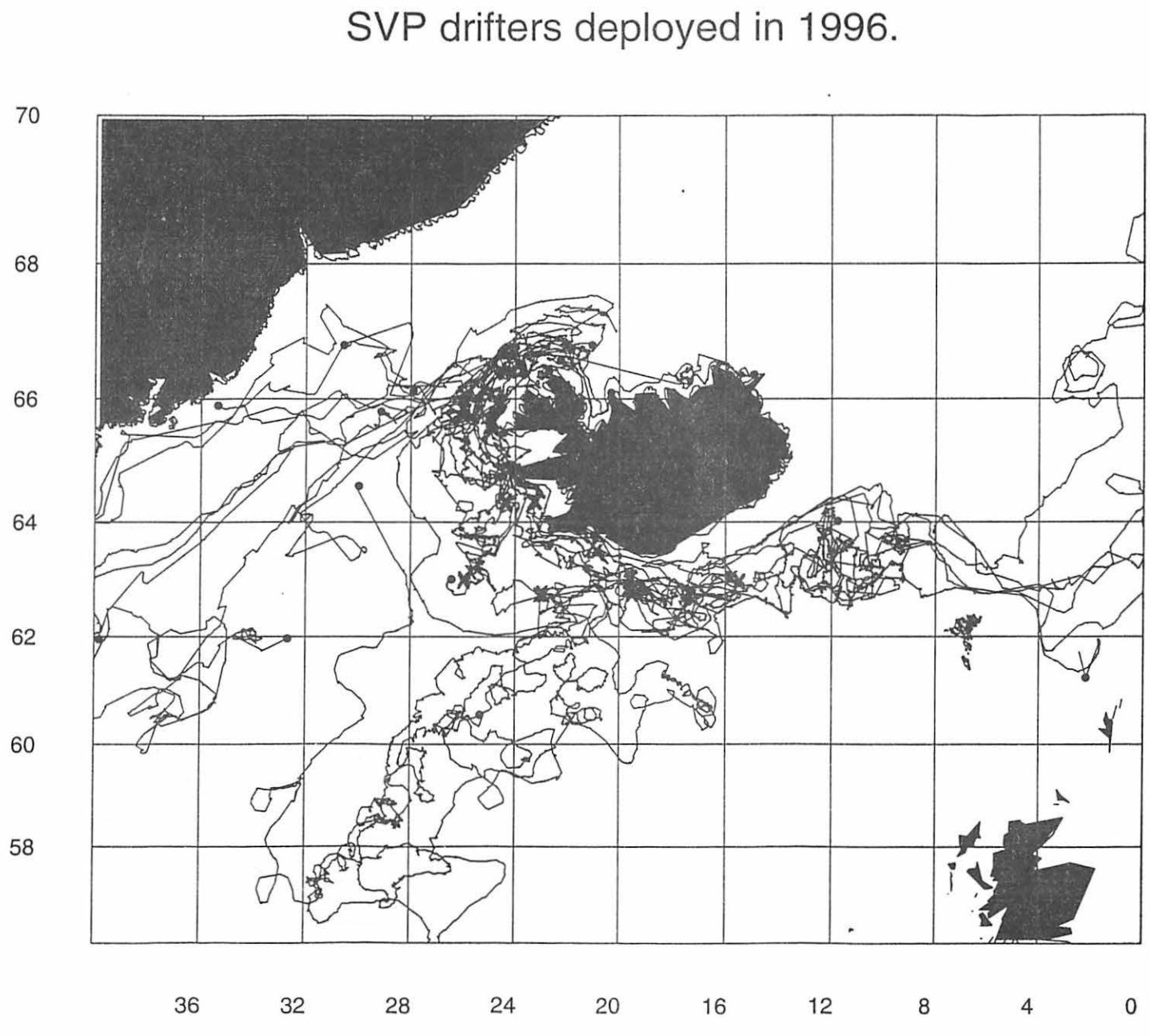

Figure 5b: Observed drift of SVP drifters in 1996.

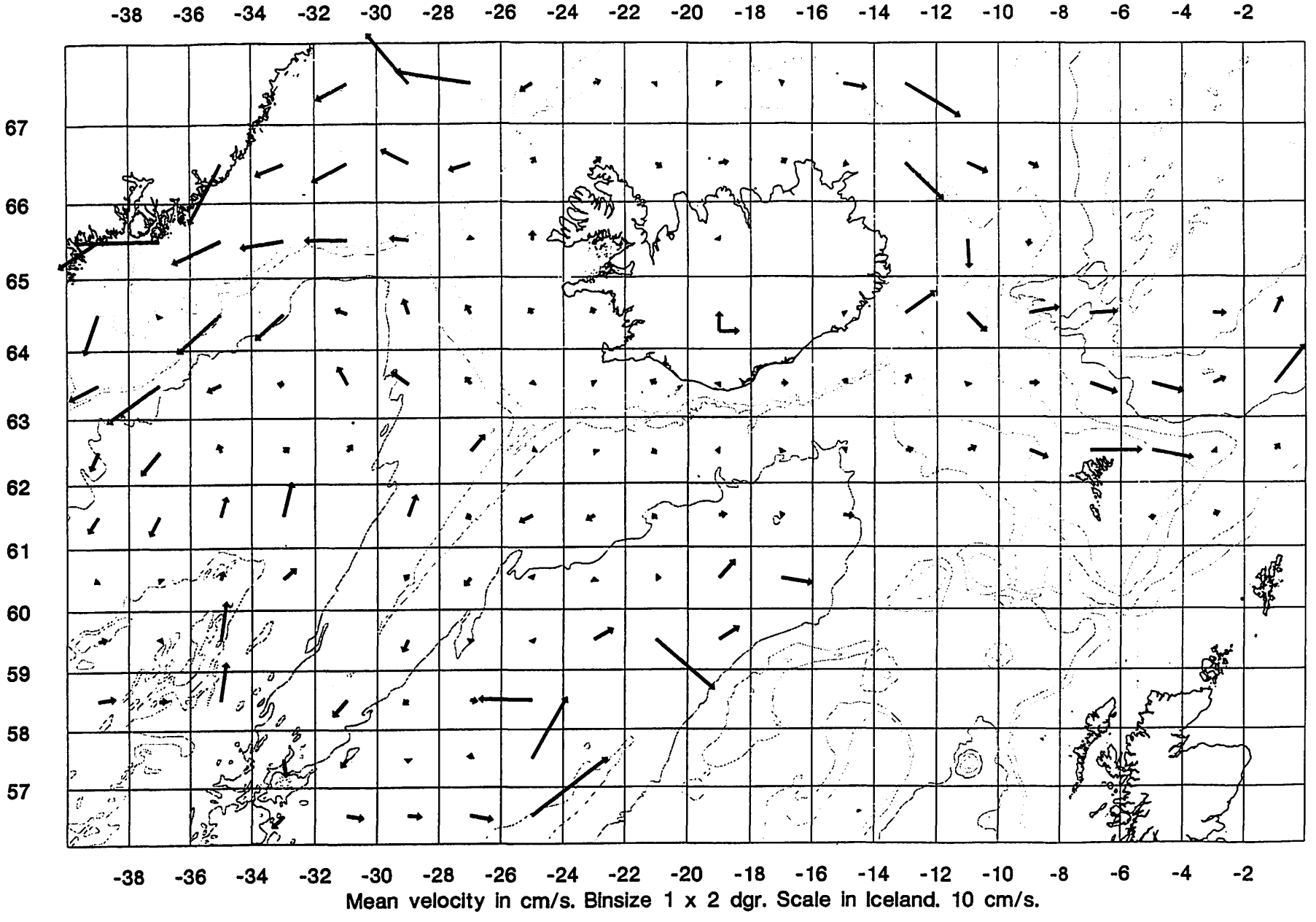

Figure 6: Mean velocity vectors, 1 x 2 degree bin. Scale in Iceland, 10 cm/s.

FURTHER RESULTS FROM GPS DRIFTER DEPLOYMENTS

D T Meldrum

Dunstaffnage Marine Laboratory, Scotland - UK

ABSTRACT

GPS allows locations to be determined with greater precision than is possible with Argos, and at times that the user chooses. Furthermore, an extension to GPS, Differential GPS (DGPS), permits errors present in the fixes to be reduced to a few metres. A scheme is described which allows DGPS and Argos positions to be combined in a way that permits efficient position determination for a drifter at user-chosen time intervals as short as a few minutes.

Results from GPS-Argos drifter deployments in the north Atlantic and in the pancake ice of the Greenland Sea are presented.

INTRODUCTION

This paper describes novel applications of the Global Positioning System (GPS) in two marine research programmes of the UK Natural Environment Research Council.

- The **Land-Ocean Interaction Study (LOIS)** Drifter Programme was devised to study the Hebrides slope current and nearby circulation patterns, with particular emphasis on exchanges between the shelf and the deep ocean. The vast majority of the 49 drifters released used the World Ocean Circulation Experiment (WOCE) Surface Velocity Programme (SVP) drifter as the basic design element (Sybrandy and Niiler (1)), modified to accommodate additional sensors and processing. These drifters have been tracked using the well-established Argos satellite system. This system has many limitations, and it was decided to modify a small number of drifters to demonstrate the advantages that could accrue from incorporating a GPS antenna and receiver as part of the sensor suite.

- The **European Subpolar Ocean Programme (ESOP)** includes a sea-ice dynamics project to study the small-scale processes within Odden ice tongue, a feature which may well be associated with the initiation of deep convection through its profound effect on the stability of the water column (Wadhams *et al* (2)). Collaboration between the Dunstaffnage Marine Laboratory (DML) and the Scott Polar Research Institute (SPRI) at the University of Cambridge has led to the development of GPS-equipped ice drifters for detailed tracking of ice trajectories. The drifters re-use the GPS-Argos technology developed within LOIS, and are constructed to mimic in shape and size the 'pancake' floes amongst which they are deployed.

THE GLOBAL POSITIONING SYSTEM (GPS)

The system is implemented using a constellation of 24 or so satellites in high orbit, ensuring global operability round the clock. The GPS user equipment is passive - it does not transmit - and estimates its range from each satellite in view by measuring the transit time of signals broadcast by the satellites. Ranges thus determined are called 'pseudo-ranges', as the receiver's clock is not initially synchronised to the satellites' clocks. The receiver computes the position of each satellite using a set of orbital parameters (the ephemeris) contained in the broadcast signal, and thus is able to infer its own position. A 2-dimensional solution (latitude, longitude and time) requires ranging to three satellites. The system is operated by the US Departments of Defense and Transportation; the former currently exercise the right to degrade the accuracy available to civilian users by introducing errors into the satellite clocks, the broadcast ephemeris, or both. Full accuracy denial is termed Selective Availability (SA), and currently increases the 2-σ error in computed GPS locations from a few metres to about 100 m. In our applications, these errors may be removed by various differential techniques (DGPS) if required. For a fuller description of GPS, see, for example, Daly (3).

THE LOIS ARGOS-GPS DRIFTERS

In order to understand the design philosophy of the combined Argos-GPS drifters that were developed for the LOIS Shelf Edge Study, it is important to be aware of some of the salient properties of both the Argos and GPS systems.

Gaps in Argos coverage

The Argos data collection system is carried on board the NOAA weather-imaging satellites. The prime purpose of these satellites is to collect daytime imagery of the earth and its weather systems, and the orbits of the spacecraft are arranged to image a swath on either side of a given point on the earth's surface at roughly the same local solar times each day. The general picture can be seen in Figure 1, which shows every pass of the two operational NOAA satellites that would have been seen by a drifter at 57°N during September 1995. A salient feature of the graph, and one of concern to many users of Argos, is the several hour gap in coverage around midnight local time, a direct consequence of the orbital configuration described above.

An experiment that aims to recover an uninterrupted time series must ensure that a sufficiently large stack of

Figure 1. Overpass durations for the month of September 1995 at 57°N. Note the gap of several hours around midnight, which normally means that no data are collected at these times.

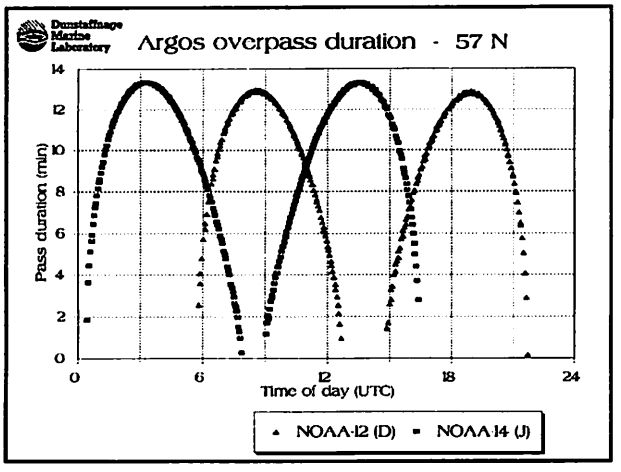

Figure 2. Gap size as a function of time of day. The size of the midnight hole is more than five hours on occasion, and will be worse at lower latitudes.

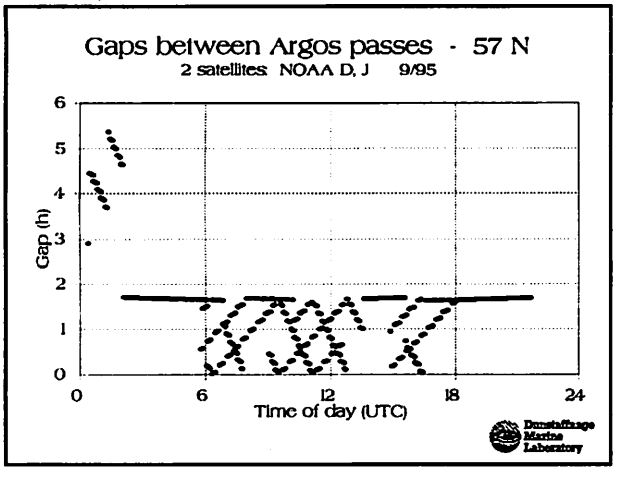

historical data is transmitted to bridge the largest expected gap in the satellite coverage. In our case, at a latitude of approximately 57°N, gaps in coverage can exceed five hours (Figure 2), which implies a stack of at least that length. The situation is, however, better for experiments lying closer to the poles, because of the convergence of the sub-satellite tracks of polar orbiters at high latitudes.

Argos location accuracy

Because of the data that we have accumulated recently from Argos transmitters (Seimac and Telonics) under test at our laboratory, an opportunity arose to perform an independent verification of Argos accuracy. Figure 3 shows the ensemble of 412 fixes of Argos classes 1, 2 and 3 that were collected. Table 1 lists the measured accuracy for the various location classes, and for GPS.

Figure 3. Measured Argos location accuracies at Dunstaffnage for transmitters under test.

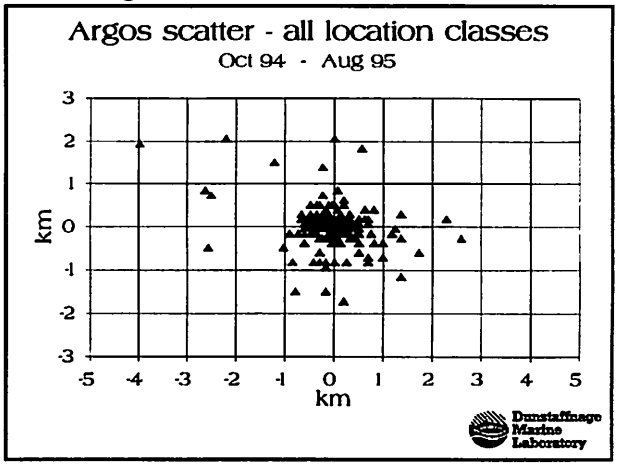

A GPS-Argos drifter

The design goals to be addressed using GPS were:

- Fix accuracy of 50 m or better (compared to ~500 m with Argos);
- Fix interval of 20 minutes (compared to ~2-3 hours with Argos);
- No gaps in the fix record, despite gaps in the satellite passes (compared to gaps of up to 6 or more hours with Argos).

A five-hour stack of GPS fixes plus other sensor data at 20 minute intervals is too big to transmit over Argos in a straightforward way. The solution we have employed is to compress the GPS data by transmitting only the significant parts of it, namely the fine-scale resolution which is not achievable by Argos, and by using the Argos location to define the coarse position, or 'lane'. For a fuller technical description, see Meldrum (4). Three prototype GPS drifters have been built (Figure 4)

	East (m)	North (m)	No of fixes
ARGOS			
Location quality 1	1440	790	130
Location quality 2	540	390	150
Location quality 3	310	390	132
GPS			
Uncorrected for SA	36	21	94
Post-corrected for SA (DGPS)	4	6	94

Table 1 - Standard deviations of various systems measured at Dunstaffnage in 1995.

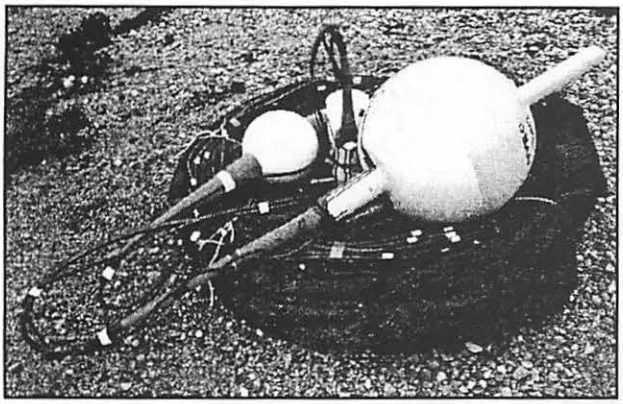

Figure 4. A prototype GPS-Argos drifter on the beach at Dunstaffnage.

and deployed in the north Atlantic. Figure 5 shows Argos and GPS tracks over a period of about five days; Figure 6 expands the scale to show a one-day section of track. In both cases the greatly improved resolution of the GPS track in both space and time is evident. Data recovery exceeds 95%, though some loss of data around midnight is still evident.

Differential post-processing (Inverse DGPS)

The intentional errors introduced by Selective Availability may be largely removed by noting the position errors at a fixed base station, and subtracting them from drifter positions computed using the same set of satellites at the same time. This form of DGPS was implemented in the LOIS GPS drifters by inserting the satellite IDs and exact time of fix into the data stream sent over Argos. Figure 7 shows the improvement in location accuracy that results from DGPS. The noise in the position measurements is probably below 10 m.

The SPRI-DML ice drifter

These drifters were designed to mimic as closely as possible the pancake shaped ice floes amongst which they were deployed (Figures 8 and 9). The electronics was more or less identical to that fitted to the LOIS drifters, and three complete units were built and deployed in the Greenland Sea in the spring of 1997. For an example of the drift tracks, see Figure 10. One drifter (No 2668) failed to report any GPS locations, though it was still located successfully by Argos. Another (No 2665) suffered an outage for several days, probably as a result of being turned upside down by adjacent floes. Apart from these instances, data recovery of GPS locations and temperatures was very close to 100%. A particular advantage of the use of GPS in this project was the ability to derive a highly accurate and noise-free velocity signal for use in detailed dynamical studies.

Further deployments, using similar hardware, are planned for 1998 or 1999.

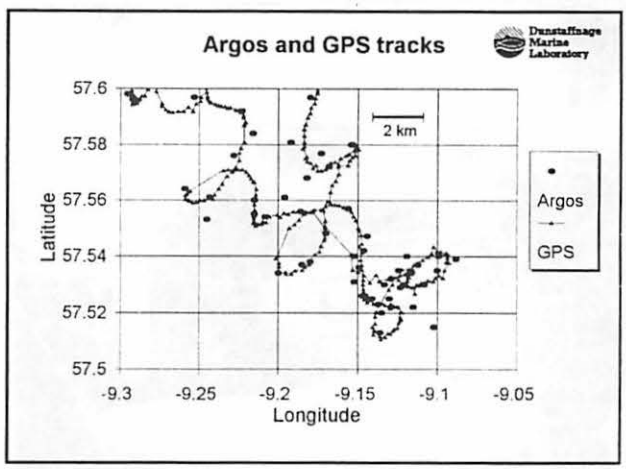

Figure 5. The GPS track over a five day period. Argos locations are shown as dots. The GPS track is of much finer resolution.

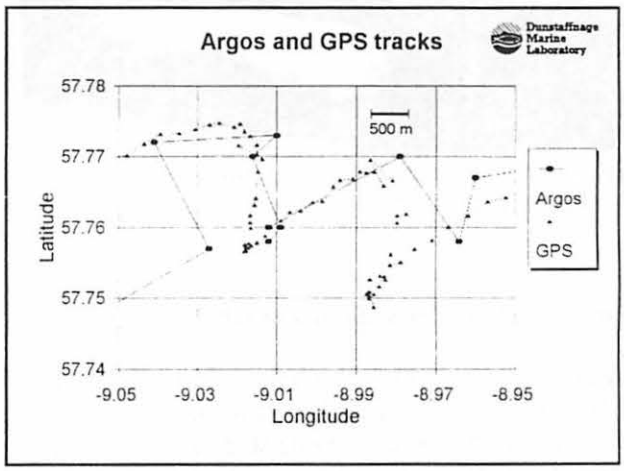

Figure 6. GPS and Argos tracks over a one day period. The detailed drift is very difficult to infer from the Argos locations alone.

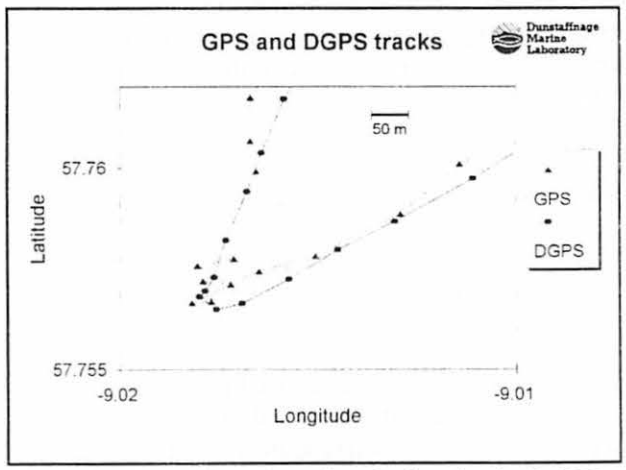

Figure 7. A small section of track showing both GPS and DGPS positions. The increased accuracy available by using DGPS is evident in the smoothness of the DGPS track.

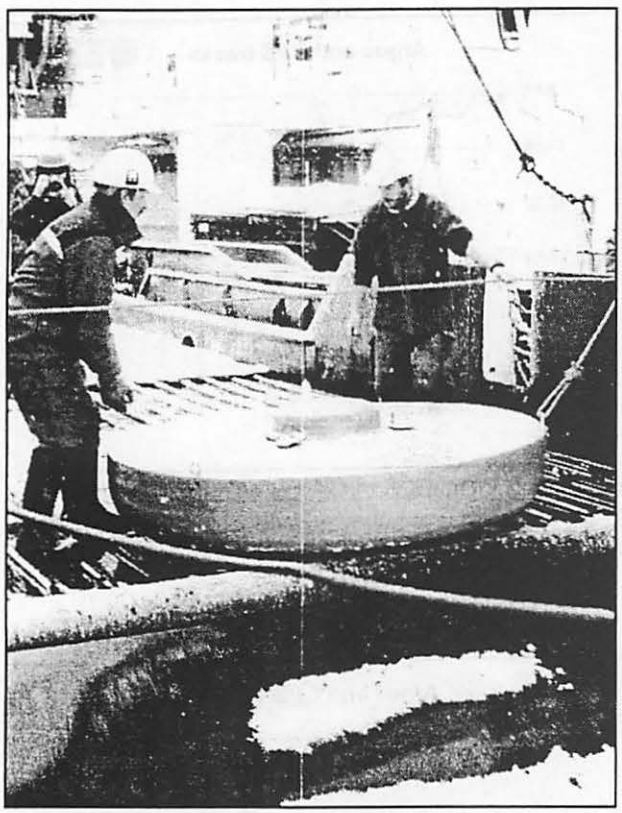

Figure 8. A SPRI-DML GPS ice drifter is deployed in the Greenland Sea.

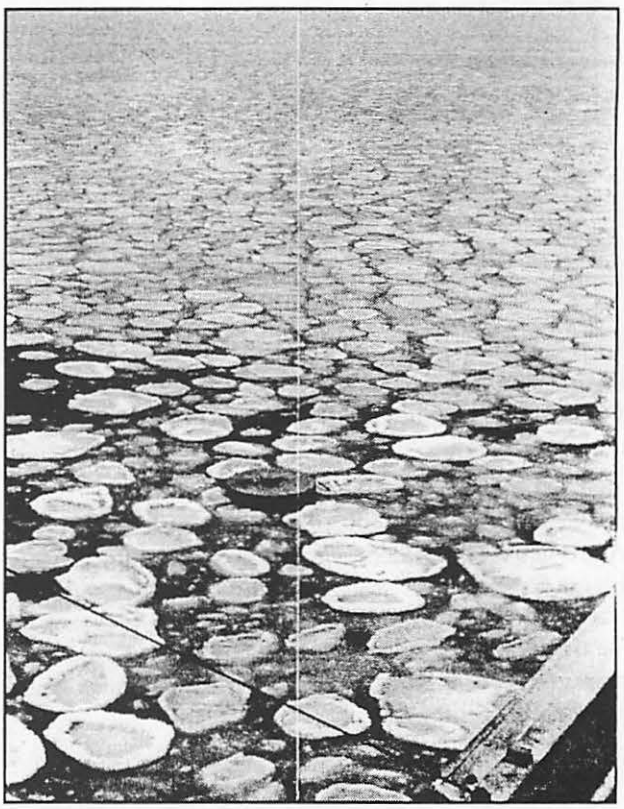

Figure 9. An ice drifter surrounded by pancake floes of similar size.

Summary of some possibilities of GPS for drifters

The precision attainable with GPS may not be of use to all investigators - it depends largely on the length and time scales of the processes being studied as to whether the additional complexity and energy penalty introduced by the GPS receiver is worthwhile.

However, GPS does bring important advantages which are not simply related to location precision. The key point is that both position and precise time are known to a drifter carrying a GPS receiver. This opens up a whole host of possibilities for the drifter of the future, capable of adapting its behaviour in response to this knowledge.

In summary, some of the advantages of GPS are:

- Accurate Argos satellite pass prediction, permitting transmitter scheduling and dynamic data stack management;
- Activity control according to position, permitting (for example) the drifter to shut down when leaving a pre-defined area of interest, and to re-start on re-entering it;
- Activity control according to time (of day, of year);
- More accurate locations, at user-defined intervals (ideal for small- and meso-scale studies), with the possibility of achieving 10-m precision using differential post-processing.
- Much better velocity estimates than can be obtained using Argos.

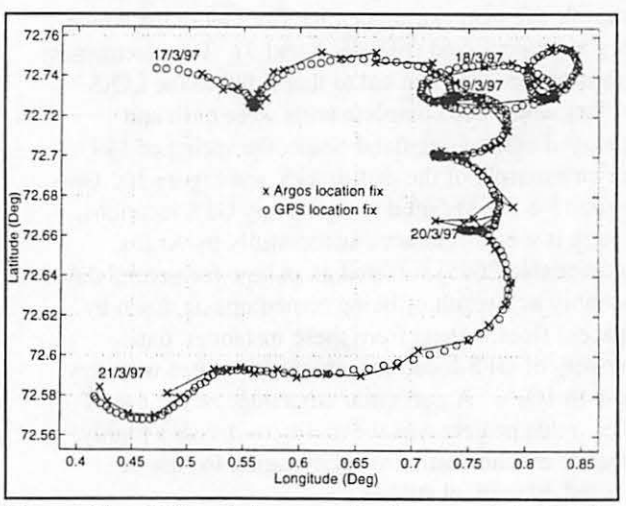

Figure 10. GPS and Argos tracks for one of the SPRI-DML ice drifters, showing the greater detail available from the GPS record.

ACKNOWLEDGEMENTS

This work was supported by the UK Natural Environment Research Council, and has depended heavily on the painstaking effort of a number of colleagues here at DML and at SPRI. In particular the invaluable and cheerful help given by Neil MacDougall before his tragic death in a car accident is gratefully acknowledged.

REFERENCES

1. Sybrandy, A L and Niiler, P P, 1991, "WOCE/TOGA Lagrangian drifter construction manual", WOCE Report No 63, Scripps Institution of Oceanography, La Jolla, California.

2. Wadhams, P, Prussen, E, Comiso, J C, Wells, S, Crane, D R, Brandon, M, Aldworth, E, Viehoff, T, and Allegrino, R, (in press). "The development of the Odden Ice Tongue in the Greenland Sea during winter 1993 from remote sensing and field observations", Journal of Geophysical Research.

3. Daly, P, 1993, "Navstar GPS and GLONASS: global satellite navigation systems", Electronics and Communication Engineering Journal, 349-357.

4. Meldrum, D T, 1996, "Integrating GPS and Argos - a drifting buoy application", in "Developments in Buoy Technology and Enabling Methods", Data Buoy Co-operation Panel Technical Document Series, 7, 71-94, World Meteorological Organization, Geneva.

THIRTEENTH SESSION OF THE DATA BUOY CO-OPERATION PANEL
SCIENTIFIC AND TECHNICAL WORKSHOP
(La Réunion Island, France, 13-17 October 1997)

LIST OF PARTICIPANTS

Mr Alaor Moacyr Dall' Antonia Jr
Head of the Marine Weather Forecast Division
Diretoria de Hidrografia e Navegação
Rua Barão de Jaceguay, S/No
NITERÓI, RJ
CEP-24048-900 Brazil
Tel: +55-21 620 8861
Fax: +55-21 620 8861
E-mail: dhn25.hinave@mhs.mar.br
meteo.hinave@mhs.mar.br

Mr César Belandia
Head, Observations and Instruments
Apartado 285
28070 MADRID
Spain
Tel: +34-1 56 19 651
Fax: +34-1 56 19 846
E-mail: cesar.belandia@inm.es

Mr Paul-André Bolduc
Marine Environmental Data Service
200 Kent Street
OTTAWA
Canada K1A 0E6
Tel: +1-613 990 0231
Fax: +1-613 993 4658
E-mail: bolduc@ottmed.meds.dfo.ca

Mr Graeme Brough
Superintendent, Instrument Engineering
Bureau of Meteorology
GPO Box 1289 K
MELBOURNE, VIC 3001
Australia
Tel: +61-3 9669 4163
Fax: +61-3 9669 4168
E-mail: g.brough@bom.gov.au

Mr Mark Bushnell
Manager, Global Drifter Center
R/E/AO/PHOD
NOAA/AOML
4301 Rickenbacker Causeway
MIAMI, FL 33149-1026
USA
Tel: +1-305 361 4353
Fax: +1-305 361 4412
E-mail: bushnell@aoml.noaa.gov

Mr Etienne Charpentier
DBCP Technical Co-ordinator
CLS Argos
8-10 rue Hermès
Parc Technologique du Canal
31526 RAMONVILLE ST-AGNE
France
Tel: +33-5 61 394 782
Fax: +33-5 61 751 014
E-mail: charpentier@cls.cnes.fr

Dr Peter Dexter
Chief, Ocean Affairs Division
WMO
CP 2300
CH-1211 GENEVA 2
Switzerland
Tel: + 41-22 730 8237
Fax: + 41-22 733 0242
Email: dexter@www.wmo.ch

Dr Rex J Fleming
Program Manager, Climate Observations
NOAA/ERL
3300 Mitchell Lane, Suite 175
BOULDER, CO 80301
USA
Tel: +1-303 497 8165
Fax: +1-303 497 8158
E-mail: fleming@ncar.ucar.edu

Ms Julie Fletcher
Marine Meteorological Officer
Meteorological Service of NZ Ltd
PO Box 722
WELLINGTON
New Zealand
Tel: +64-4 4700 789
Fax: +64-4 4700 772
E-mail: fletcher@met.co.nz

Mr François Gérard
Ingénieur en chef de la météorologie
Chef du Département 'Réseau' de la Direction
Générale des Opérations de Météo-France
1 quai Branly
75340 PARIS Cedex 07
France
Tel: +33-1 45 56 70 24
Fax: +33-1 45 56 70 05
E-mail: francois.gerard@meteo.fr

Mr Frank Grooters
Co-ordinator, International Observation Programmes
Royal Netherlands Meteorological Institute
PO Box 201
3730 AE DE BILT
Netherlands
Tel: +31-30 220 6691
Fax: +31-30 221 0407
E-mail: grooters@knmi.nl

Commanding Officer, attn: Ms Elizabeth Horton, N31
U.S. Naval Oceanographic Office
Stennis Space Center, MS 39522-5001
USA
Tel: +1-228 688 5725
Fax: +1-228 688 5514
E-mail: ehorton@navo.navy.mil

Mr Pekka Järvi
Product Manager
Vaisala Oy
PO Box 26
FIN-00421 HELSINKI
Finland
Tel: +358 9 894 9491
Fax: +358 9 894 9485
E-mail: pekka.jarvi@vaisala.com

Mr D Wynn Jones
The Meteorological Office
Beaufort Park, Easthampstead
WOKINGHAM RG40 3DN
United Kingdom
Tel: +44-1344 855603
Fax: +44-1344 855897
E-mail: dwjones@meto.gov.uk

Mr Piet Le Roux
South African Weather Bureau
Private Bag X97
PRETORIA 0001
South Africa
Tel: +27-12 309 3024
Fax: +27-12 309 3020
E-mail: pleroux@cirrus.sawb.gov.za

Mr Ron McLaren
Head, Marine Operations
Atmospheric Environment Branch
Pacific and Yukon Region
Environment Canada
700-1200 West 73rd Avenue
VANCOUVER, BC
Canada V6P 6H9
Tel: +1-604 664 9188
Fax: +1-604 664 9195
E-mail: ron.mclaren@ec.gc.ca

Mr Svend-Aage Malmberg
Marine Research Institute
Skúlgata 4
121 REYKJAVIK
Iceland
Tel: +354-552 0240
Fax: +354-562 3790
E-mail: svam@hafro.is

Mr Eric Meindl
Chief, Data Systems Division - W/DB3
NOAA National Data Buoy Center
Stennis Space Center, MS 39529-6000
USA
Tel: +1-228 688 1717
Fax: +1-228 688 3153
E-mail: emeindl@ndbc.noaa.gov

Mr David Meldrum
Group Leader, Marine Technology
Dunstaffnage Marine Laboratory
PO Box 3
OBAN PA34 4AD
Scotland - UK
Tel: +44-1631 567873
Fax: +44-1631 565518
E-mail: dtm@dml.ac.uk

Dr Peter Niiler
Scripps Institution of Oceanography
LA JOLLA, CA 92093-0230
USA
Tel: +1-619 534 4100
Fax: +1-619 534 7931
E-mail: pniiler@ucsd.edu

Mr Christian Ortega
CLS Argos
8-10 rue Hermès
Parc Technologique du Canal
31526 RAMONVILLE ST-AGNE
France
Tel: +33-5 61 394 729 / 5 61 394 720
Fax: +33-5 61 394 797
E-mail: ortega@cls.cnes.fr

Mr Derek Painting
WMO Consultant
5 The Sycamores
Darby Green, Blackwater
CAMBERLEY
United Kingdom
Tel: +44-1252 876804
Fax: +44-1252 654612
E-mail: 101527.1533@compuserve.com

Mr Richard W Reynolds
NCEP/NWS/NOAA
5200 Auth Road, Room 807
CAMP SPRINGS, MD 20746
USA
Tel: +1-301 763 8000 ext 7580
Fax: +1-301 763 8125
E-mail: richard.w.reynolds@noaa.gov

Mr Jean Rolland

Météo-France
13 Rue du Chatellier
29273 BREST Cedex
France
Tel: +33-2 98 22 18 53
Fax: +33-2 98 22 18 49
E-mail: jean.rolland@meteo.fr

Mr Flosi Hrafn Sigurõsson
Head of Department / Meteorologist
Dept of Instruments and Observations
Icelandic Meteorological Office
Bustadavegur 9
IS-150 REYKJAVIK
Iceland
Tel: +354-560 0600
Fax: +354-552 8121
E-mail: flosi@vedur.is

Mr Alain Soulan
Directeur du Service Météorologique
Météo-France
BP 497 491
STE CLOTILDE Cedex
La Réunion
Tel: +262 921 100
Fax: + 262 921 147
E-mail: alain.soulan@meteo.fr

Dr Mark Swenson
Director, Global Drifter Program
NOAA/AOML
4301 Rickenbacker Causeway
MIAMI, FL 33149-1026
USA
Tel: +1-305 361 4363
Fax: +1-305 361 4412
E-mail: swenson@aoml.noaa.gov

Mr Michel Taillade-Carrière
General Manager
CLS Argos
8-10 rue Hermès
Parc Technologique du Canal
31526 RAMONVILLE ST-AGNE
France
Tel: +33-5 61 394 704 / 5 61 394 836
Fax: +33-5 61 751 014
E-mail: taillade@cls.cnes.fr

Mr Yves Tréglos
UNESCO
Intergovernmental Oceanographic Commission
1, rue Miollis
75015 PARIS
France
Tel: +33-1 45 68 39 76
Fax: +33-1 45 68 58 12
E-mail: y.treglos@unesco.org

Mr Gary Williams
Clearwater Instrumentation Inc
304 Pleasant Street
WATERTOWN, MA 02172
USA
Tel: +1-617 924 2708
Fax: +1-617 924 2724
E-mail: wgwill@world.std.com

Mr William E Woodward
NOAA/OAR/AOML
SSMC #3, Room 11142
1315 East-West Highway
SILVER SPRING, MD 20910
USA
Tel: +1-301 713 2790 ext 180
Fax: +1-301 713 4499
E-mail: william.e.woodward@noaa.gov

Mr Louis Vermaak
South African Weather Bureau
Private Bag X 097
PRETORIA 001
South Africa
Tel: +27-12 309 3834
Fax: +27-12 309 3020
E-mail: vermaak@cirrus.sawb.gov.za

TECHNICAL DOCUMENTS ISSUED WITHIN THE DATA BUOY COOPERATION PANEL SERIES

No.	Title	Year of issue
1	Annual Report for 1994	1995
2	Reference Guide to the GTS Sub-system of the Argos Processing System	1995
3	Guide to Data Collection and Location Services using Service Argos	1995
4	WOCE Surface Velocity Programme Barometer Drifter Construction Manual	1995
5	Surface Velocity Programme - Joint Workshop on SVP Barometer Drifter Evaluation	1996
6	Annual Report for 1995	1996
7	Developments in Buoy Technology and Enabling Methods - Technical Presentations Made at the Eleventh Session of the DBCP	1996
8	Guide to Moored Buoys and Other Ocean Data Acquisition Systems	1997
9	Annual Report for 1996	1997
10	Developments in Buoy and Communications Technologies	1997
11	Annual Report for 1997	1998
12	Developments in Buoy Technology and Data Applications	1998

These publications can be ordered from: Etienne Charpentier, Technical Coordinator of the DBCP, CLS/Service Argos, 8-10 rue Hermès, Parc Technologique du Canal, F-31526 Ramonville Saint-Agne, France - *Internet mail:* charpentier@cls.cnes.fr - *Telefax:* +33-5 61 75 10 14 *Telephone:* +33-5 61 39 47 82